Title

Augmenting Real-World Haptic Interactions

Author

Kawazoe, Anzu

Publication Date

2023

Peer reviewed|Thesis/dissertation

University of California
Santa Barbara

Augmenting Real-World Haptic Interactions

A dissertation submitted in partial satisfaction
of the requirements for the degree

Doctor of Philosophy
in
Media Arts and Technology

by

Anzu Kawazoe

Committee in charge:

Professor Yon Visell, Chair
Professor Misha Sra
Professor Jennifer Jacobs
Professor Taku Hachisu

September 2023

The Dissertation of Anzu Kawazoe is approved.

Professor Misha Sra

Professor Jennifer Jacobs

Professor Taku Hachisu

Professor Yon Visell, Committee Chair

June 2023

Augmenting Real-World Haptic Interactions

by

Anzu Kawazoe

This dissertation is dedicated to my parents, Sayuri and Tetsuji, and grand mother, Nobuko who have always been my rock and supported me through every step of this journey. To my siblings, Gumi and Mitsuoki, who have cheered me on and kept me laughing through the tough times. Thank you all for being my constant support and inspiration.

Acknowledgements

First of all, I'd like to acknowledge the invaluable guidance and inspiration provided by my Graduate Advisor, Yon Visell. His patience, knowledge, and commitment to high standards greatly benefited this research. I would like to extend my gratitude to my collaborator, Massimiliano Di Luca, whose partnership and expertise significantly contributed to the research. To my PhD dissertation committee: Misha Sra, Jennifer Jacobs, and Taku Hachisu, thank you for your time, insights, and constructive feedback. Your expert perspectives enriched the final version of this dissertation. I owe deep gratitude to my co-authors: Gregory Reardon, whose advising formed the backbone of this study; Dustin Goetz, who supported crafting the cool actuators; Shriniwas Patwardhan and Erin Woo for their exceptional cooperation and collaboration in our research endeavors. Special thanks to the alumni, Yitian Shao, Bharat Dandu, and Mengjia Zhu. Your advice and encouragement were invaluable in the completion of this study. I am fortunate to have worked alongside amazing labmates, Stejara Dinulescu, Neeli Tummala, Max Linnander, and Chris Cheney. Your passion for research and unwavering support made our lab an environment of learning and growth. My sincere gratitude goes to Katja Seltmann for her kindness and support. Adela Contreras (Lolly), your exceptional mentorship has profoundly enriched my English learning journey, and for that, I am immensely grateful.

To my friends Anshul Pendse and Mart Toka, who provided an abundance of support and encouragement throughout my life and this journey. I cannot forget the warm companionship of Anshul Pendse's cat, Byron. Jungah Son, Sahar Sajadieh, and Saki Hachisu your friendship is highly appreciated. A word of gratitude for the MAT folks who participated in the experiment: Samuelle Bourgault, Pau Roselló, Jenni Hutson, Yixuan Li, Nefeli Manoudaki, Iason Paterakis, Ashley del Valle, and Alejandro Aponte. Your participation and commitment made this research possible. Special thanks to Miyuki

Kawasaki, my best friend back home, for your unwavering friendship and moral support despite the distance.

Lastly, to my family: Sayuri Kawazoe, Tetsuji Kawazoe, Gumi Kawazoe, Mitsuoki Kawazoe, and Nobuko Miyaguchi. Your love, encouragement, and unwavering belief in my capabilities have been the pillar of my strength throughout this journey. I dedicate this work to you.

Curriculum Vitæ

Anzu Kawazoe

Education

2023	**Ph.D.** in Media Arts and Technology (Expected), University of California, Santa Barbara.
2016	**M.S.** in Engineering, Information System Science, Soka University, Tokyo, Japan
2014	**B.E.** in Engineering, Information System Science, Soka University, Tokyo, Japan

Publications

Journal articles:-

1. **A. Kawazoe**, G. Reardon, D. Goetz, M. D. Luca and Y. Visell, "Effect of Time Delay and Masking Effects in the Perception of Tactile Feedback Accompanying Finger-Surface Contact," in preparation.
2. S. Biswas, B. Dandu, Y. Shao, D. Goetz, **A. Kawazoe**, M. Zhu, and Y. Visell "Stretchable Optoelectronic Skin for Haptic Feedback via Light Fields", in preparation.
3. **A. Kawazoe**, G. Reardon, E. Woo, M. D. Luca and Y. Visell, "Tactile Echoes: Multisensory Augmented Reality for the Hand," in IEEE Transactions on Haptics, 2021.
4. Peng, Y., Serfass, C.M., **Kawazoe, A.** et al."Elasto-hydro dynamic friction of robotic and human fingers on soft micropatterned substrates" Nature. Material, 2021.
5. S. Patwardhan, **A. Kawazoe**, D. Kerr, M. Nakatani, and Y. Visell. Dynamics and Perception in the Thermal Grill Illusion. in IEEE Transactions on Haptics. 2019.

Peer-reviewed conference papers:-

1. **A Kawazoe**, M Di Luca, Y Visell, "Tactile echoes: A wearable system for tactile augmentation of objects," 2019 IEEE World Haptics Conference (WHC), 2019.
2. Ishikawa, Y., **Kawazoe, A.**, Chernyshov, G., Fujii, S., Nakatani, M. (2019). The Thermal Feedback Influencer: Wearable Thermal Display for Enhancing the Experience of Music Listening. AsiaHaptics 2018.
3. S. Patwardhan, **A. Kawazoe**, D. Kerr, M. Nakatani and Y. Visell, "Too hot, too fast! Using the thermal grill illusion to explore dynamic thermal perception,"IEEE Haptics Symposium (HAPTICS), 2018.

Non Peer-reviewed domestic conference papers:-

1. **Anzu Kawazoe**, Masashi Nakatani. A Trial Production for Ambient Display. VRSJ the 22 th Annual Conference. September 2017.
2. **Anzu Kawazoe**, Masashi Nakatani, Kouta Minamizawa, Susumu Tachi. Vibrotactile Signal Synthesis for Haptic Rendering. The 16th SICE system integration division Annual Conference. December 2015.
3. **Anzu Kawazoe**, Kazuo Ikeshiro and Hiroki Imamura.A Trial Production for A Haptic Device of Finger Mounted Typeby PID Contorol UsingARToolKit.VRSJ the 16th Annual Conference. CD ROM:pp. 500-501, 2011.

Patents

1. **Anzu Kawazoe**, Kazuo Ikeshiro, and Hiroki Imamura. Haptic device based on an approximate plane, 2012. Japan.Patent application number 2012-198778

Media

1. Michelle Hampson, New AR System Alters Sight, Sound and Touch Tactile Echoes allows users to freely interact with any surface IEEE Spectrum, July 2021 `https://spectrum.ieee.org/new-ar-system-alters-sight-sound-and-touch`

Awards

1. **Best Application paper award Finalist** at the 2021 IEEE Transactions on Haptics.
2. Awarded the UC Santa Barbara MAT Dept. **MAT MERIT SUPPLEMENT SUPPORT research stipend**, 2020.

WorkShops

1. Masashi Nakatani, Yon Visell, Xuan Duan, Hsin-Yun Yao. Introduction to Haptic Media Design: Basics and Implementations, organized workshop and presented psychophysics technique demonstration at IEEE Haptics Symposium 2016, Pennsylvania USA.

Abstract

Augmenting Real-World Haptic Interactions

by

Anzu Kawazoe

Future haptic augmented reality systems could transform our interactions within many environments by furnishing haptic feedback that augments touch interactions with physical objects. However, most prior haptic technologies involve controllers, wearables, or devices that either impede free-hand interactions or make it impossible to directly touch physical objects with the skin. This Ph.D. presents several haptic design approaches and findings that can overcome these limitations, and that provide new methods for augmenting free-hand interactions with physical objects.

The first part of the Ph.D. presents a new haptic augmented reality system for the hand. It introduces Tactile Echoes, a finger-wearable system that provides responsive haptic feedback that augments touch interactions with physical surfaces. It renders these effects by capturing touch-elicited vibrations in the skin and processing them in real-time in order to enliven tactile experiences. Using computational and spatial tracking techniques, different haptic effects may be spatially painted onto different objects or surfaces. This chapter presents experiments characterizing how these novel haptic effects are perceived, demonstrations of several applications, and a user study showing how they can enhance augmented or mixed reality applications.

The second part of this Ph.D. was motivated by observations obtained using Tactile Echoes that indicate that the perceived strength of haptic feedback increases when it is supplied tens of milliseconds after a touch event. This observation is consistent with findings from prior perception research on tactile forward masking. However, prior studies

of forward masking have been confined to passive conditions rather than active touch, as occurs in Tactile Echoes. This chapter presents research revealing prominent modulatory effects of the timing, amplitude, and perceptual similarity between the feedback and the transient skin oscillations elicited via touch contact. Forward masking produced a greater attenuation of the perceived intensity of feedback as delay time decreased, with the maximum attenuation reaching nearly 10 dB. These findings shed light on the interplay between perception and action in the haptic system and have important implications for the design of haptic interfaces.

The third part of this Ph.D. presents another method for augmenting touch interactions that exploits mechanical wave propagation in the skin. This method, called Beatactile, involves supplying vibrations on the finger and on the surface with slightly different frequencies. When a surface is touched, the two vibration sources interfere, producing beat frequencies between vibrations in the finger that cause a flat surface to feel coarsely textured. The BeaTactile hardware and software system enables parametric control over these novel effects.

The final part of this Ph.D. concerns thermal augmentations of touch interactions, based on the thermal grill illusion. It presents a newly developed thermal grill haptic interface that exploits juxtaposed warm and cool areas to render surprisingly intense thermal sensations. The results revealed perceived intensity to increase, and response time to decrease, monotonically with temperature differences. An augmented reality demonstration highlights potential applications of this technique haptic design and engineering. This research contributes to knowledge about thermal perception and suggests new design approaches for thermal interfaces.

Contents

Chapter 1

Introduction

Touch is the most fundamental interaction with the world. In daily life, we physically perceive our surroundings and use tools to live. For example, when we can grasp a cup and drink water in the cup, we adjust the force of holding the cup based on the touch sensation and move our limb based on the proprioception, which is kinetic information to let us perceive location, movement, and action of the body from muscle joint. Based on the input from the touch sensation, we can drink water without dropping the cup and spilling water. In the same context, we also can sense if the touching piece of fabric is smooth or rough, even if we do not rely on the visual cue. The ability to perceive and identify the properties of the object using the sense of touch is often referred to as haptics or haptic sensing [1]. The word haptics is derived from the Greek word hapkitos which means "able to grasp or perceive."

With multisensory information including touch, vision, and auditory sense, we can sense the world better. The visual and auditory display has been developed to provide real vision and sound. The development of Virtual reality (VR) and augmented reality (AR), and mixed reality (MR) is one of the real displays to interact or access information in an immersive way. Comparing these research achievements of vision, and auditory display, haptic technology has not progressed to provide real touch sensation in free-hand interaction which is touch interaction in the daily life of humans. As previously mentioned, we use touch information to identify the object property and manipulate it intuitively. However, the loss of touch sensation with free-hand interaction is a lack of real, immersive, and intuitive interaction in VR and MR.

The development of haptic technology presents a significant challenge due to the skin's ability to sense various sub-modalities, including vibration, pressure, temperature, and pain. Additionally, the brain integrates touch information temporally and spatially to perceive touch sensation. As a result, the perception of touch sensation can easily be influenced by the properties of touch stimuli and the conditions of body movement or touch interaction. This complexity makes it challenging to design tactile displays that can provide a real touch sensation during natural touch interactions. Therefore, it is essential to design tactile devices that allow for free-hand interaction and to clarify the characterization of touch responses in these sub-modalities to enable haptic augmentation of touch interaction. Achieving this engineering goal would enhance the quality of feedback from tactile displays, enable users to interact freely with virtual objects using their hands, and enhance immersive experiences in VR, AR, and MR.

This PhD dissertation contributes knowledge in several areas toward the overarching goal of designing and engineering technologies for haptically augmenting surfaces, objects, environments, or interactions. Haptics research is necessarily very multi-disciplinary because it involves aspects of engineering, mechanics, and perception. Thus, this research uses methods drawn from engineering, psychophysics, and other areas.

Following this introduction, and a survey of related research (Chapter 2), the dissertation introduces a new technique and wearable system, called Tactile Echoes, for haptically augmenting touch interactions in physical environments, for augmented and virtual reality and human-computer interaction (Chapter 3). This chapter presents methods for designing such interactions and presents findings from perception studies that characterized how Tactile Echoes are perceived, and how the experiences they provide are described by users. A further observation from the research of Chapter 3 was that the feedback supplied in Tactile Echoes felt stronger when it was delivered after a brief time delay. This motivated the research presented in Chapter 4, which describes scientific investigations of the effect of time delay on the perception of tactile feedback, particularly tactile forward masking in active touch. The findings from Chapter 4 characterize how the perceptual intensity of tactile feedback is increased as the latency with which tactile feedback is provided is increased. Chapter 5 describes an exploration of a further method for augmenting touch interactions with surfaces, using feedback supplied not only to the finger but also via the touched surface. This system exploits vibrations supplied to a finger and a surface to augment surfaces with spatial vibration patterns formed by beat frequency interference. Chapter 6 departs from the previous methods of tactile augmentation in investigating methods for augmenting surfaces with thermal sensations, using the thermal grill illusion. It presents a new thermal grill display device and findings from experiments characterizing how perception varies with the temperature differences in the thermal grill.

1.1 Overview

This PhD dissertation consists of several chapters presenting key investigations that comprise this research (Fig. 1.1). Following this introduction, Chapter 2 describes the background knowledge of human haptics. This includes the mechanical receptors, perceptual sensing mechanisms, characterization of perception in vibration, and thermal sensation. It also introduces haptic technologies such as wearable tactile displays and thermal displays. As a foundational concept of tactile augmented reality, the Tangible

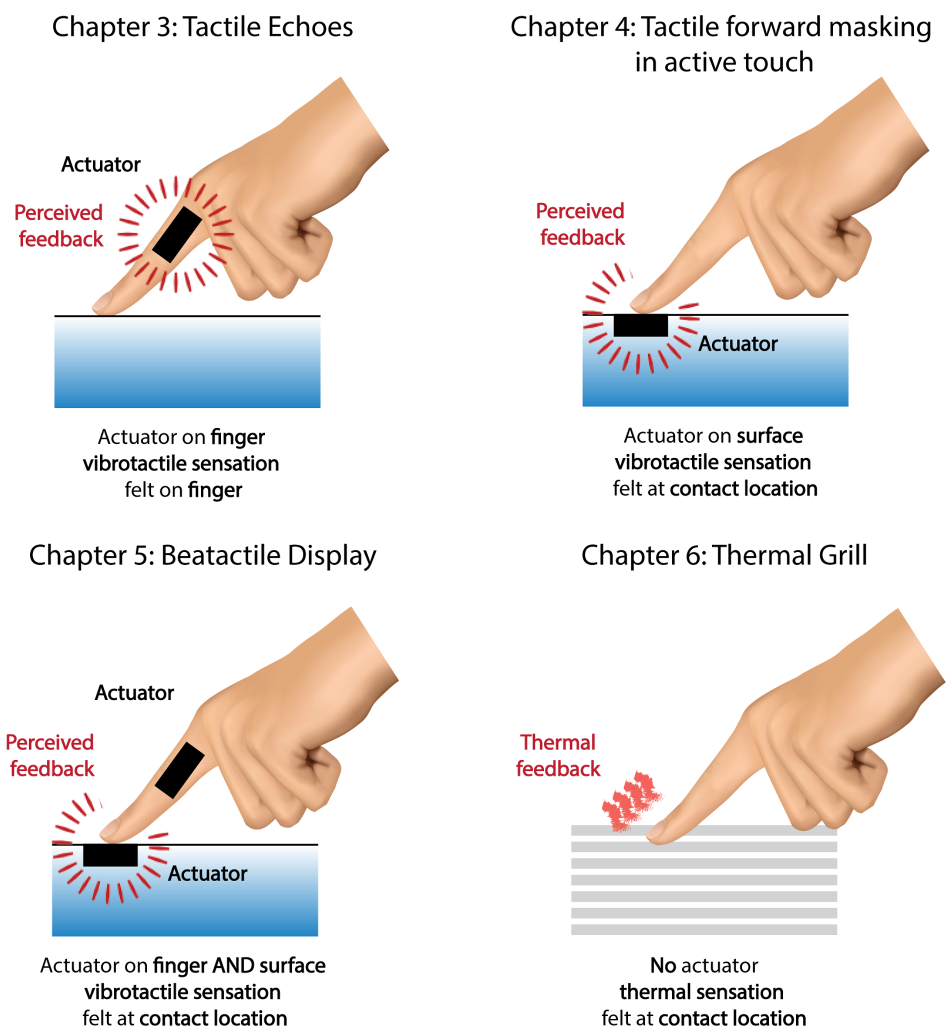

Figure 1.1: This figure shows the different approaches to tactile augmentation of surfaces presented in this dissertation.

User Interface (TUI) application and rendering methods used to modify touch sensations on tangible surfaces are discussed.

Free-hand interaction is a natural method we use daily to identify and manipulate objects in our surroundings. However, due to their design, most haptic interfaces inhibit this free-hand interaction, providing non-responsive tactile sensations based on touch interactions. Prompted by this constraint, in Chapter 3, we developed a wearable tactile device named “Tactile Echoes”, which facilitates free-hand interaction in VR and AR applications, as reported in our publication [2]. Tactile Echoes employs a unique tactile rendering method that leverages audio processing techniques, such as delay, frequency modification, and amplification. Additionally, we incorporated Tactile Augmented Reality, which maps tactile sensations onto physical objects. Following a series of perceptual experiments, we found that the tactile feedback from Tactile Echoes can be described using 12 descriptors, including terms such as “hard”, “shallow”, and “echoing”. The stimuli generated from 35 Tactile Echoes settings were plotted within perceptual 2D and 3D spaces. We further conducted a user study, which involved using Tactile Echoes in a gaming context. The study results indicated that Tactile Echoes offers responsive, engaging interactions and enhances the users’ sense of agency when interacting with buttons that provide tactile feedback from the device.

The following chapter of this dissertation presents an investigation of tactile forward masking in active touch. When employing Tactile Echoes, we observed a fascinating phenomenon: tactile feedback provided a short delay after touch is more challenging to perceive than when a longer delay is given. We hypothesized that this can be attributed to tactile forward masking, wherein touch-elicited vibration acts as a masker to reduce the perception of tactile feedback provided after the touch. In Chapter 4, we sought to understand how the perceptual intensity of tactile feedback is affected by the latency with which vibration feedback in response to touch is supplied. To this end, we conducted a series of perceptual experiments. Our findings revealed that each 15 ms of delay yielded an increase of about 2 dB in perceived intensity. Furthermore, we hypothesized that, in line with previous tactile masking studies, the degree of similarity between the masking stimulus and test stimulus impacted the extent of masking. To clarify this, we conducted additional perceptual experiments. The results confirmed our hypothesis: in active touch-induced tactile forward masking, feedback that was more similar to the masker (a touch-elicited vibration) produced more masking.

Utilizing two vibrations, it is able to generate interfering vibrations in the finger. Here, in Chapter 5, we describe a novel method for synergistically integrating vibrotactile feedback provided via a wearable device on the finger with feedback from a touch screen device. One actuator is placed on the surface that the user touch and another is attached to the finger phalanx. As a result of the measurement, the beat frequency is captured from the piezo sensor on the fingertip. In the demonstration, the user reported that a bumpy surface can be felt from the surface during stroking with this BeaTactile system.

The thermal grill illusion is one of the tactile illusions to provide a burning sensation without pain. Taking account of VR use or medical check application, in Chapter 6, we conducted a perceptual study to characterize response time and perceptual intensity of burning sensation in each combination of cold and warm temperature settings of the aluminum bar in the thermal grill. As a result, the large temperature difference between the warm and cold aluminum bar in the thermal grill provides the most intensive burning sensation and makes the response of the participant quickly.

Finally, Chapter 7 summarizes the achievement of research in this PhD and its findings, and presents future research direction or application of this work.

1.2 Contributions

The research makes significant contributions to haptic science and technologies, with applications in augmented reality. The key contributions are summarized as follows:

1. This research presents a novel approach to haptically augmenting free-hand interactions with physical objects, within a tactile augmented reality paradigm, and the design of a wearable tactile display for user-free-hand interaction. This work is detailed in Chapter 3 and published in IEEE Transactions on Haptics (publication [2]).

2. The PhD investigates how users perceive tactile sensations generated through touch interaction with Tactile Echoes, a device for haptic feedback. The findings of this investigation have significant implications for the development of wearable tactile systems in virtual reality. The research suggests that responsive and engaging tactile feedback can enhance user experience and usability, leading to an immersive experience. This published paper was nominated for an honorable mention in IEEE Transactions on Haptics Best Application Paper 2021.

3. Chapter 4 of this PhD presents new insights into the perceptual characterization of tactile forward masking in active touch. This study investigates how touch-elicited vibrations can mask tactile sensations felt after touch contact. This work is currently being prepared for submission to the journal Scientific Reports.

4. The research of Chapter 4 also highlights the surprising finding that increasing the latency of tactile feedback increases perceptual intensity. These findings have significant implications for the design of haptic and tactile displays.

5. Chapter 5 of this PhD also presents a new method for rendering coarsely textured,

bumpy surfaces via beat frequencies generated within the finger (Chapter 5). This method has the potential to inform the design of new forms of haptic feedback.

6. Chapter 6 of this PhD presents a new study of the thermal grill illusion. It characterizes the perceptual intensity of thermal sensations produced via this feedback technique.

7. The findings presented in Chapter 6 also show that thermal grill stimuli, which are non-harmful, can elicit surprisingly rapid sensations and behavioral responses, in contrast to many thermal feedback techniques that yield slower responses. These findings have significant implications for the creation of thermal haptic devices for augmented reality or human-computer interaction.

Chapter 2

Background

This chapter serves as a broad overview of the background literature and prior knowledge that frames the research presented in this PhD dissertation. Further detailed background literature associated with each research project is included in the introductory sections of Chapters 3 through 6.

Haptics is an interdisciplinary field that delves into the sense of touch from the perspectives of science, engineering, and psychology. The goal of haptics is to understand the mechanisms underpinning touch and to develop engineering methods for delivering touch feedback in human-computer interactions. This includes examining how humans perceive tactile information through touch interactions and designing and constructing devices and software methods capable of providing evocative touch experiences. Over the past few decades, considerable efforts have been devoted to understanding perception mechanisms, the anatomy and physiology of touch, and the development of technologies that provide evocative touch experiences or feedback.

A significant engineering challenge in haptics is designing devices or methods that provide a sense of touch without restricting hand movement or interfering with free-hand interaction. Existing haptic technologies often inhibit free-hand interaction and direct touch due to their hardware configuration and the method used to provide touch feedback. A gap remains between the interaction with existing tactile devices and natural touch interaction in daily life.

Recent advancements in visual and audio displays have spurred rapid technological progress in virtual reality (VR), augmented reality (AR), and mixed reality (MR). In VR technology, users can fully immerse themselves in a virtual world displayed via a head-mounted display (HMD) and interact with virtual objects. AR and MR technologies overlay visual information onto the real world to aid or guide awareness and access to digital information. These technologies find applications in gaming, education, fabrication, and rehabilitation [3]. Nevertheless, there is scope for enhancing the provision of touch sensation and usability to further enrich applications or interactions. The field of human-computer interaction (HCI) research aims to understand how humans can naturally utilize digital information, considering factors such as design, perception, and human behavior. The concept of a Tangible User Interface (TUI) in HCI originates from the idea of natural interaction with digital information, such as directly touching and grasping objects like everyday tools. In VR and MR technologies, the concept of TUI has been integrated into applications. TUI research in VR has demonstrated that direct natural interaction improves usability, enabling users to use digital applications more intuitively. In these immersive worlds, like VR and AR, the potential of directly touching and manipulating objects in a natural way with tactile sensation has been explored.

In the realm of haptic research, understanding the biomechanics of the human body, the psychophysics of touch, and the techniques of natural touch interaction using TUI methods in HCI is crucial. The research presented in this thesis focuses on vibrotactile perception, interface research using free-hand interaction with physical objects, and rendering methods with vibrotactile devices for haptic augmentation.

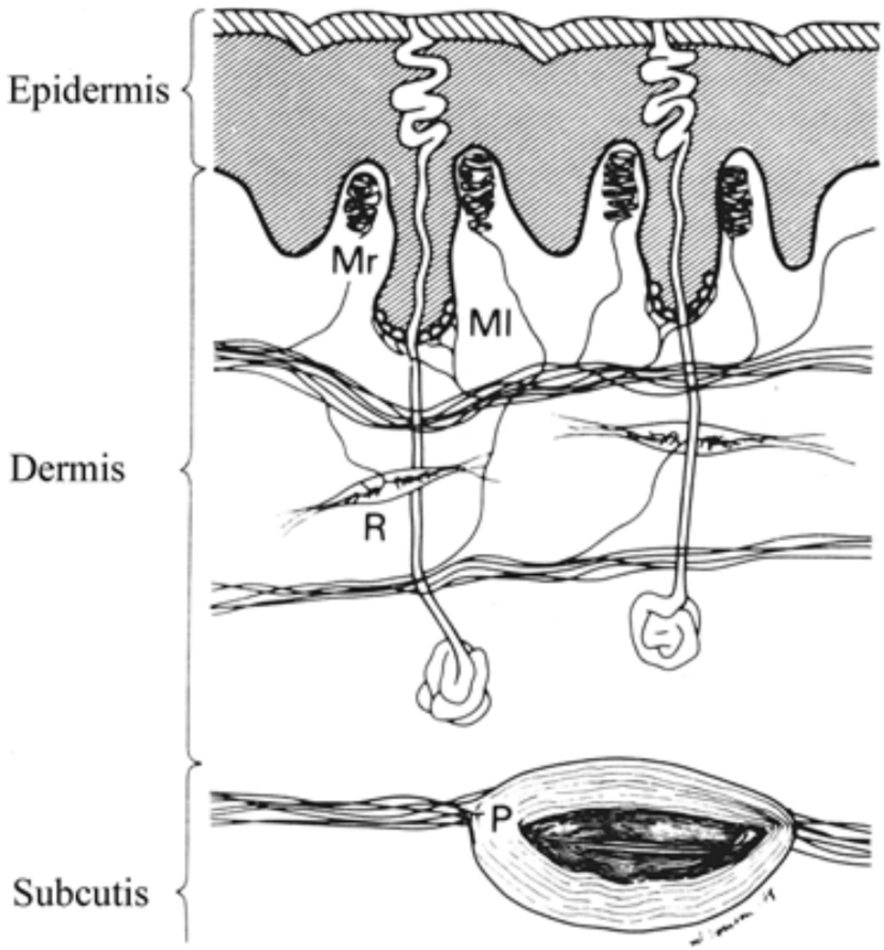

Figure 2.1: The grabrous skin is palm of hands and finger in body of human. There are four mechano-receptors in grabrous skin. Mr, Meussner corpuscle; P, Pacinian corpuscle; MI, Merkel disk receptor; R, Ruffini endings. This figure is reffered from [4]. ©2009, Psychonomic Society, Inc.

2.1 Human haptics

The skin, the largest and heaviest sensory organ in the human body, primarily serves four senses: touch, temperature, pain, and itch [1]. These senses provide essential information about touch properties, such as allowing us to turn on the light in a dark room or judge the proper temperature of shower water based on its temperature.

Human skin is divided into two types: glabrous skin and hairy skin. Glabrous skin covers the palmar surface of the hands and feet, while hairless skin, different from glabrous skin due to its lack of sweat glands and mucosal surface, covers the lips and genitalia. The distribution of touch receptors varies based on whether the skin is glabrous or hairy. As illustrated in Fig. 2.1, glabrous skin houses four types of touch receptors: Meissner corpuscle (RA1), Pacinian corpuscle (RA2), Merkel disk receptor (SA1), and Ruffini ending (SA2). Each receptor possesses a unique structure and sensing property, including the rate of adaptation and receptive field, the latter referring to the area responsive to stimuli. Receptive fields are classified into two types: type I, small (2-8 mm in diameter), and type II, larger (10-100 mm in diameter).

In terms of adaptation property, Meissner corpuscles and Pacinian corpuscles are classified as rapid-adapting receptors. Fig. 2.2(c) illustrates the neural spike activity when pressure is applied to a finger. The stimulus plot shows pressure being gradually applied, maintained constant, and then immediately released. During rapid adaptation, Meissner corpuscles and Pacinian corpuscles predominantly evoke neural spikes at the beginning and end of the stimulus. These rapid-adapting receptors react when the skin is actively indented by a stimulus but do not respond when the skin displacement ceases. Consequently, these receptors are crucial for sensing minor skin movements, such as tapping or grabbing objects. Meissner corpuscles and Pacinian corpuscles have different receptive field sizes, with Meissner corpuscles (type I) being smaller than Pacinian corpuscles (type II), as shown in Fig. 2.2.

Merkel cells and Ruffini endings are slow-adapting receptors, evoking responses even when the stimulus is continuously applied, often at the beginning and end of the stimulus (Fig. 2.2). These slow-adapting receptors respond when the skin is both stationary and moving. They are essential for perceiving the shape and direction of a finger moving along an object. Merkel cells are type I, and Ruffini endings are type II.

These mechanoreceptors react to vibrations applied to the skin, with a frequency range of 0 to 1000 Hz. Meissner corpuscles respond to a frequency range of 1 to 300 Hz, Pacinian corpuscles to 5 to 1000 Hz, and Merkel cells to 0 to 100 Hz. The optimal responsive frequencies for Meissner, Pacinian, and Merkel cells are 50, 200, and 5 Hz, respectively.

Sensory afferent fibers innervating the hand transmit tactile and other somatosensory information, such as muscle and joint movement, to the central nervous system. Two ascending pathways convey somatosensory information from the limbs and trunk: the dorsal column-medial lemniscal system (represented by the orange-colored pathway in Fig. 2.3) and the anterolateral system (represented by the brown-colored pathway in Fig. 2.3). These two pathways transmit different types of sensory modalities. The dorsal column transmits touch and limb proprioception signals to the spinal cord and brain stem through large-diameter myelinated nerve fibers and then to the thalamus. Tactile and proprioceptive information is sent to the primary somatosensory cortex. In the anterolateral system, pain, itch, temperature, and visceral sensation information is conveyed to the spinal cord by small-diameter myelinated and unmyelinated fibers, with the destination being the ipsilateral dorsal horn. This information is transmitted across the midline by neurons within the spinal cord to the brainstem and thalamus in the contralateral anterolateral system.

2.1.1 Vibrotactile Perception

When vibrotactile feedback is applied to the finger, each type of mechanoreceptor responds to a specific frequency range (Fig. 2.19B) [7]. SA1 fibers are the most sensitive population below 5 Hz, RA1 fibers are sensitive between 10 and 50 Hz, while RA2 fibers respond in the range of 50 to 400 Hz. The perceptual threshold differs based on the frequency of the vibrotactile signal. As seen in Fig. 2.19A, the perceptual threshold

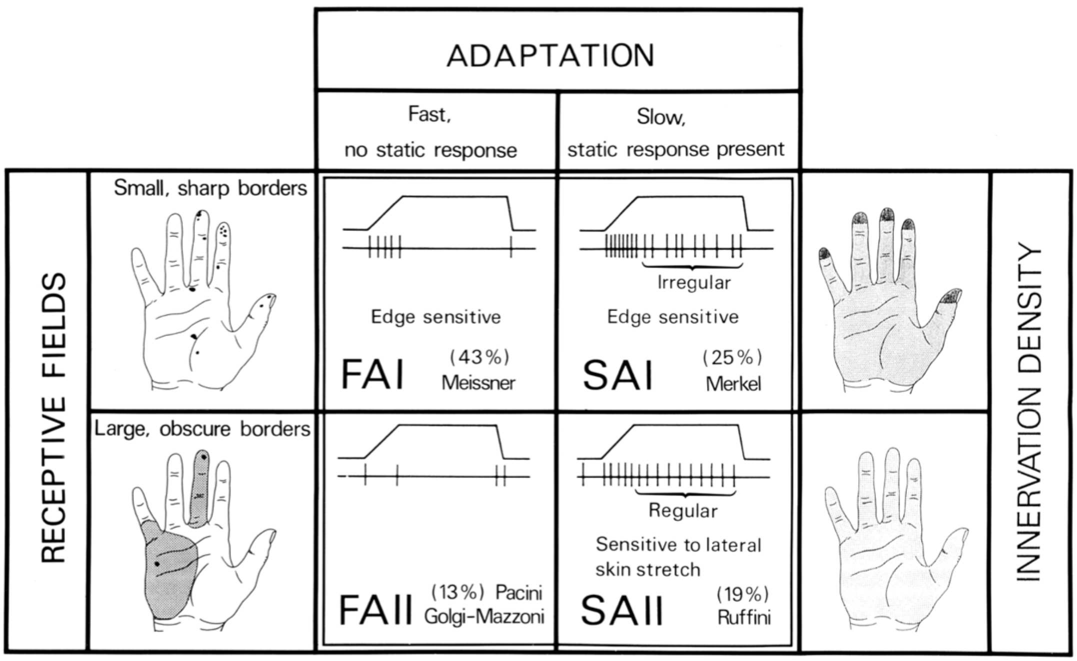

Figure 2.2: Four types of mechanoreceptors are classified according to their unique structures, receptive field sizes, and rates of adaptation. Pacinian corpuscles and Ruffini endings have larger receptive fields, while Meissner corpuscles and Merkel cells have smaller receptive fields. This figure is cited from [5].

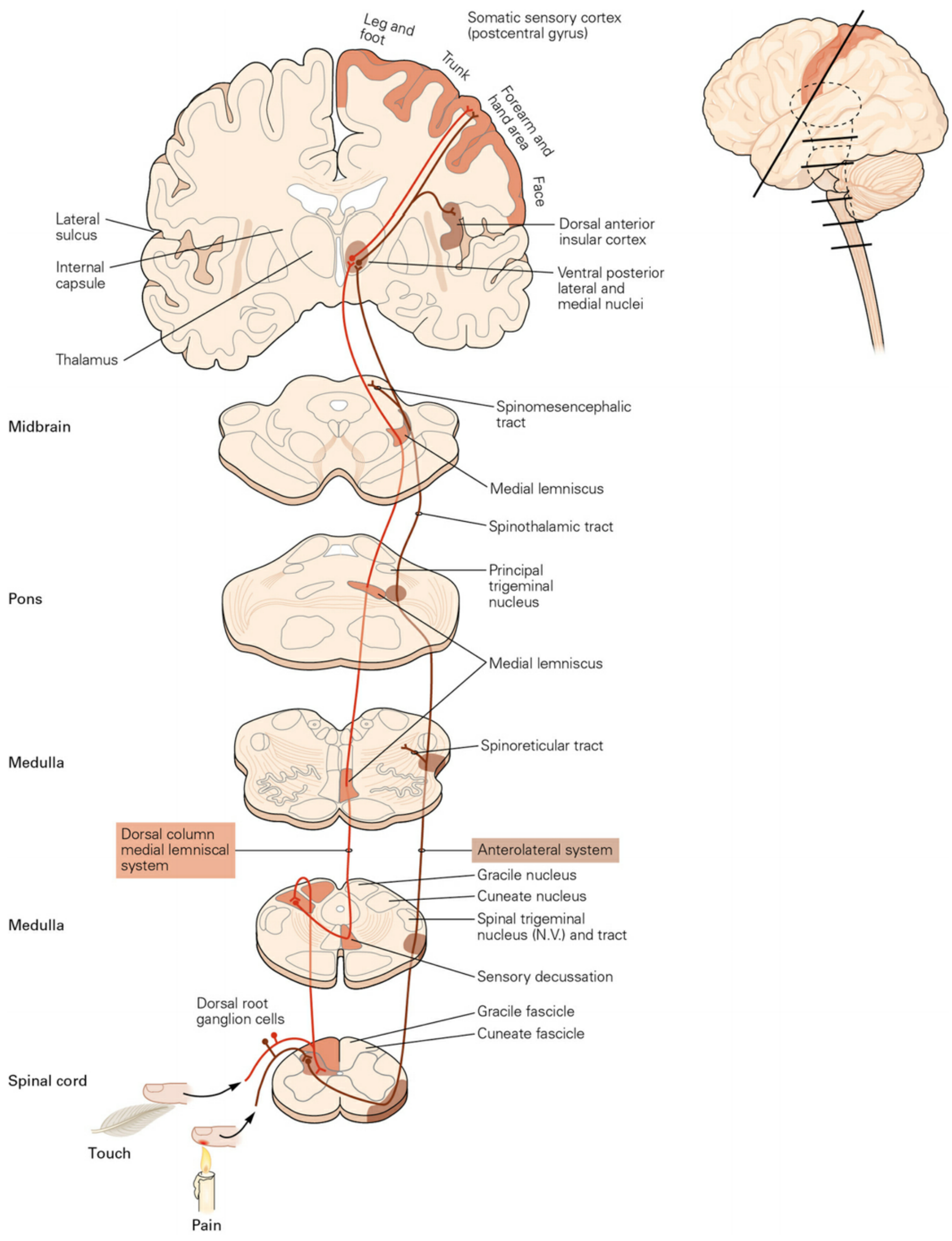

Figure 2.3: There are two neural pathways for conveying somatosensory information from the limbs and trunk to the thalamus and central cortex. The dorsal column (represented by the orange-colored pathway) transmits touch and proprioception signals to the spinal cord and brainstem. In contrast, the anterolateral system conveys pain, itch, temperature, and visceral information to the brainstem and thalamus. This figure is cited from [6]. ©2020 McGraw-Hill Education.

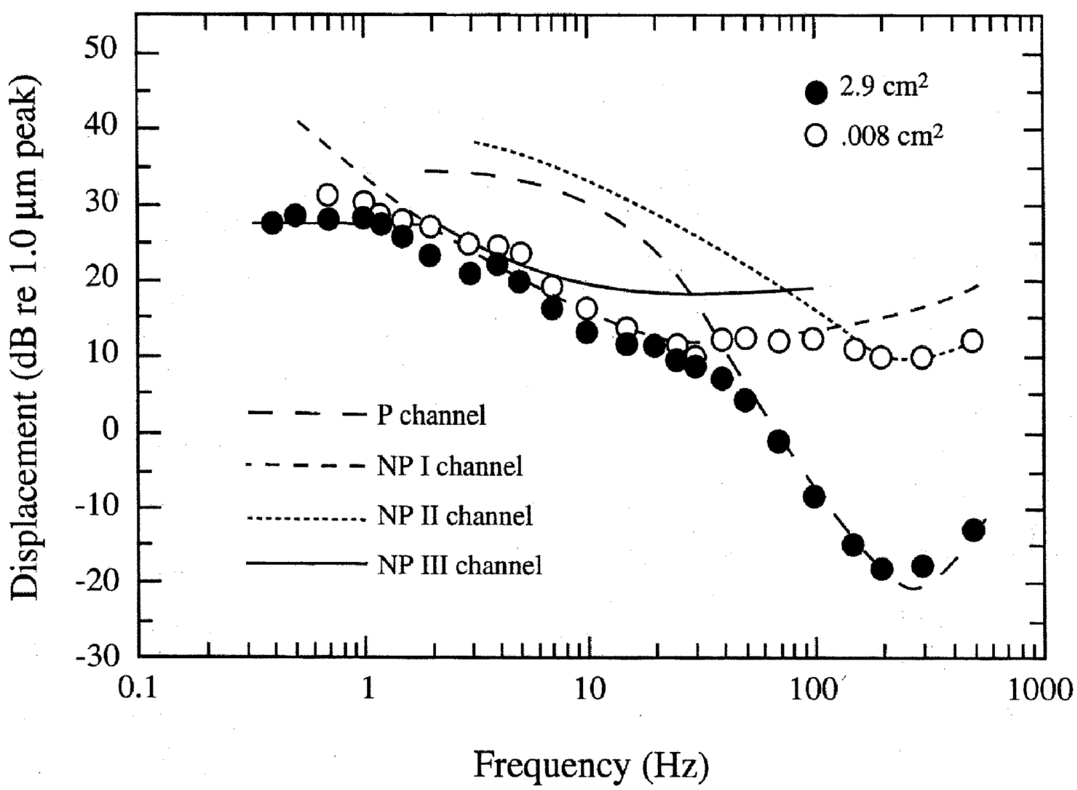

Figure 2.4: The threshold of detection varies across the frequency range. Humans are most sensitive to vibrations around 200-250 Hz. Each mechanoreceptor is activated within a specific frequency range of vibration. This figure is cited from [8]. The image reproduced with permission.

for detection is the lowest for a sinusoidal signal of the vibration around 200-250 Hz. This means that humans can detect the smallest amplitude vibration in the 200-250 Hz range. Numerous factors influence this threshold. In addition to frequency, the perceptual threshold for vibration detection can differ based on the vibrator's contact area, the probe size, contact force, anatomical location, skin's mechanical properties, temperature, gender, and age.

When multiple vibrotactile stimuli are presented sequentially, the sensitivity to such stimuli also changes. Specifically, when two vibrotactile stimuli are applied to the skin, the perceptual threshold for vibrotactile detection is higher than when a single vibrotactile stimulus is presented. This indicates that humans are less sensitive when two tactile stimuli are applied to the skin simultaneously, a phenomenon known as tactile masking. The effect of tactile masking depends on the order of vibrotactile stimuli, the duration of the signal, the interval between stimuli, the frequency and amplitude combination of two stimuli, and the distance between the locations where the vibrotactile stimuli are applied. This phenomenon is described in more detail in Section 4.2.

Body movement reduces sensitivity to vibrotactile stimuli, a mechanism termed tactile suppression. Similar to tactile masking, tactile suppression occurs when body movement generates proprioception information that shares the same neural path as vibrotactile stimuli. The temporal integration of proprioception and vibrotactile stimuli results in reduced sensitivity to vibrotactile feedback.

The sensitivity to vibration varies based on frequency. The human hand is most sensitive to vibrations of 200-250 Hz (Fig. 2.19A). This suggests that it is easier to perceive a low-intensity 250 Hz vibration than vibrations at other frequencies. According to the neural thresholds, Pacinian corpuscles respond most to vibrations around 200-250 Hz. Sensitivity to vibration is also influenced by the size of the vibrator (actuator) producing the vibration. As demonstrated by [9], Verrillo et al. measured the absolute threshold for six different sizes of vibrators and seven frequencies on the thenar eminence of glabrous skin. They found that when the contact area of the vibrator was doubled, participants perceived the vibration as 1.5 dB more intense. However, at lower frequencies (under 40 Hz), the intensity of the vibration was unaffected by the size of the contact area of the vibrator.

When additional stimuli are applied before, during, or after the vibration, the sensitivity to the vibration is affected by these additional stimuli. Tactile masking is a phenomenon where the sensitivity of a vibrotactile stimulus changes when another vibrotactile stimulus is applied before, during, or after it [10]. The type of tactile masking is categorized based on the order of the two stimuli. In tactile forward masking, the first vibrotactile stimulus acts as a mask to the perception of the second (test) stimulus. Conversely, in backward masking, the masking vibrotactile stimulus comes after the test stimulus. Other masking techniques include simultaneous (masking stimulus and test stimulus start and end at the same time), pedestal (test stimulus is applied during the masking stimulus), sandwich (test stimulus is sandwiched between two masking stimuli), and common-onset masking (masking and test stimulus start simultaneously, but the test stimulus ends earlier) [11]. Tactile masking is described in more detail in Chapter 4.

2.1.2 Thermal Perception

Changes in skin temperature are detected by two types of receptors: cold and warm thermoreceptors. These receptors are found in the free nerve endings in the epidermis (Fig. 2.1). Warm thermoreceptors are located 0.3 to 0.6 mm beneath the surface of the epidermis, while cold thermoreceptors are situated 0.15 to 0.17 mm below the surface. The distribution of thermoreceptors varies depending on the body part, but typically, there are more cold thermoreceptors than warm thermoreceptors in a given region [12]. A study on afferent nerve transmission found that the transmission speed in cold receptors, which is between 5 and 30 m/s, is faster than that in warm receptors, which is between 0.5 and 2 m/s [13].

Figure 2.5 displays the frequency of impulses generated in response to thermal stimuli. Warm fibers respond to a temperature range of 30 to 50 °C, with the most frequent response occurring around 45 °C. Cold fibers respond to temperatures spanning from 5 to 43 °C, with the most frequent response observed between 22 and 28 °C [12, 15]. Within the skin temperature range of 30 to 36 °C, neither coldness nor warmth is perceived, and both warm and cold fibers evoke nerve spikes at a low rate. If the skin temperature shifts above 45 °C or below 15 °C, conditions potentially harmful to the skin, nociceptors

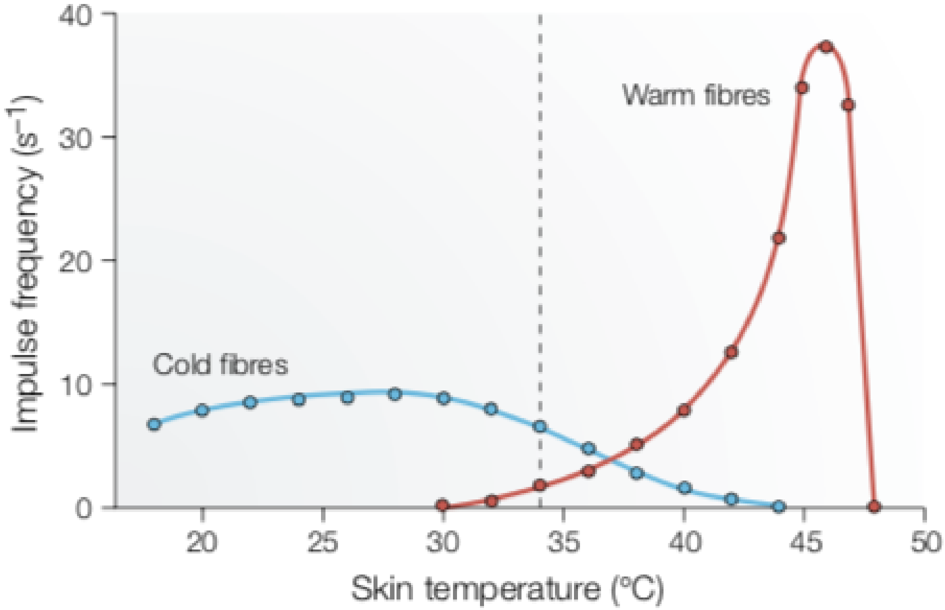

Figure 2.5: The average discharge frequency of individual cold and warm sensitive fibers responds to changes in skin temperature. Cold fibers are most active in the range of 22 to 28 °C, while warm fibers are most active around 45 °C. This figure is referenced from [14]. ©1969, Springer Nature Limited

respond to these stimuli and individuals perceive a sensation of pain.

Temperature stimuli are converted into signals for transmission via temperature-activated transient receptor potential (thermo TRP) channels. TRP channels are composed of six putative transmembrane segments and cytoplasmic amino and carboxyl termini [14]. Figure 2.6 shows the response characteristics of TRPs to temperatures. TRPV 1, 2, 3, and 4 are activated by heating stimuli. TRPV 1 and 2 respond to hot stimuli that cause a painful sensation, while TRPV 3 and 4 respond to warm stimuli that do not cause a painful sensation. TRPA1 (Anktm1) and TRPM8 respond to cold sensations. Anktm1 is activated by cold temperatures that cause a painful sensation, while TRPM8 responds to cold temperatures that do not induce pain. Interestingly, TRPM8 also responds to menthol, which is present in mints, and TRPV1 reacts to capsaicin, the hot ingredient in chili pepper. These responses to menthol and capsaicin serve as

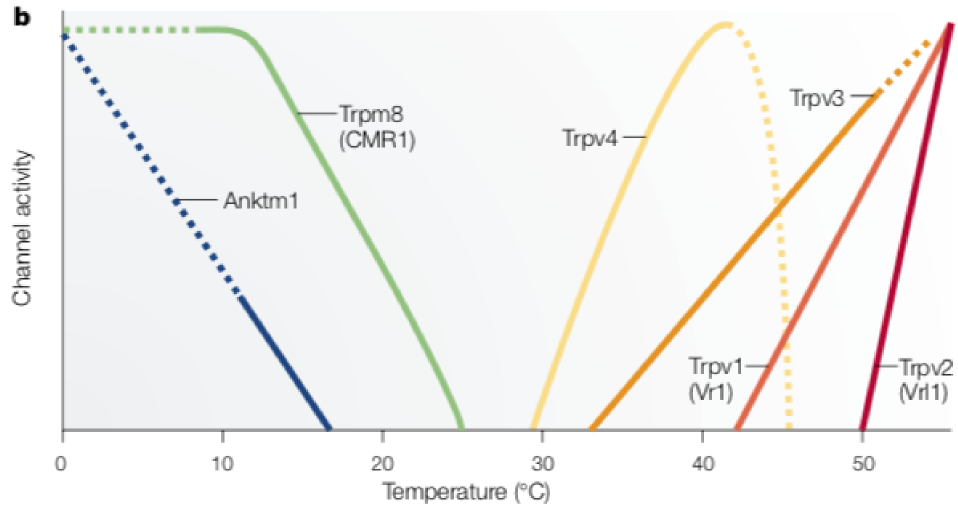

Figure 2.6: Six temperature-activated Transient Receptor Potential (thermo TRP) channels are activated, each corresponding to a specific range of temperature stimuli. Thermo TRPs are ion channels that convert thermal stimuli into signals for transmission to the brain. This figure is referred to from [14]. ©1969, Springer Nature Limited.

non-thermal activators.

The sensitivity to temperature varies across different body parts. Figure 2.7 illustrates the temperature thresholds for each body part, with the temperature threshold being the minimal difference in temperature required for an individual to discern between two temperature stimuli. For instance, when two thermal stimuli are applied to the finger, individuals aged between 18 and 28 can discern a temperature difference of approximately 0.0218°C under warm conditions. The lip, having the lowest temperature threshold for both warm and cold temperatures, is the most sensitive to disparities in temperature stimuli. In contrast, limbs display a lesser sensitivity to temperature differences. With skin temperature at 33°C, the threshold for discerning temperature differences is 0.20°C for warm sensations and 0.11°C for cold sensations. In comparison, the fingertip has a temperature threshold of 0.55°C for warm sensations and 0.3°C for cold sensations. As shown in Figure 2.7, sensitivity to temperature alters with age, with older individuals exhibiting a reduced sensitivity to temperature differences. For all body parts, there is

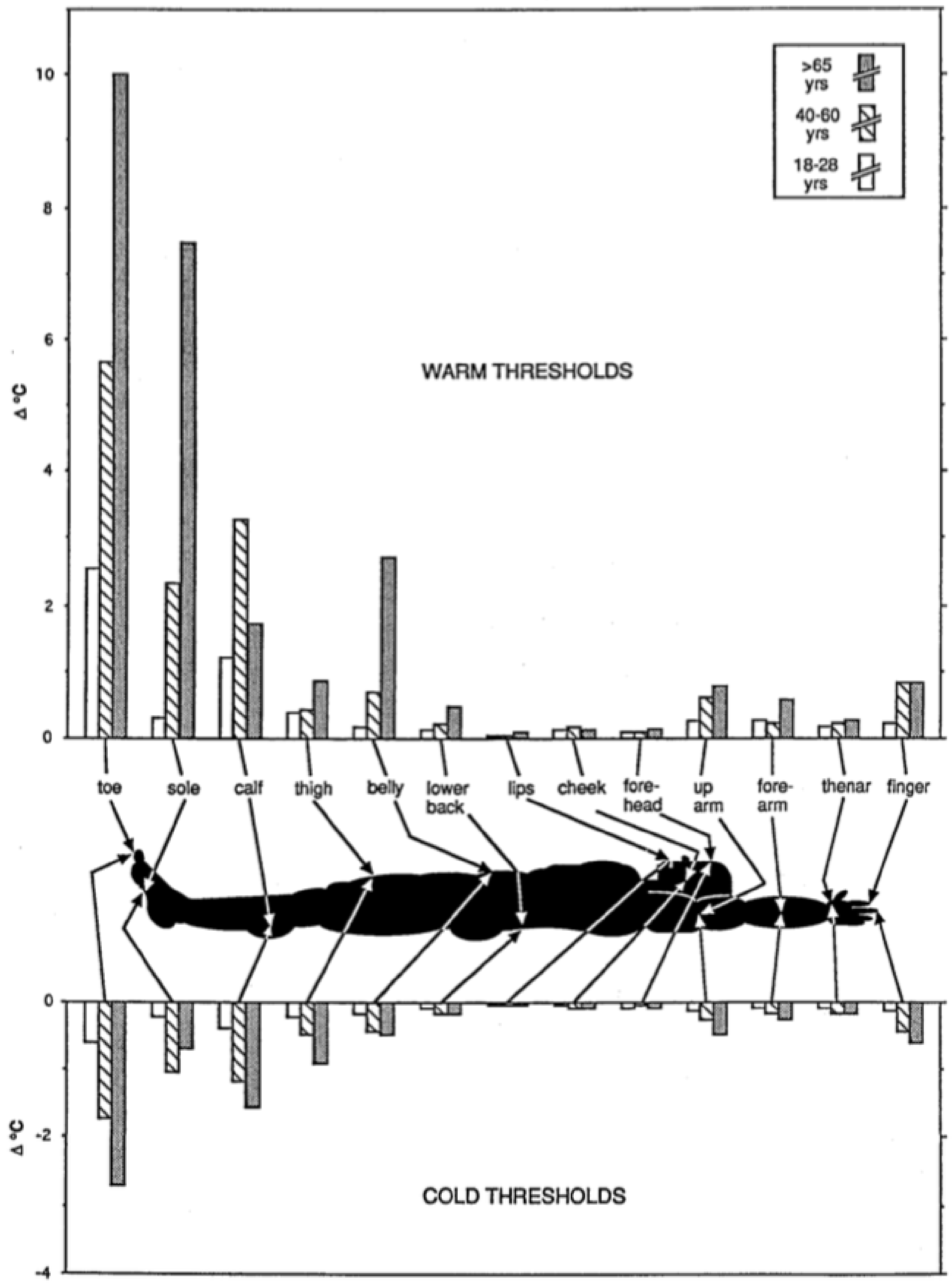

Figure 2.7: The body map of warm and cold sensitivity varies by age. The lips are the most sensitive area for perceiving differences between two thermal stimuli in both warm and cold categories, while limbs are the least sensitive to detecting these differences. Humans are generally more sensitive to cold stimuli than to warm stimuli. Thermal sensitivity tends to decrease with age. This figure is adapted from [16]. This Image reproduced with permission.

a higher sensitivity to warm stimuli as compared to cold stimuli [16].

Psychological experiments reveal that thermal sensations can influence emotions and social behavior by eliciting feelings of comfort or discomfort. For instance, in a study exploring human impressions, participants who held a hot coffee cup during an elevator ride evaluated an unknown co-rider as significantly warmer (more humane, trustworthy, and friendly) than those who evaluated the same individual while holding an iced coffee. This brief experiment illustrates that physical warmth experienced on the skin of the hand can foster interpersonal warmth [17]. Environmental warmth encourages people to evaluate others more positively and promotes the establishment of closer social relationships [18]. These observations regarding how physical warmth can influence social behavior stem from physical experiences such as childhood hugs, which can evoke feelings of affection [19].

2.2 Haptic Technologies

This dissertation provides a detailed exploration of methodologies for designing haptic displays that facilitate interaction in Virtual Reality (VR) and Augmented Reality (AR). These designs are covered in Chapters 3, 4, 5, and 6. The displays in question offer surface sensations by means of vibrotactile feedback, a topic that is discussed extensively in Chapters 3, 4, and 5. Additionally, the concept of thermal sensation, another critical aspect of these displays, is discussed in Chapter 6.

2.2.1 Haptic device and haptic interaction

Numerous haptic devices have been developed over the past few decades. These devices can be categorized based on their designs, which largely include grounded devices, handheld devices, and wearable devices [20]. The distinctions are depicted in Fig. 2.8.

The nature of our interaction with the environment varies depending on the design of the haptic device.

- **Grounded Devices**: These haptic devices are not intended to be worn or affixed to the human body during operation. The design of grounded devices is unrestricted by size or shape considerations, as there's no need for them to be worn on the body. Therefore, a diverse range of haptic feedback methods can be incorporated into grounded devices, such as large and powerful actuators, pneumatic actuators, magnetic actuation, and ultrasound (See Fig. 2.9).

- **Handheld Devices**: These haptic devices can be comfortably held in the hand without the need for attaching straps. They are designed to be lightweight and offer larger workspaces, enabling more interaction compared to grounded devices. Handheld devices can deliver tactile feedback or kinetic feedback, both of which can be achieved by integrating actuators or using thin or small tactile feedback systems like electrodes (electrotactile displays) (See Fig. 2.10).

- **Wearable Devices**: These haptic devices can be affixed not just to the hand, but also to various other body parts. Haptic gloves and exoskeleton systems are amongst the most popular examples of wearable device designs. Wearable devices can be further subdivided into three categories: exoskeletons, finger-worn devices, and arm-worn devices [20] (See Fig. 2.11).

2.2.2 Vibrotactile displays

Vibrotactile displays, which deliver stimuli through vibration, have been developed for grounded, handheld, wearable, and finger-worn haptic devices. Eccentric Rotating Mass (ERM) motors are often utilized as actuation technology in finger-worn vibrotactile displays, with smaller ERM motors designed for wear on individual fingers.

Vibrotactile feedback is capable of conveying a diverse range of sensations to the human hand and various body parts. It allows devices to render textures and aid in human motion and communication activities. Such feedback can supply or adjust the perception of texture [33, 34, 35], roughness [35, 36], friction [35, 36], softness, and hardness [37]. Furthermore, vibrotactile feedback can signify direction and motion through the utilization of spatial and temporal vibrotactile illusions and human finger perception [38, 39, 40, 41, 42, 43].

Many vibrotactile displays have been implemented for interaction within virtual real-

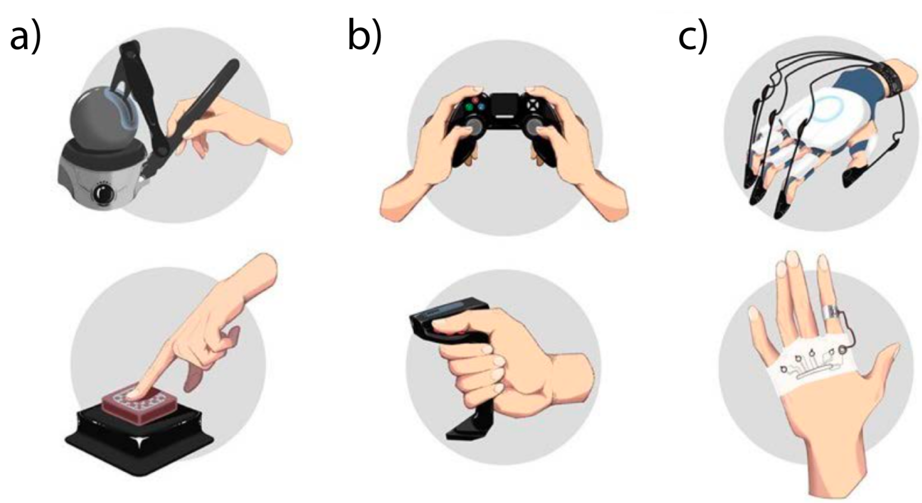

Figure 2.8: The graphic illustrates the classification of haptic devices according to structural differences. a) Grounded devices are those affixed to a table or similar surface. These devices cannot be worn or attached to a person's body. b) Handheld devices are those that can be picked up and held with the hand. c) Wearable haptic devices can be attached not only to the fingers but also to various other body parts. This figure is cited from [20]. This image reproduced with permission.

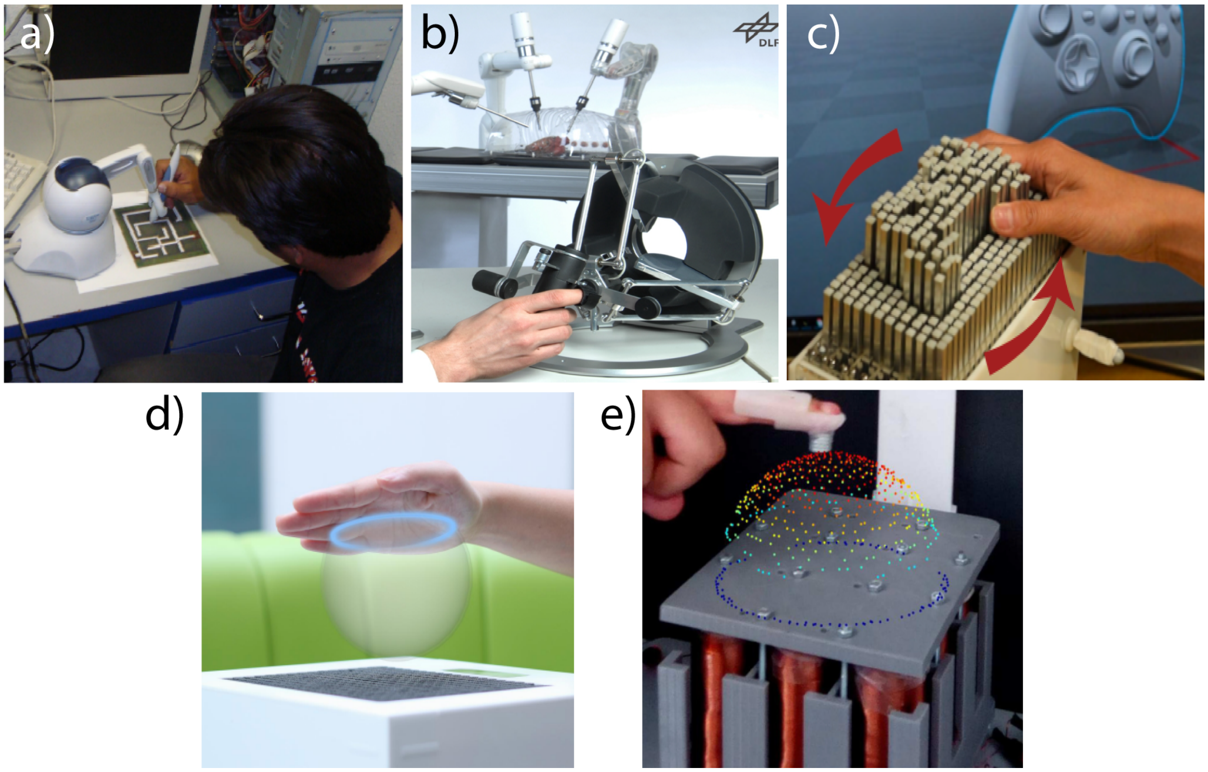

Figure 2.9: The grounded haptic device category encompasses a variety of design examples and methods for providing haptic feedback. a) Phantom, produced by Sensable Technologies, is a tabletop, graspable device designed for interaction in Virtual Reality and 2D applications [21]. ©2009 IEEE b) Omega is another tabletop haptic device featuring a kinetic structure. Users grasp the device's attached grip to interact with haptic feedback [22]. ©2013 IEEE c) ShapeShift is a tabletop shape display for haptic interaction. The device uses actuators to control the height of individual pins, creating a 2D shape. This device can be moved around on the tabletop to enable interaction [23]. d) Grounded mid-air ultrasound haptic displays leverage focused ultrasound to generate haptic shapes in mid-air [24]. e) The volumetric shape haptic display is an electromagnetic-based haptic interface. It arranges coils in an array to generate a magnetic field that provides haptic feedback to a magnet-attached finger. This volumetric shape display is used in virtual reality applications for interacting with 3D shapes [25]. ©2018 IEEE. The images of c) and d) reproduced with permission.

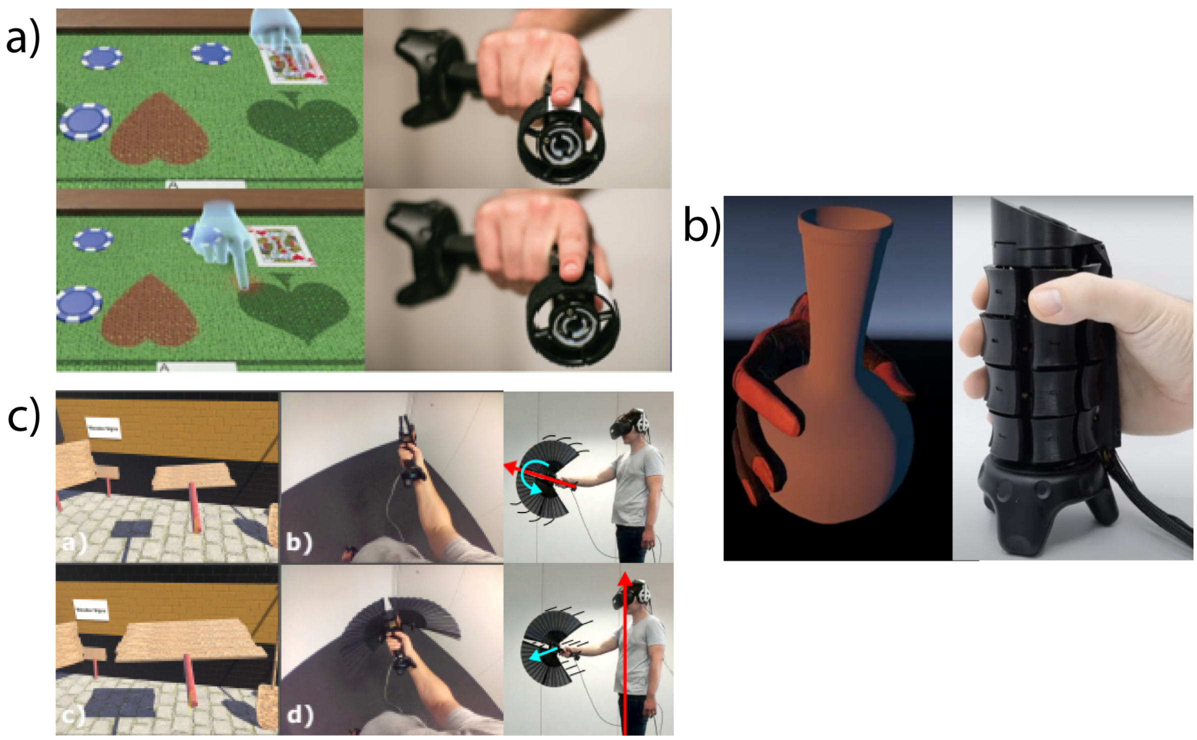

Figure 2.10: Handheld haptic devices are designed to be picked up and held by the user's hand, facilitating a range of haptic feedback properties. (a) The Haptic Revolver is a handheld VR controller designed to provide texture, shape, and touch sensations. A textured component is attached to the controller. As the user's finger glides over an object, this textured part rotates to provide a textured sensation [26]. (b) X-Rings is a handheld 3D shape display that offers grasping force. A modular stack of motor-driven expandable rings renders the shape of the surface. Users can perceive the 3D shape of an object in VR using their whole hand [27]. (c) Drag:on is a VR controller that provides drag and weight shift sensations. Users hold an expandable structure of rods, facilitating interaction with objects in VR [28]. These images reproduced with permission.

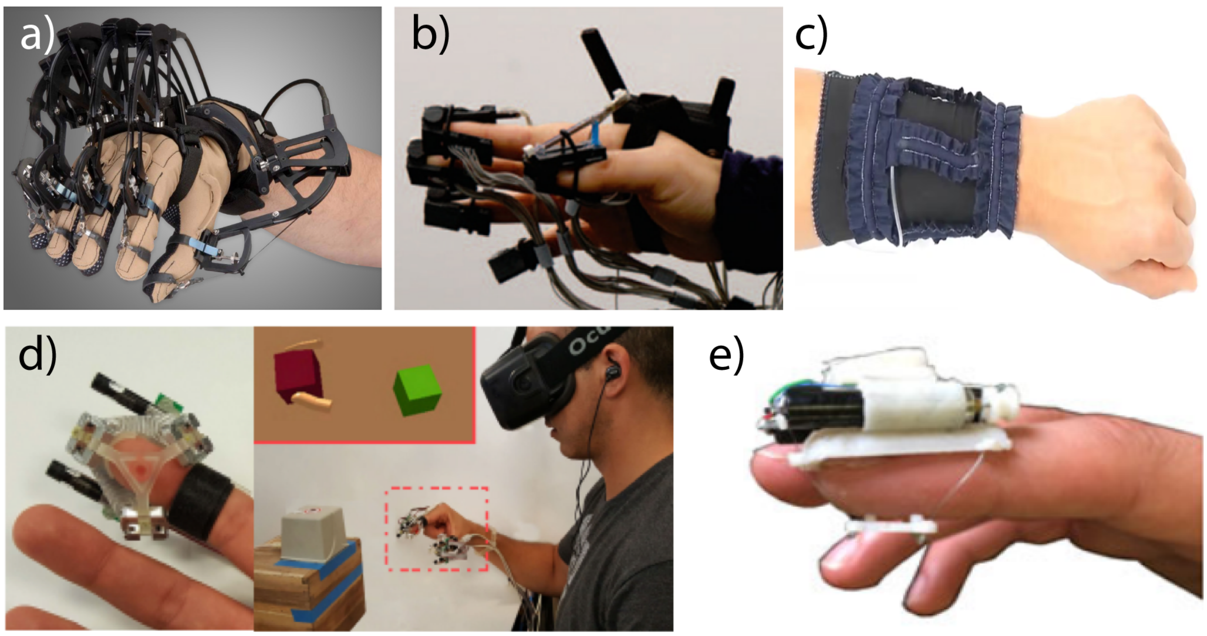

Figure 2.11: Wearable haptic devices can be attached to various parts of our body, including hands, fingers, and arms. (a) CyberGrasp features an exoskeleton structure that delivers force feedback to the user [29]. (b) A lightweight electrotactile feedback device uses haptic feedback to enhance grasp interactions in a virtual environment [30]. (c) PneuSleeve employs a pneumatic actuator integrated into a fabric sleeve to provide vibrotactile feedback to the arm [31]. (d) The fingertip tactile device features a miniature kinetic structure on the fingertip to deliver haptic feedback when the user touches an object in VR. This device improves object manipulation and exploration [30]. (e) A 3-DoF wearable device offers cutaneous force feedback [32]. ©2013 IEEE. The images of (a), (b) and (c) reproduced with permission.

ity (VR) or augmented reality (AR) environments. Providing sensations of texture and hardness during interaction with VR objects enriches the experience, making it more akin to daily real-world interactions and thus improving the immersive quality of VR.

In Chapter 3, we introduce our custom-designed wearable tactile device, which can be used to enhance usability and immersion within VR and AR experiences. This chapter also offers room for further exploration of the variation of sensations provided by vibrotactile feedback and examines the range of tactile sensations that vibrotactile feedback can deliver during touch interaction.

Vibrotactile devices also have potential applications as communication tools for deaf-blind individuals [39], guides for wheelchair users [41], tools for rehabilitation tasks [41], and aids for interpersonal touch communication for children with developmental disorders [43].

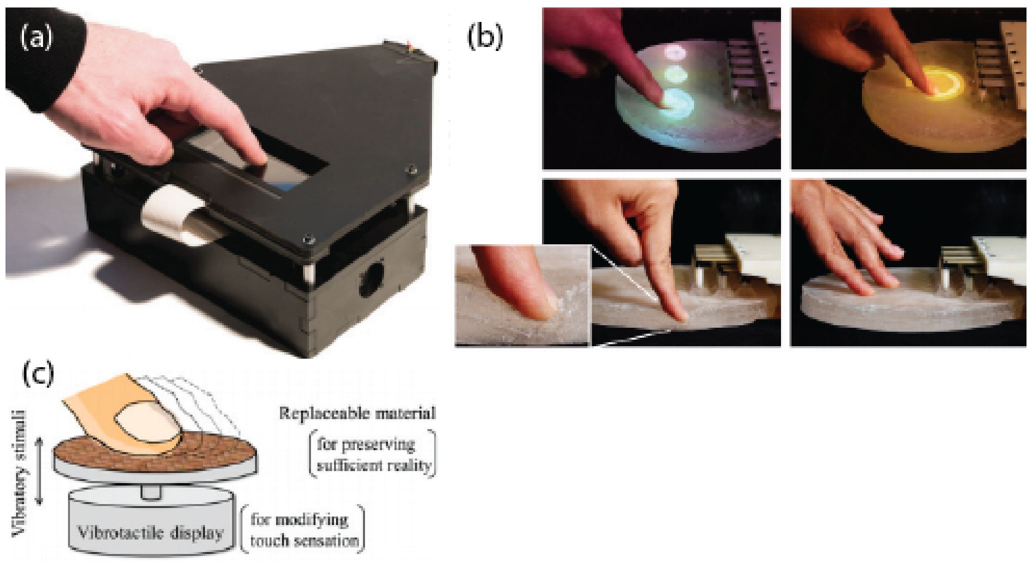

Figure 2.12: These are examples of grounded vibrotactile displays: (a) Wiertlewski et al. developed a high-fidelity surface haptic device that renders textures on a bare finger. The device provides ultrasound vibration on a glass plate, where the user touches and the display presents friction during the touch interaction with texture [33]. (b) Elastowave is a soft haptic interface that provides localized tactile feedback. Employing an array of piezo actuators on a gel phantom, Elastowave focuses vibrotactile feedback on the user's finger [38]. ©2020 IEEE. (c) Asano et al. developed a vibrotactile display capable of rendering textures based on real materials, such as fabric, wood, and leather [34]. ©2015 IEEE. The image reproduced with permission.

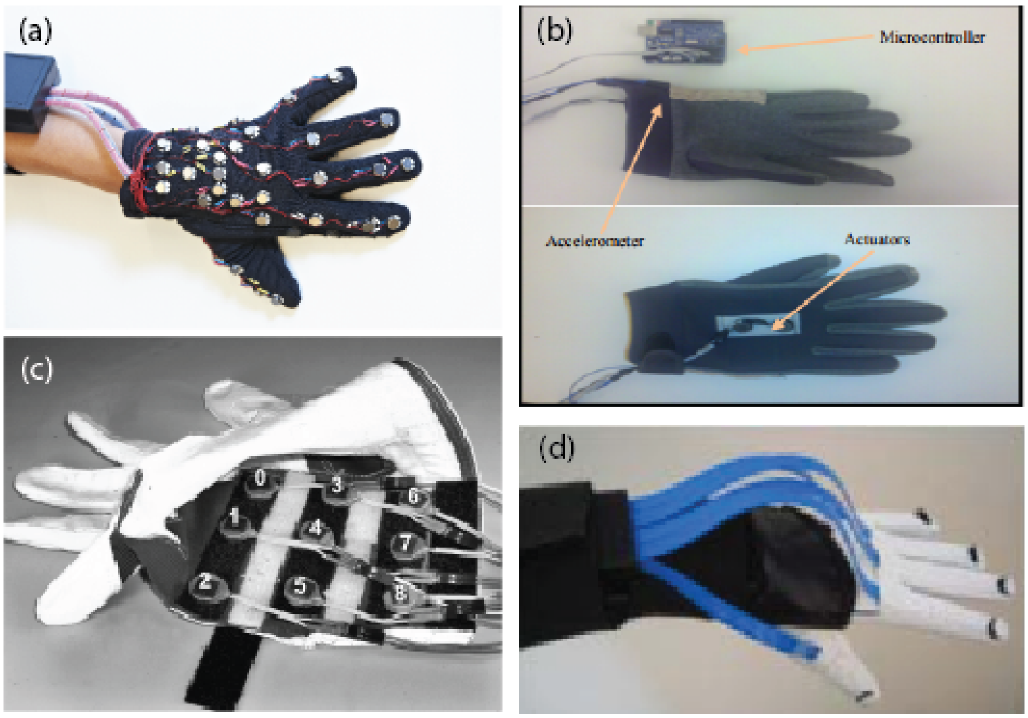

Figure 2.13: These are examples of glove-type tactile devices, which employ a small actuator structure that allows for the attachment of multiple actuators:(a) The Mobile Lorm Glove is a communication device designed for deaf-blind people that utilizes vibrotactile feedback. An array of actuators delivers the vibrotactile feedback necessary to present the tactile hand-touch alphabet [39]. (b) E-Glove provides vibrotactile feedback to the wrist for the rehabilitation of post-stroke patients. An attached accelerometer captures the rotation of the wrist, and the actuator vibrates to indicate to patients the state of the game task for rehabilitation [41]. ©2011 IEEE (c) A vibrotactile glove was developed to guide semi-autonomous wheelchair operations. A 3 by 3 array of small actuators on the backside of the glove provides stimuli to indicate direction [40]. (d) Sizebig et al. developed a VR system that uses vibrotactile feedback with the ShapeHand device. Six actuators are attached to the palm of the hand and fingertips to provide vibrotactile feedback during interaction with the VR environment [44]. ©2009 IEEE. Images reproduced with permission.

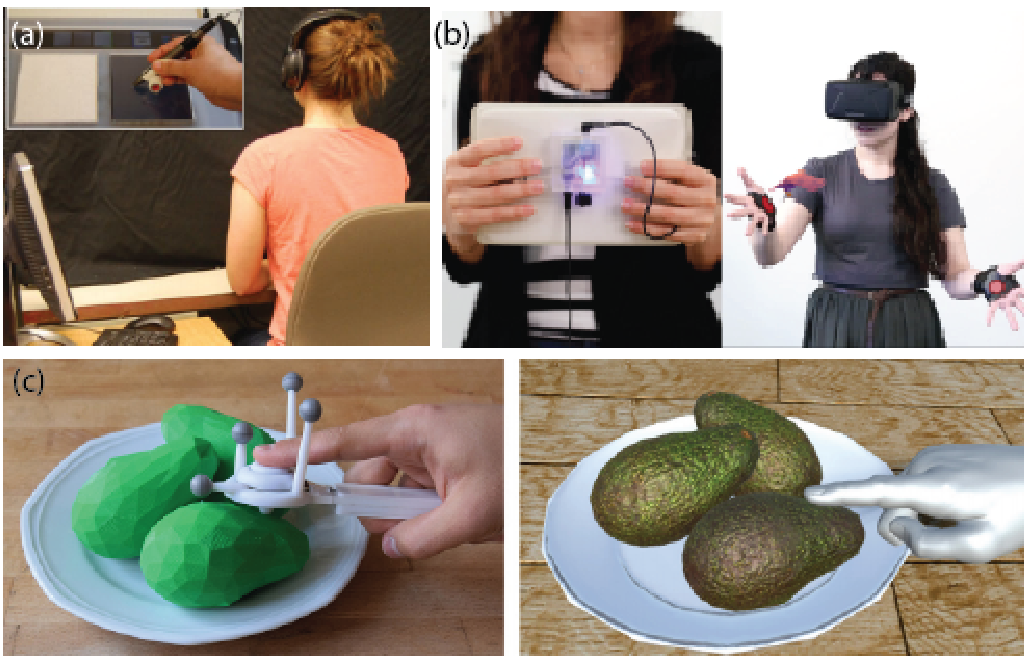

Figure 2.14: The structure of hand-held vibrotactile displays varies based on their purpose. (a) The texture rendering system incorporates a haptuator on the stylus. The stylus is equipped with a six-axis force torque sensor, two-axis accelerometers, and a magnetic motion tracking sensor to record texture sensations during interactions [35]. ©2014 IEEE. (b) Po2 is a haptic technology for augmented haptics in interactive gameplay. It utilizes two actuators to provide vibration, creating an illusory tactile motion between the user's hands [42]. (c) Choi et al. developed a device that enhances the perceived softness while interacting with haptic proxy objects in VR through the use of vibrotactile feedback and visuo-haptic illusion [37]. ©2020 IEEE. Images reproduced with permission.

Figure 2.15: The wearable display can be attached to various body parts, including the finger, hand, wrist, and other body parts. (a) The Haptic Ring provides vibrotactile feedback for rendering textures. The ring can be attached to the tip of the finger, finger phalanx, and wrist as well [45]. ©2019 IEEE. (b) FinGAR is a finger glove designed for augmented reality. It utilizes a DC motor attached to the finger to provide sensations of macro roughness, friction, fine roughness, and hardness [36]. ©2017 IEEE. (c) The finger-worn device aims to modify stiffness using vibrotactile feedback during interactions with virtual objects [46]. ©2017 Maereg, Nagar, Reid and Secco. (d) EnhauncedTouchX is a smart bracelet designed to augment interpersonal touch interactions. During hand-to-hand touch interactions, vibrotactile feedback is transferred from one hand to the other [43]. (e) HapTip enables multi-finger interaction in VR environments and provides sensations of a rough virtual surface, inertia, or weight of virtual objects [47]. ©2016 Girard, Marchal, Gosselin, Chabrier, Louveau and Lécuyer. Images reproduced with permission.

2.2.3 Thermal displays

A haptic display that provides thermal or temperature sensation is known as a thermal display. Primarily, two methods exist for providing thermal sensation: utilization of Peltier devices and thermo-resistive heaters. Most thermal displays leverage Peltier devices to deliver thermal feedback [57]. A Peltier device consists of two flat surfaces, one of which imparts a sensation of heat while the other induces a feeling of coolness. The degree of cooling and heating can be manipulated by the amount of induced voltage. Traditionally, Peltier devices possess a rigid structure and are not designed for stretching or folding. Nevertheless, recent studies have seen the development of flexible Peltier devices. These flexible devices can be stretched and folded, thereby broadening their applications [58]. Alternatively, thermo-resistive heaters generate heat by exploiting the heat emanating from the electricity applied to a conducting material. This technique allows for a swift response time to achieve 90% of the steady-state temperature [57].

Thermal displays are utilized for interactions within Virtual Reality (VR) applications. A multitude of thermal devices have been developed specifically for VR environments (Fig. 2.16). The thermal module can be attached to the hand [50, 48] or the fingertip [49] to facilitate interaction with VR objects. Recent advancements have led to the development of stretchable Peltier devices, allowing for natural hand interactions in everyday life. The compactly designed thermal module can be integrated into the existing haptic interface [49, 51]. When attached to a haptic device, the thermal module can convey multiple properties of an object and has the potential to provide haptic feedback akin to interaction with a real object. Some thermal devices are designed to be attached to other body parts, such as the back of the neck [52], or the forehead [53]. This design consideration is intended for use with head-mounted displays. In a VR environment, the primary role of a thermal device is to convey the thermal sensation of an object. How-

Figure 2.16: Thermal devices are widely used in VR applications. (a) Kim et al. developed a flexible thermal glove for VR interaction. This glove enables users to engage in haptic interactions such as grasping and pinching virtual objects, utilizing thermal feedback [48]. (b) The thermal module is integrated into the Haptic Thimble, an existing haptic device. This device provides heat sensations to the fingers, rendering thermal feedback in VR experiences [49]. ©2018 IEEE. (c) Chernyshov et al. developed thermal feedback displays on the hand within virtual environments to reduce the time delay of thermal feedback [50]. (d) Gallo et al. developed a small thermal display that can be integrated into existing haptic devices like Falcon and OMEGA3. This compact thermal display leverages the capabilities of other haptic devices to provide multiple sensory properties [51]. ©2015 Gallo, Rognini, Santos-Carreras, Vouga, Blanke and Bleuler. (e) Ambiotherm is a thermal device used in conjunction with a VR head-mounted display (HMD). The thermal module is attached to the neck, allowing the ambient temperature in the virtual environment to be rendered through thermal feedback [52]. (f) Peiris et al. used thermal feedback on the forehead to enhance spatial awareness in VR experiences [53]. ©2017 IEEE. (a) is is licensed under Creative Commons 4.0. Images reproduced with permission.

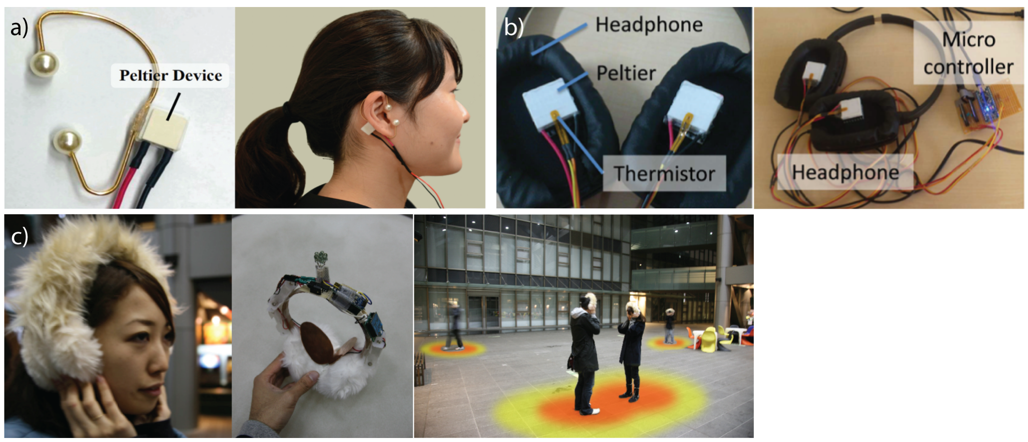

Figure 2.17: Thermal devices can be utilized to enhance emotional and social experiences, as discussed in section 2.1.2, where warmth and cold sensations were found to impact emotions and social behavior. (a) The Thermal Feedback Influencer aims to enhance the experience of music listening. This device is attached to the ears and provides cold and warm sensations based on the mood of the music being played [54]. ©2019, Springer Nature Singapore Pte Ltd. (b) ThermOn, when attached to headphones, provides warm and cold sensations to enhance the emotional experience of music [55]. (c) Thermotaxis is a system designed to support social interaction between individuals. It promotes closeness by providing a comfortable temperature when someone with the device comes closer, and a non-comfortable temperature when they are far away [56]. ©2009, Springer-Verlag Berlin Heidelberg. Images reproduced with permission.

ever, when affixed to body parts near the face, the thermal display can provide ambient temperature feedback in VR [52], thereby increasing spatial awareness and enhancing navigation in VR [53].

Moreover, thermal displays can enhance emotional and social experiences. For instance, thermal feedback paired with music listening can enhance mood. Ishikawa et al. provided thermal feedback based on the mood of the music. In their user study, some subjects reported experiencing goosebumps while listening to music [54]. Thermal sensation can also facilitate social interaction. Narumi et al. developed the Thermoaxis system to support social interaction. This device emits a warm, comforting sensation when another person equipped with the device is nearby, and conversely, it imparts a cold, uncomfortable sensation when the person is farther away. These responses promote closer social interaction. As mentioned previously in Section 2.1.2, thermal sensation is anticipated to enhance or improve social behavior and evaluation.

2.3 Applications of Haptic Technologies in HCI, AR, VR

2.3.1 Augmenting physical surfaces and objects

Haptic Augmented Reality (HAR) is a branch of haptic technology designed to enhance interactivity and usability in Virtual and Mixed Reality environments. It accomplishes this by augmenting surfaces and physical objects in direct touch interactions. Notably, HAR is compatible with Tangible User Interfaces (TUI), thereby enhancing the user experience within these interfaces. TUI represents a mode of human-computer interaction that facilitates the direct and intuitive manipulation of digital information. It employs direct skin contact and freehand interaction with various shapes, surfaces, and objects. For instance, these interfaces may take the form of pucks [59], boxes [60], bottles [61], architecture [62], brushes [63], and skeletal preparations [64]. HAR offers the potential to expand the variations of touch sensations when interacting with these shapes and surfaces, depending on the use cases. To delve into the unexplored aspects of HAR research, this section reviews prior works on TUI applications categorized by use cases. It also elaborates on the diverse types of freehand interactions, shapes, and surfaces found in tangible interfaces.

Landscape and Urban Planing

The Urp system is designed for urban planning, wherein tangible architectural models of varying shapes are positioned on a tabletop [62]. Each model allows for the simulation of wind and shadows. As depicted in Fig. 2.18(a), each distinct architectural model casts a different shadow. As time transitions from morning to afternoon, the shadow elongates based on the time of day, demonstrating how a shadow might appear with time changes.

The direction of the wind is visualized using arrows, which depend on the orientation and position of the tangible objects on the table.

The GeoSpace system, in conjunction with the metaDesk system, enables the visualization and interaction with geographical space [65]. Users employ phycons, three-dimensional icons of tangibles, to represent buildings and visualize geographical spaces. Lens, phicons, and instruments are integral to this application. Users are enabled to grasp, place, and rotate these tangibles while peering into the lens (Fig. 2.18(c)).

The SandScape system uses grass beads in the form of sand to delineate the geometry of a landscape model [66]. Users can shape the landscape model using grass beads. The arrangement of these beads is captured by recording the intensity of light that passes through the volume from the high-power infrared LEDs located beneath the beads (Fig. 2.18(d)). Illuminating Clay offers a more precise system to adjust the form.

Illuminating Clay is a system designed for the real-time computational analysis of landscape models [67, 68]. Users manipulate a thin layer of Plasticine, a modeling clay supported by a metal mesh core and combined with a light and flexible thin layer of material, to maintain the desired topography. Variations in slope, shadows, and solar radiation are projected onto the surface of the Plasticine. Users create a form and this arbitrary form is used as input (Fig. 2.18(b)).

Modeling Simulations

Sensetable, a wireless object-tracking platform, was developed to enable various tabletop simulations [59]. In the workspace on the tabletop, users grab and drag tangible pucks, pressing and turning a dial with these pucks (Fig. 2.19(a)). The system can simulate a chemical reaction, where users move each molecule using individual pucks, and attach them to each other (Fig. 2.19(b)). Additionally, system dynamics simulations comprising nodes and lines are used to model business and social sciences (Fig. 2.19(c)).

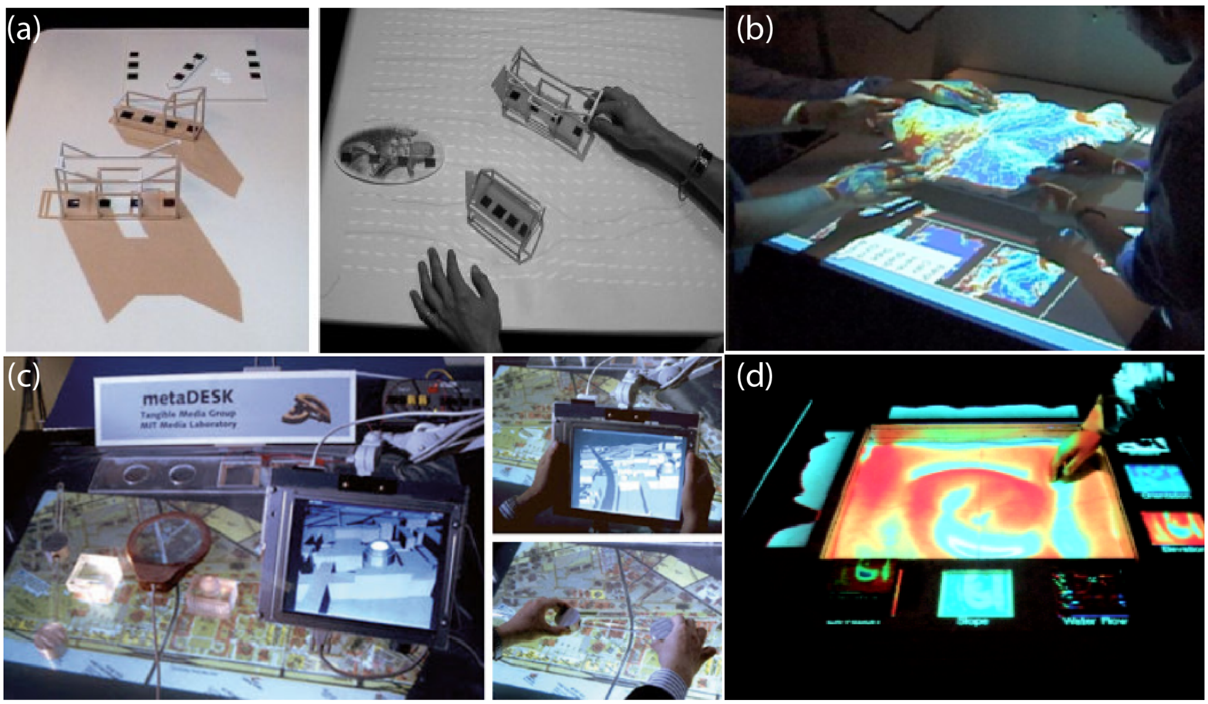

Figure 2.18: The applications for landscape and urban planning are as follows: (a) The Urp system is used for urban planning with architectural models [62]. (b) Illuminating Clay is utilized for analyzing landscape models [67]. (c) GeoSpace is integrated into the metaDESK system to visualize and simulate geographical space [65]. (d) SandScape employs sand as a material for creating geographical models [66]. Images reproduced with permission.

Utilizing this system, Kobayashi et al. created simulations for disaster management and networking.

Kobayashi et al. also developed a system for an IP Networking simulation, employing pucks used in the disaster measures system [69] (Fig. 2.19(d)). Each puck can adjust the parameter settings of a link, client, and server by being rotated and pressed. The parameter changes are based on the location of the pucks. This real-time simulation visualizes network performance onto the tabletop workspace.

Kobayashi et al. further developed a disaster simulation system that aids in the collaborative planning of disaster measures [70] (Fig. 2.19(e)). A map is projected onto the tabletop, and users manipulate pucks that act as tangibles within the system. A Geographic Information Systems (GIS) database estimates the damage from a hazard. Users can alter parameters such as refuge area capacity, population, the impact of the fire break, and the size of the restricted area by rotating the pucks at the location where they are placed. Pucks also serve to monitor the damage situation. For example, users can check the damage by placing a puck on the map, revealing the number of evacuated and injured individuals.

Digital Media Container

In the Bottles project [61], perfume bottles are repurposed as tangible objects to offer access to information at any time and any place, thereby encapsulating the idea of "ubiquitous computing". Through the simple physical act of opening and closing these bottles, users can access various types of information (Fig. 2.20). Each perfume bottle acts as a distinct container for specific information. For instance, upon opening one bottle, users might be greeted with jazz music, while opening another bottle might lead to the sound of classical music. Additionally, distinct bottles can deliver weather updates from a variety of locations. As such, these bottles act as digital vessels containing music,

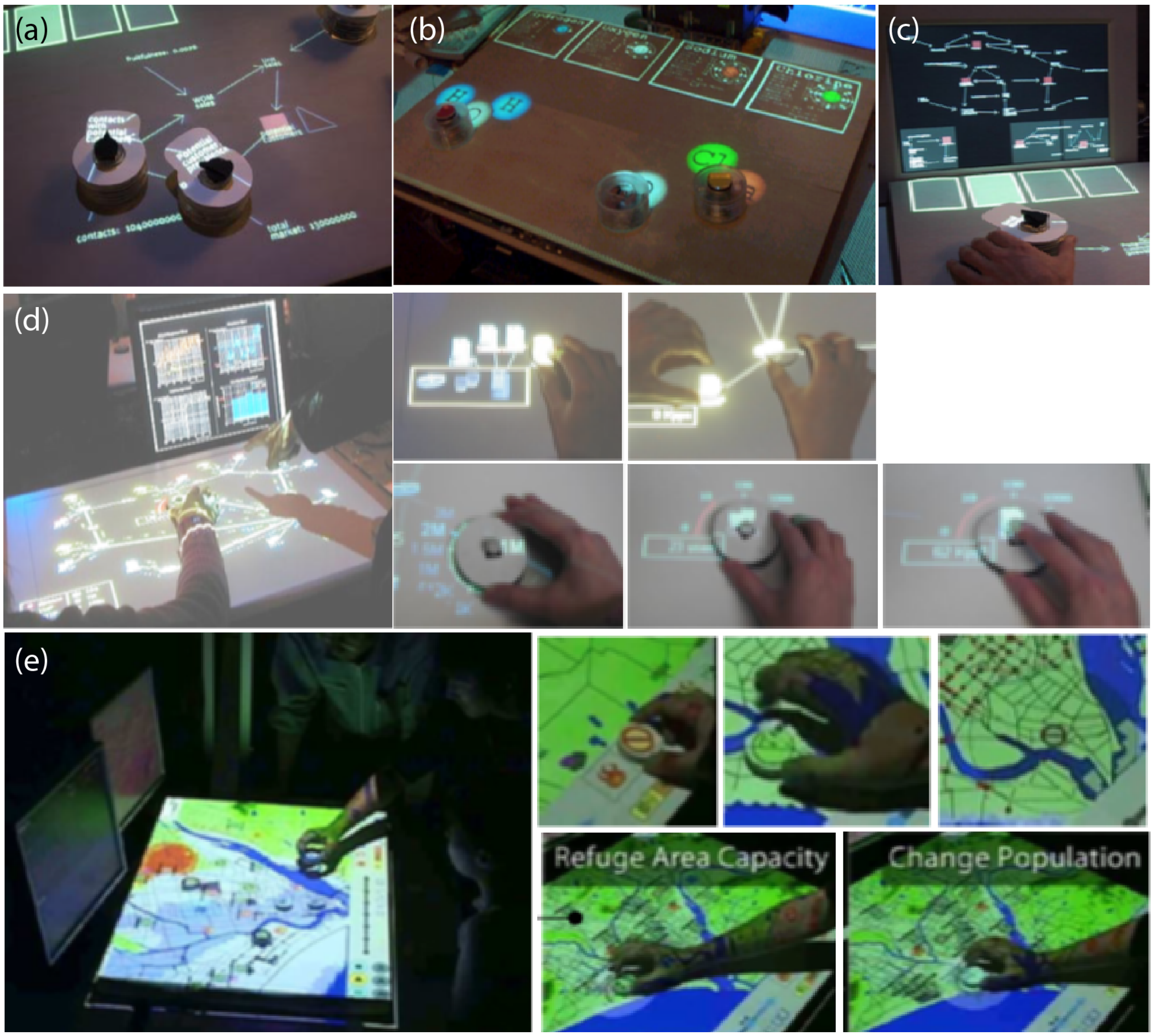

Figure 2.19: The applications of tangible user interfaces (TUIs) for computer simulations are as follows: (a) Sensetable can be applied for (b) chemical reaction simulation and (c) system dynamics simulation, as demonstrated by Patten [59]. (d) In a network simulation, tangible interactions allow for the modification of client and server settings [69]. (e) In a disaster simulation system, parameters such as refuge area capacity or population can be adjusted by grabbing and turning pucks, as illustrated by Kobayashi et al. [70]. Both (d) and (e) are presented by Kobayashi et al. Images reproduced with permission.

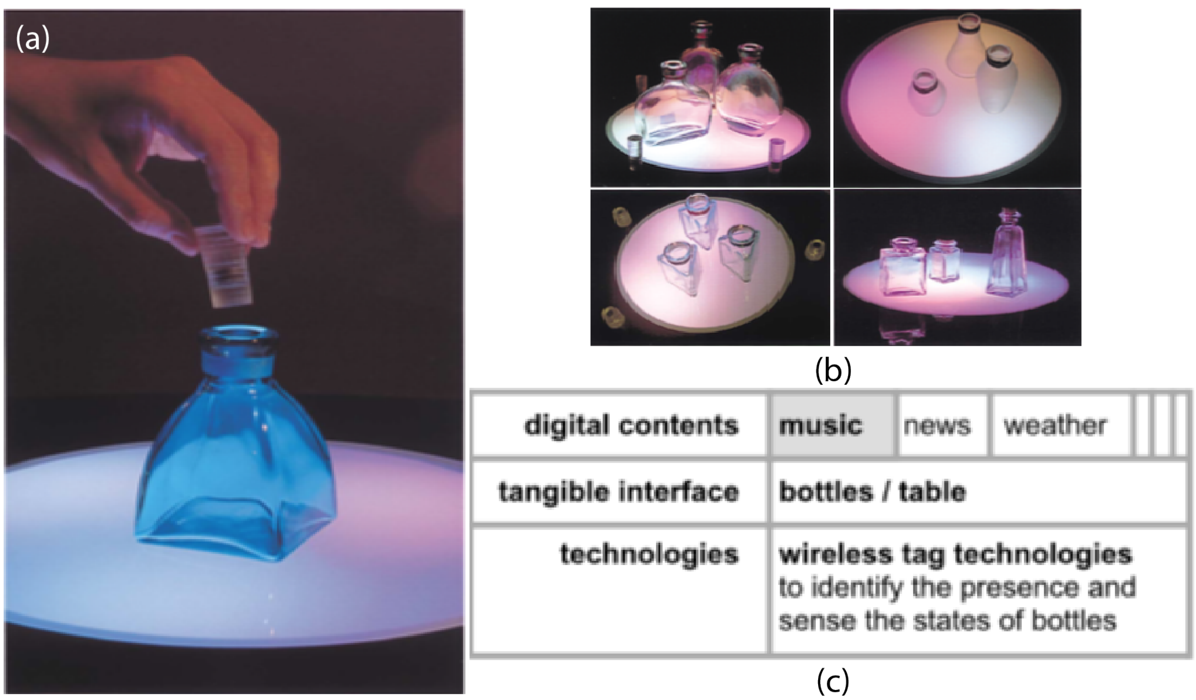

Figure 2.20: (a) In Bottles, users can access information by opening the bottles. (b) Each bottle, with its unique size and shape, contains different music, traffic sounds from different locations, and various news. (c) The figures depict the three layers of Bottle interfaces, as presented by Ishii [61]. ©2004 IEICE. Images reproduced with permission.

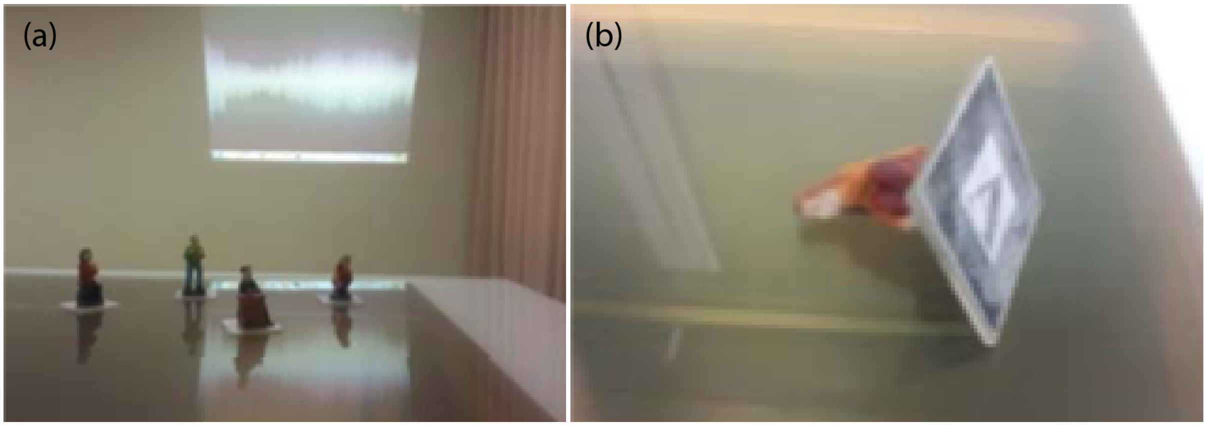

Figure 2.21: (a) TMusic is a music player manipulated by human model objects. (b) The position of the human model on the table can be tracked using markers attached to the human model objects. The figures are taken from the paper written by Zhang et al. [71]. Images reproduced with permission.

news, weather, and more. Through the straightforward manipulation of opening and closing, users can conveniently access this digital information.

Music Player

TMusic, a tangible music player, alters both music and its visual effects through the manipulation of tangible objects (Fig. 2.21) [71]. Users can determine the playability of different music tracks by augmenting different shapes of tangibles. In this system, human model objects are employed as tangibles. On the workbench, users rotate and move these tangibles, and the position and rotation of the tangibles subsequently influence the volume and visual effects of the music. The human model is tracked through object tracking, and different music is played based on the presented model. Manipulations such as grasping, placing, dragging, and rotating are available for user interaction.

Musical Performance and Patching

Patten et al. developed interaction techniques for musical performances using a table-top tangible interface [72]. The position of objects on the table top surface (Fig. 2.22) is tracked and translated into commands for a musical synthesizer. Tangible objects are used to adjust the volume and parameters of audio effects. For instance, the volume is determined by the distance between the objects. The interface includes three different object shapes: star, circle, and large circle. The star shape functions as a menu, while the circle is used for selection and adjustment. Users can interact with these objects by grasping, dragging, and pushing the tangibles.

The reacTable [60] is a well-known musical table, with tangibles positioned on the tabletop display (Fig. 2.23). It allows for dynamic patching of music. On the table, connections between each tangible, and the location and rotation of tangible parameters can be adjusted. Each tangible is a specific object type, with its shape corresponding to a distinct audio function in audio processing. For example, as shown in Fig. 2.23(c), square-shaped tangibles are used as generators, while circular tangibles function as controllers for filters. Each shape of the tangible object allows the user to interact by grasping, placing, and turning the knob to adjust the parameters.

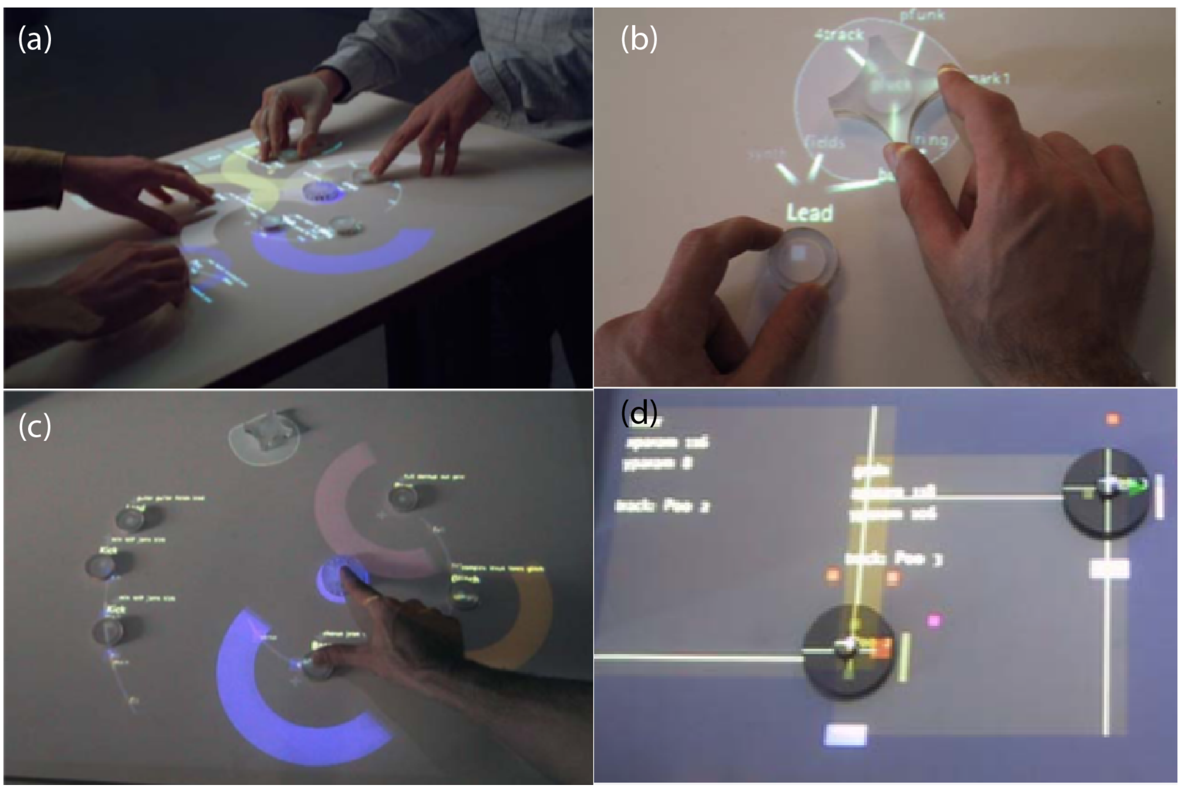

Figure 2.22: (a) Interaction techniques for musical performance with a tabletop tangible interface. (b) Star-shaped and circle-shaped tangibles are utilized for menu selection. (c) and (d) The user engages in dragging and placing the circle-shaped objects to adjust the volume and parameters of the audio effects. These figures are from Patten's paper on interaction techniques [72]. Images reproduced with permission.

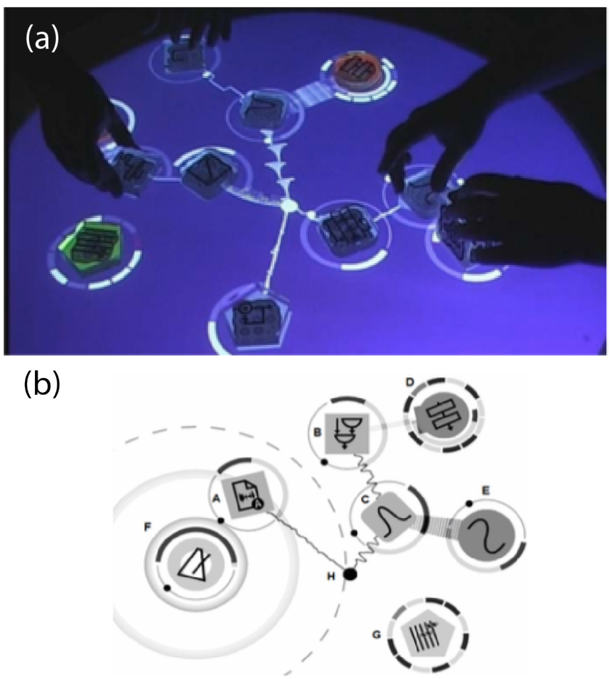

	Connections	Shape	Examples
Generators	• 1 audio out • N control in	(square)	• square wave • sampler player
Audio filters	• 1 audio in • 1 audio out • N cntrl in	(rounded square)	• resonant filter • flanger
Controllers	• 1 cntrl out	(circle)	• sine wave low frequency oscillator • 12-step amplitude sequencer
Control filters	• 1 cntrl in • 1 cntrl out	(octagon)	• decimator • sample & hold
Audio mixers	• 2 audio in • 1 audio out • N cntrl in	(pentagon)	• mixer bus • ring modulator
Global	• N cntrl in	(double circle)	• metronome • tonalizer

(c)

Figure 2.23: (a) An overview of the reacTable is presented. (b) The tangibles are connected on the worktable, and the connections between them are visualized. (c) Each shape of the tangible represents a specific function, such as generators, audio filters, and audio mixers. These figures are depicted in the paper by Jorda et al. [60]. Images reproduced with permission. Images reproduced with permission.

Drawing and Interactive Arts

Spindler et al. developed a system featuring dynamic Tangible User Interface (TUI) palettes, called WorkZone (Fig. 2.24(a)(b)) [73]. In this system, users utilize a handheld display palette to select colors using a tool pen. The handheld display can host multiple tool palettes simultaneously. The position of the handheld display is tracked, allowing users to quickly access different attributes for each tool palette based on the position of the WorkZone. For example, when the handheld palette is on the left side of the WorkZone, users can select the thickness of the drawing pen. When the handheld palette is on the right side, users can select the color of the pencils. In the WorkZone, they use palettes and pencils to create their artwork. Using the position of the palettes, they can access multiple tools that are necessary for drawing.

The I/O Brush [63] uses a digital brush that allows users to capture the color of everyday objects and use it as ink. The tips of the I/O Brush are equipped with touch sensors, lights, and a camera surrounded by optical fibers. When the tips of the I/O Brush come into contact with an everyday object, the user can capture the color of the object and use it for drawing. Users can draw pictures with the same motion as drawing in the real world. They can pick the color by grabbing the objects and touching them with the brush.

The Sensetable [59] is also employed in interactive art applications, where the user creates with a node controlled by pucks. The connections between pucks are visualized on the tabletop. Users can grab and place pucks anywhere on the table.

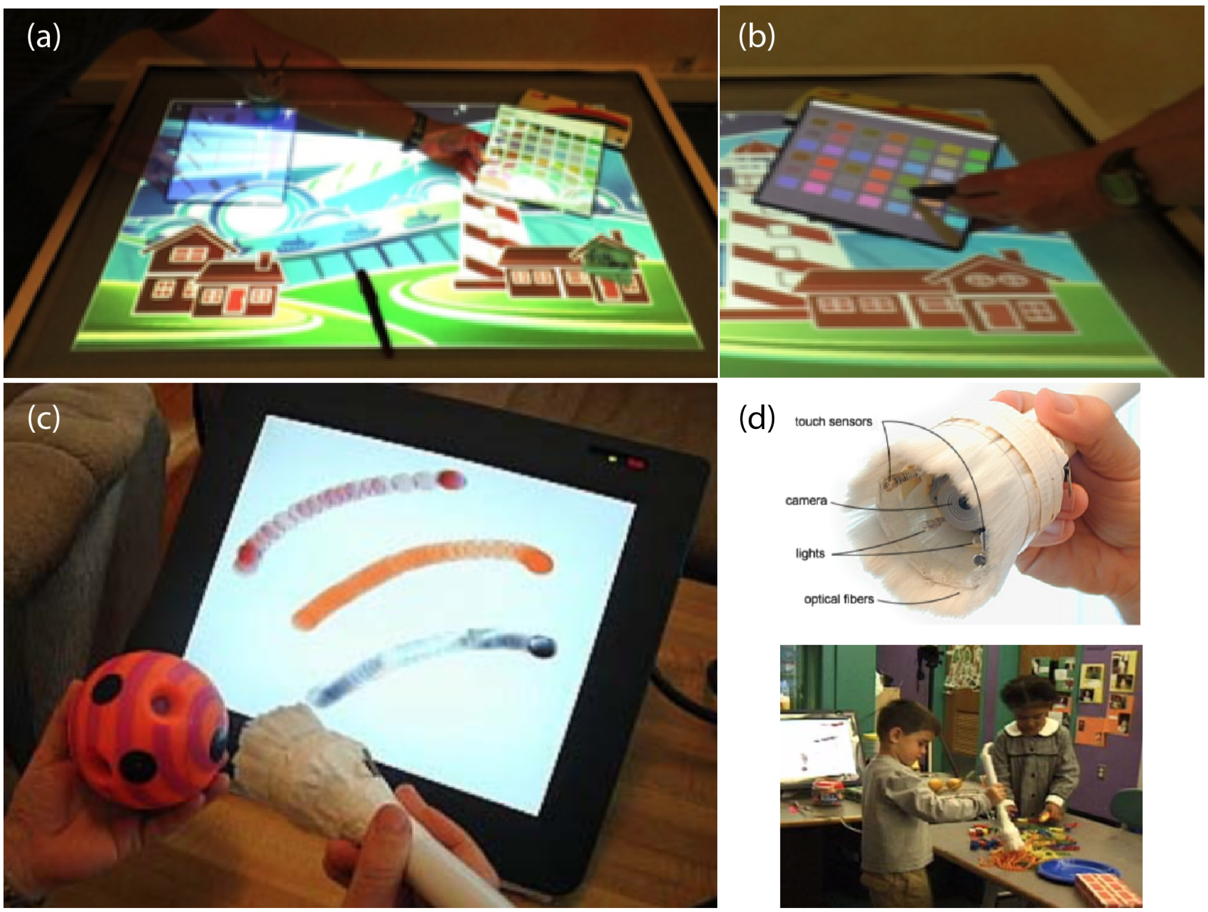

Figure 2.24: (a) The system featuring dynamic tangible user interface (TUI) palettes is known as WorkZone. ©2013, Springer-Verlag Berlin Heidelberg. (b) In this system, color selection is performed using the palette, and when the palette is moved to the left side, the user can choose the thickness of the pen. Figure (a) and (b) are presented by Spindler et al. in their paper [73]. (c) Color is captured from everyday objects in the system described. (d) I/O Brush consists of touch sensors, lights, and cameras. Children use the I/O Brush to select colors and draw pictures. Figure (c) and (d) are described by Ryokai et al. in their paper [63]. Images reproduced with permission.

2.3.2 Perceptual effects from augmentation

Existing research on the perceptual dimensions of tactile textures has identified various properties perceivable through tactile interactions with objects. These include attributes like roughness/smoothness, hardness (stiffness)/softness, moisture/dryness, stickiness/slipperiness, and coldness/warmth [74]. Haptic feedback can influence the perception of these surface properties during touch-based interactions. As indicated by previous studies, vibrotactile feedback can alter perceptions of softness [75, 76], hardness or stiffness [77, 78, 79], roughness [80], friction or texture [35], and material properties [81]. Thermal feedback also has the potential to change perceptions of material properties. These techniques for adjusting surface properties can be implemented in various human-computer interaction applications.

Softness

Past studies have demonstrated that low-frequency vibrotactile stimuli, within the frequency range of 3 to 5 Hz, can evoke sensations of material softness [82, 76]. Okamoto and Yamauchi [75, 76] performed an experiment to assess the impact of low-frequency vibrations on the perception of softness. Their experiment compared the softness sensation elicited by a 5Hz low-frequency vibrotactile surface to that produced by a physically soft sample. Participants were asked to judge which stimulus felt softer. The experimental methodology was founded on the method of constant stimuli, with the experimental setup depicted in Figure 2.25 (a). Their findings suggested that vibrotactile amplitudes of 0-1.6 mm under a sustained load of 0.5 N corresponded to soft cylindrical silicone rubber samples with spring coefficients ranging from 4.7-22.3 N/mm (Figure 2.25 (b)). Furthermore, perceived hardness was found to decrease as a function of the vibration amplitude. Moreover, low-pass-filtered white-noise vibrations were perceived as soft [83].

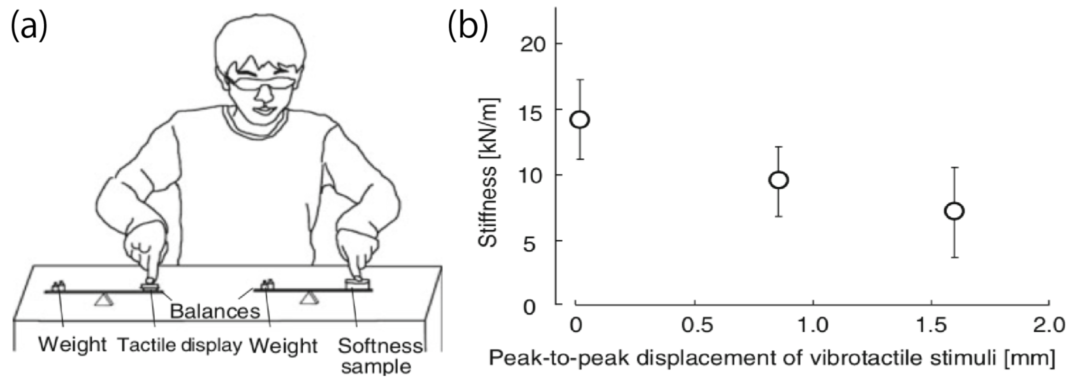

Figure 2.25: (a) The experimental setup was designed to evaluate the softness of materials when low-frequency vibrotactile feedback was applied to their surfaces. (b) The experimental results demonstrate that the stiffness of materials, ranging from actual softness of 5 to 15 kN/m, corresponds to the displacement of vibrotactile stimuli, which ranges from 0 to 1.8 mm [75, 76]. Figures (a) and (b) are cited from [84]. ©2014, Springer-Verlag London.

Upon making direct or indirect contact with an object, vibrations are generated on the surface as the object's volume compresses and releases energy [84]. These vibrations can provide potential cues for perceiving volumetric softness. Several published perceptual studies have indicated that vibrotactile feedback can influence perceived volumetric softness [85, 86]. Kildal et al. developed a vibro-actuator-included stylus interface to alter volumetric compliance during a press interaction with mobile computational devices (Figure 2.26). They synthesized vibration signals based on the contact point and captured force. Additionally, a 156 Hz sinusoidal signal was overlaid on the force gain envelope. In their experimental study, they found that 80.3% of all explicit statements suggested that users perceived an illusion of compliance [85].

Hardness and Stiffness

The use of vibrotactile feedback from a stylus has been explored to simulate variations in the stiffness of objects within virtual reality environments. This involves utilizing frequency differences in the vibrotactile feedback when an object is tapped, thereby

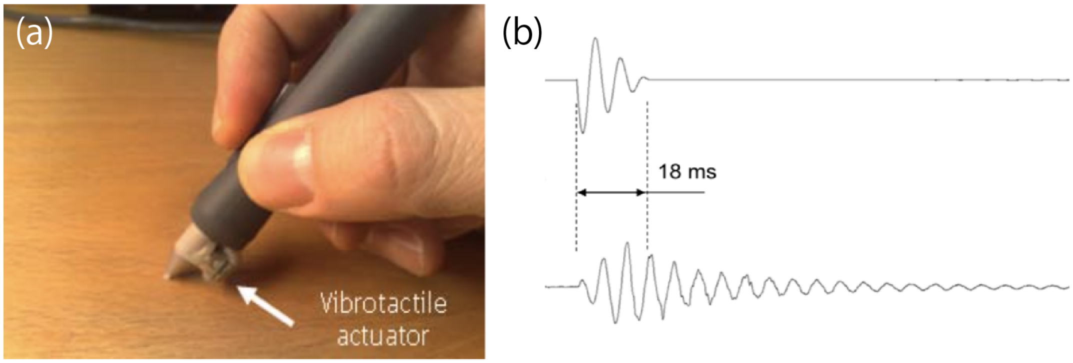

Figure 2.26: (a) The stylus is equipped with a vibrotactile actuator that modifies the sensation of softness on the surface. (b) The mechanism for modifying volumetric softness involves providing vibrotactile feedback that generates vibrations similar to those experienced when touching a soft surface. Figures (a) and (b) are cited from [85, 86]. ©2012, Springer-Verlag Berlin Heidelberg. Images reproduced with permission.

conveying the sensation of different stiffness levels. Okamura et al. [77] proposed a method to model the decaying sinusoidal wave to render the sensation of material tapping in virtual reality. This approach is based on experimental data obtained by tapping real objects with a stylus equipped with an accelerometer. They employed a decaying sinusoid model, expressed as

$$Q(t) = A(v)e^{-Bt}\sin(2\pi\omega t) \tag{2.1}$$

where $A(v)$, B, and ω represent the amplitude as a function of impact velocity, the decay rate of the sinusoid, and the sinusoid frequency, respectively. They created tapping feedback for rubber, wood, and aluminum materials. In the experiment, three materials of the same stiffness were used, and each material randomly used the vibration feedback model for rubber, wood, or aluminum. Consequently, participants were capable of identifying each material (the correct rate was 83.3%).

To enhance the realism of the contact, Kuchenbecker et al. [78] proposed an event-based haptic feedback system, which uses pre-recorded acceleration profiles to provide

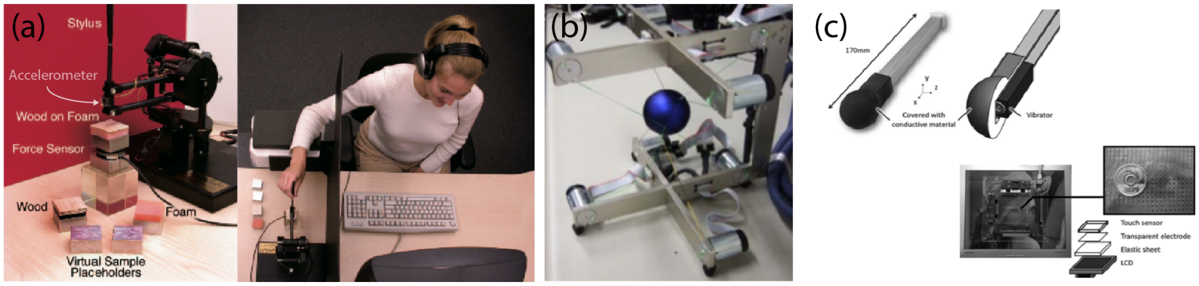

Figure 2.27: Material property modifications with a haptic feedback approach are as follows:(a) Kuchenbecker proposed an event-based haptic feedback method, and the figure shows their experimental setup for tapping on real and virtual objects [78]. ©2006 IEEE. (b) Ikeda et al. used the haptic interface "SPIDER" in their experiment to investigate the perceived stiffness changes using event-based haptic feedback [79].(c) Hachisu et al. utilized a rod device to modify material perception during tapping interactions [89]. ©2017 IEEE. Images reproduced with permission.

haptic feedback based on the incoming velocity of the stylus tip when users tapped an object (Fig. 2.27 (a)). Ikeda et al. [79] studied how event-based haptic feedback improved the perceived stiffness of the tapping object using a system called SPIDAR (Fig. 2.27 (b)). They suggested that the frequency of the feedback vibration serves as a cue for stiffness.

Subsequent studies aimed to identify the frequency components of vibrotactile feedback in tapping, which users perceive as stiffness [87, 88]. These studies found that stiffness is perceived at a peak of around 300 Hz and decreases or disappears at higher frequencies due to perceptual capabilities' limitations.

Conversely, research has indicated that the latency of haptic feedback can alter the perceived stiffness of an object. Hachisu et al. [89] developed a haptic rod device that provided vibration feedback with a latency of 0.1 ms. Their findings suggest that higher latency tends to make users perceive the surface as being softer (Fig. 2.27 (c)). Similarly, when using a PHANToM stylus, the perceived elasticity was found to be less than the actual elasticity when feedback force was delayed [90]. Kaaresoja et al. [91] also found that tactile feedback that was delayed for longer periods was perceived as being heavier and required a greater amount of force during a button press interaction.

Roughness

Indeed, several studies have explored the use of vibration to enhance the sensation of roughness. Hollins et al. [92] suggested that altering the friction between a material and a finger through vibration could modify the sensation of texture. Culbertson et al. [35] expanded on this by creating a haptic texture model from data recorded during natural and unconstrained tool-surface interactions. They developed a custom stylus to record accelerometer data, stylus position and orientation, and contact force on six different surfaces (rough plastic, canvas, floor tile, silk, vinyl, and wood). With an Autoregressive (AR) model structure, they used these textures to generate vibration signals for texture rendering.

Focusing on the augmentation or modification of roughness from real-life material properties, Asano et al. [80] proposed a method to modify the sensations of fine and macro roughness. They used two vibration models to adjust roughness sensations (Fig. 2.28 (a)). First, sinusoidal based texture models from prior studies [93, 94] were used to modify the perceived fine material. The displacement that applied to the acrylic plate was expressed as

$$y_1(t) = A_1 \sin\left(2\pi \frac{x(t)}{\lambda}\right) \tag{2.2}$$

where A_1, $x(t)$, and λ were the amplitude, position of the finger, and the wavelength of the augmented wave, respectively. This wavelength is a parameter to alter the roughness perception. For the altering micro roughness, they used decayed sinusoidal wave models based on the prior work to render the tapping sensation which Okamura et al. proposed

[95]. The displacement to the finger pad was expressed as

$$y_2(t) = A_2 \exp(-at) \cdot \sin(2\pi f t) \tag{2.3}$$

where A_2, a, and f are the amplitude, damping ratio, and damped natural frequency of the finger pad, respectively. The value of f was fixed at 200 Hz based on the prior study [96]. As a result of the studies, they confirmed that the perceived fine and macro roughness sensations of materials were able to be selectively modified while maintaining their tactile characteristics using slight modification instead of total modification. In addition, they reported that their approach to combined vibro-tactile stimuli and real materials is effective regardless of the type of material such as cotton cloth or taurillon leather. Maeda et al. [97] presented the method to augment the material surface with vibration. Their system captures the touch signal from a vibration sensor and it modulated with a frequency filter and provides vibration from the wrist band. They reported that the roughness of sandpaper was changed when they applied the low-pass filter with the cutoff frequency between 30 and 250 Hz (Fig. 2.28 (c)).

Material Property

Ochiai et al. [81] indeed proposed a novel method to reduce or even eliminate the sensation of real textures, using what is known as the squeeze film effect (Fig. 2.28 (b)). This approach manipulates the air layer between the object and the user's fingers to modulate the friction and consequently, the perceived texture.

In contrast to the common approach of attaching vibrators or other tactile devices to objects, Bau et al. [98] proposed an ingenious method for modifying tactile sensations without physical alterations to the object. They employed the principles of reverse electro-vibration, a technique that works by injecting a weak electrical signal into any

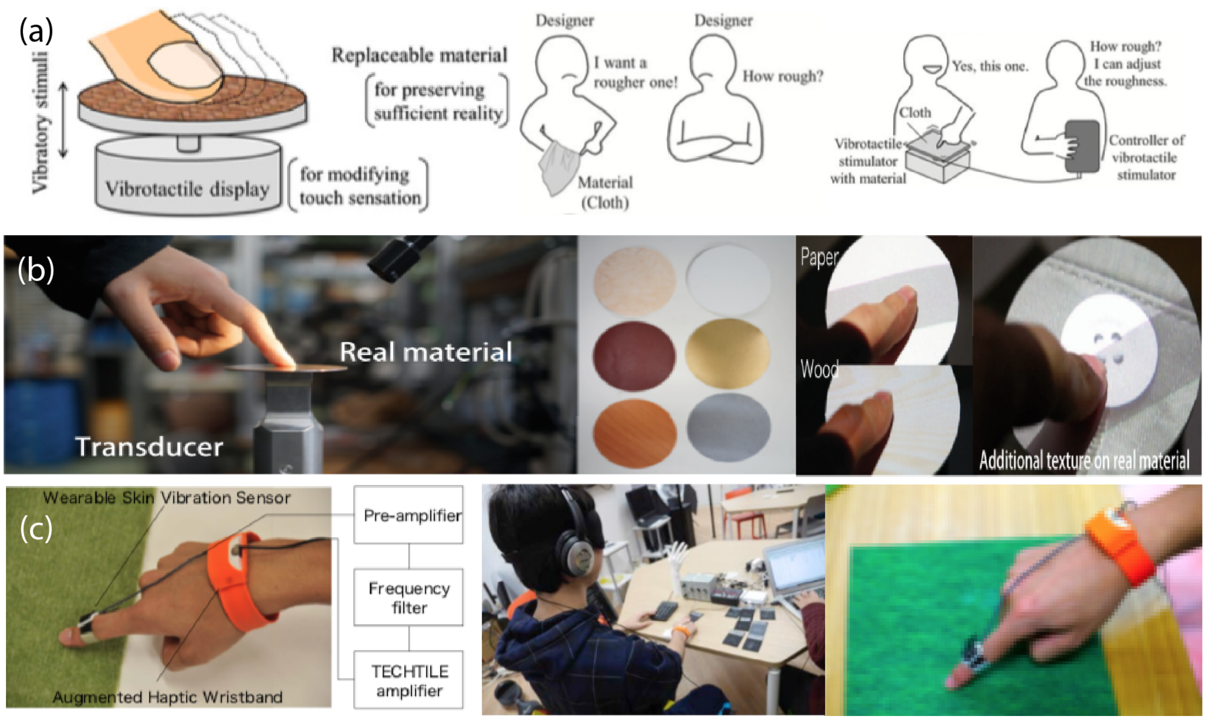

Figure 2.28: Material modification with haptic feedback is depicted in the following figure captions:(a) Asano et al. proposed a method to alter fine and macro roughness sensations using a vibrotactile display [80]. The right figure illustrates the application for communicating the tactile sensation of texture. (b) The system overview of the Diminished Haptic system developed by Ochiai et al. is presented [81]. The middle figure showcases the real material they used for recording, while the right figure demonstrates an application with their system. ©2014, Springer-Verlag Berlin Heidelberg. (c) Maeda et al. introduced a method for modifying texture with haptic feedback by processing the input tactile signal with a frequency filter [97]. Images reproduced with permission.

part of the user's body. This signal creates an oscillating electrical field around the user's fingers, leading to an altered tactile sensation when interacting with an object. This approach has the advantage of being non-invasive and not requiring any modifications to the object itself, while still providing the possibility of significantly altering the user's haptic experience.

Chapter 3

Tactile Echoes: Multisensory Augmented Reality for the Hand

Haptic interfaces in virtual and augmented reality technologies have long sought to incorporate responsive and realistic haptic feedback to accompany free-hand interaction like in tangible user interfaces, as reviewed in Chapter 2. This chapter contributes to this field by developing a wearable tactile interface, Tactile Echoes, that employs a unique tactile rendering method that leverages audio processing techniques, such as delay, frequency modification, and amplification. Additionally, we incorporated Tactile Augmented Reality, which maps tactile sensations onto physical objects. The findings in this chapter motivated rigorous perceptual studies, presented in Chapter 4, on tactile forward masking in active touch (Chapter 4). The findings of Chapter 3 are also extended through the exploration, presented in Chapter 5, of additional methods for tactile augmentation of surfaces.

The contents of Chapter 3 are reproduced from the following publication by the author and her colleagues [2]:

A. Kawazoe, G. Reardon, E. Woo, M. D. Luca and Y. Visell, "Tactile Echoes: Multisensory Augmented Reality for the Hand," in IEEE Transactions on Haptics, vol. 14, no. 4, pp. 835-848, 1 Oct-Dec 2021, ©2021 IEEE. Reproduced here with permission from the IEEE, doi: 10.1109/TOH.2021.3084117.

3.1 Abstract

Touch interactions are central to many human activities, but there are few technologies for computationally augmenting free-hand interactions with real environments. Here, we describe Tactile Echoes, a finger-wearable system for augmenting touch interactions with physical objects. This system captures and processes touch-elicited vibrations in real-time in order to enliven tactile experiences. We process these signals via a parametric signal processing network in order to generate responsive tactile and auditory feedback. Just as acoustic echoes are produced through the delayed replication and modification of sounds, so are Tactile Echoes produced through transformations of vibrotactile inputs in the skin. The echoes also reflect the contact interactions and touched objects involved. A transient tap produces discrete echoes, while a continuous slide yields sustained feedback. We also demonstrate computational and spatial tracking methods that allow these effects to be selectively assigned to different objects or actions. A large variety of distinct multisensory effects can be designed via ten processing parameters. We investigated how Tactile Echoes are perceived in several perceptual experiments using multidimensional scaling methods. This allowed us to deduce low-dimensional, semantically grounded perceptual descriptions. We present several virtual and augmented reality applications of Tactile Echoes. In a user study, we found that these effects made inter-

actions more responsive and engaging. Our findings show how to endow a large variety of touch interactions with expressive multisensory effects.

3.2 Introduction

Interacting with our environment frequently involves touching, exploring, or manipulating objects with the hands. Among the many haptic technologies that have been developed, few have been designed to augment naturally occurring touch interactions. Many existing haptic devices are based on controllers, instrumented surfaces, or hardware interfaces that must be operated by the hands. By occupying the hands, such interfaces often inhibit the great majority of manual interactions that support daily activities. We envisage new classes of electronic haptic interfaces that accommodate manual interactions involving direct skin contact with any object or surface in the surroundings. Only a few wearable devices for the hand have been designed to provide touch feedback without occluding skin-object contact [99, 100]. Addressing this gap could enable a wider range of human activities to be augmented with useful haptic information or evocative effects.

Here, we present a system for rendering effects that augment naturally occurring tactile sensations during manual interactions with objects and surfaces (Fig. 3.1. The system senses naturally occurring vibrations in the skin that are produced by contact with touched objects [101, 102] and transmitted throughout the skin [103, 104]. It processes the vibrations in real-time using a parametric signal network before returning them to the hand and ear as multisensory "echoes" of tactile interactions. Just as acoustic echoes are continuously produced in response to sound, Tactile Echoes can be continuously produced in response to touch interactions. A hard tap produces a higher-amplitude response than a light tap, and a continuous slide produces feedback that is extended through time. The system can produce a wide array of responsive and evocative effects

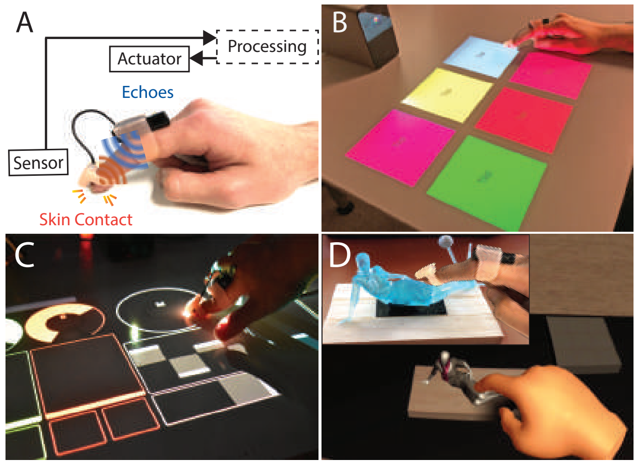

Figure 3.1: (A) Tactile Echoes system and concept. The wearable device captures vibrations in the fingertip that are produced during touch interactions, and processes them, and returns them to the finger as "echoes" of touch. (B) In this application, different Tactile Echoes are assigned to each region of the projected surface. The finger is tracked via camera, allowing different echoes to be assigned to different mapped regions on the surface. (C) In a musical controller application, a user controls a performance system by interacting with haptically augmented buttons, sliders, and knob interfaces rendered via a camera-projector system. (D) A VR experience involving a physical proxy object in which users are free to interact with miniature 3D printed objects upon which Tactile Echo feedback is superimposed.

that can be parametrically designed using ten signal processing parameters.

Different Tactile Echoes can be assigned to different touched objects or interactions (Fig. 3.1B) by tracking movements of the hand in a mapped environment via optical, electromagnetic, ultrasound, or other technologies. This can enable a variety of applications in virtual, augmented, and mixed reality or human-computer interaction. Such applications can integrate informative surface-specific tactile feedback, introducing palpable digital information layers into physical environments, or can involve responsive, playful augmentations of ordinary touch interactions, among other possibilities.

In this paper, we first contextualize our work in the literature. We then describe the hardware and software, and the considerations that informed them. We next present experiments investigating how these unique haptic experiences are perceived. We describe three behavioral experiments and a multidimensional scaling (MDS) analysis based on user-provided descriptions and ratings. Analyses of the results shed considerable light on the perceptual dimensions underlying the unique experiences provided by our system. We next present several applications in which different objects, creative interfaces, or games are realized using Tactile Echoes. We then present a study evaluating how users appraised the form of tactile feedback provided by our system in one of these applications. We conclude with a discussion of these findings, opportunities for future work, and potential future implications for haptic engineering, augmented reality, and human-computer interaction design.

3.3 Background

The Tactile Echoes haptic feedback method shares similarities with other haptic feedback methods that are based on modulating the perceived properties of real objects by imposing forces felt via a haptic interface [105, 106] or with vibrations presented from a stylus [107, 108]. Such systems rely on generating signals to be reproduced via a device in response to performed motions or forces, but do not provide feedback during direct manual contact with touched objects. Closer to the approach taken in our work is the tactile magnification system of Yao and Hayward [109], which amplifies the sensations felt via a surgical tool.

Many other approaches to providing haptic feedback have been based on electronic gloves or exoskeletons [110, 111, 112], finger-mounted haptic devices [113, 114, 115, 116, 117], or grasped controls [118]. Few of these systems have integrated feedback from both real and virtual objects during free-hand interactions (in which the motion of the hand is essentially unrestricted). The great majority also introduce a surface or material between the hand and touched object, and thus restrict natural tactile sensation felt by the hand. Overcoming these limitations, as in our system, could pave the way for more effective and engaging haptic augmented and virtual reality systems.

In contrast, several methods have been proposed for superimposing touch-dependent haptic feedback on a tactile surface explored with the skin – typically a bare finger [119, 120, 121, 122, 34, 123]. Similar to these methods, we compute tactile feedback via an algorithm that processes the sensed touch input. However, nearly all prior approaches of this kind provide feedback that is designed for a particular interaction type, such as textural sliding or tapping. The Tactile Echoes system generates feedback by processing the naturally occurring vibrations in the skin. The same algorithm can be applied to augment a wide variety of interactions – tapping, sliding, grasping, scratching with a finger, among other possibilities, all using the same system. One key difference between our work and the aforementioned examples is that our system augments real tactile interactions with unmistakably synthetic or "cartooned" haptic feedback that does not aim for realism, but rather at producing evocative effects. An analogy can be drawn to image distortion filters that are used for creative portraits, or to special effects in computer graphics, such as sparkles, glow effects, or explosions.

Recently, several researchers have described wearable electronic systems for capturing, amplifying, and reproducing natural tactile signals via skin-worn electronics. These include prior research in our lab [124, 125], and Makino et al. [126] as well as several collaborative works by Minamizawa, Maeda, Kakehi, Nakatani, Tsuchiya, Mihara, Peiris, and Tachi [127, 128, 129]. This research shows how it is possible to realize evocative experiences by concurrently sensing tactile signals elicited through skin-object contact and by amplifying the sensed signals to provide feedback on the same limb or another part of the body.

Such tactile amplification systems can yield interesting perceptual effects that are somewhat analogous to the auditory parchment skin or potato chip illusions [130, 131]. Several cross-modal effects of this type have also been uncovered. For example, in 1932, von Schiller reported tactile roughness perception to be influenced by the presence of concurrent auditory stimuli [132]. Other researchers have investigated the simultaneous use of vibrotactile and acoustic feedback associated with contact interactions. For example, Koehn and Kuchenbecker reported that users preferred haptic-auditory feedback from tool vibrations during robotic surgery [133]. Our system integrates haptic and auditory feedback in a way that is directed less at realism than at playfulness.

3.3.1 Summary of Contributions

Here, we show how both the sensing and feedback actuation may be located on the same finger. Locating both sensing and actuation near the fingertip allows the physical and virtual sensations to better fuse into a single percept during touch interactions with physical objects. Crucial to our approach is our use of signal processing methods that minimize feedback instabilities, and that increase perceptual saliency by avoiding perceptual masking effects.

Prior examples of tactile amplification systems have provided for at least limited processing of the feedback that is supplied, including amplification. Maeda et al. went further by allowing for filtering, distortion, and other effects [128]. Here, we greatly expand on this approach by showing how a plurality of parametric processing stages can be used to yield a large continuum of haptic effects. We also use psychophysical methods to reveal several distinct underlying perceptual dimensions. The parameters in our system are addressable via UDP networked communication (as demonstrated in the applications presented in later sections of this paper).

Another key contribution of our work is that we show how to realize programmable tactile augmented reality with direct skin-object contact. We achieve this aim by combining wearable sensing, processing, and amplification with spatial position tracking.

This system allows us to selectively assign distinct haptic effects to different surface regions or objects in a spatially mapped environment. In some configurations, our approach is analogous to visual augmented reality techniques that use projection mapping or head-mounted displays. Our research expands on previous approaches to haptic augmented reality that are based on users of electronic haptic feedback to supplement what is felt during interactions with real objects and environments [134, 135]. Our approach contrasts with these tool-based approaches, and instead augments interactions involving direct skin contact, similar to the projects discussed in the foregoing. Another distinctive aspect of our approach is that we supply responsive haptic feedback that, while derived from measured natural tactile signals, is unmistakably synthetic or "cartooned". Similar approaches have been used in gaming or other applications [136].

Various methods have been used to investigate the perception of haptic feedback or effects superimposed on physical surfaces [137, 138, 139]. However, the Tactile Echoes system provides augmented tactile feedback that could be compared to synthetically rendered graphic effects (e.g., explosions) superimposed on real visual scenes. Such feedback need not resemble any natural touch experience, and indeed is not intended to reproduce natural touch experiences. Informed by these observations, we studied how Tactile Echoes are perceived via behavioral experiments, using a multidimensional scaling (MDS) paradigm. Since it was unclear, a priori, what factors or descriptors would best match Tactile Echoes, we based our approach on a methodology in which we systematically collected labels from users themselves, rather than from descriptors that we judged to be appropriate. Similar MDS methods have been previously used to assess the perception of natural haptic materials [140, 141, 142] and mechanisms [143] and have also been used to characterize the perception of synthetic haptic effects [144, 145]. In addition to identifying the perceptual space that characterizes Tactile Echoes, we demonstrate opportunities for applying our system in several simple applications, including a

VR application in which passive props [146, 147] acting as haptic proxies are augmented with dynamic, programmable tactile feedback.

3.4 System Design

The responsive and multisensory (haptic and auditory) feedback provided by Tactile Echoes is delivered by a system (Fig. 3.2) that captures and concurrently processes naturally occurring vibrotactile signals in the skin during manual interactions. The embodiment presented here senses vibrations in the finger as they are produced through touch interactions. It processes the sensed vibrations in real-time via a parametric signal network running on a computer, and continuously returns them to the finger and the ear (respectively using a vibrotactile and audio output device). The resulting tactile and auditory feedback augments what would normally be experienced during the touch interaction.

The wearable portion of the system consists of a fingernail-worn piezoelectric vibration sensor and a wide-bandwidth inertial voice coil actuator. The sensor, actuator, and cables are mounted in custom, ring-like brackets that were designed in CAD and fabricated in synthetic rubber via industrial molding (Fig. 3.1A). The piezoelectric sensor signals are amplified (Puremini Amplifier, K&K Sound) and digitized in real-time using an audio analog-to-digital converter (Model 624, Mark of the Unicorn). The sampling rate is 44100 Hz. They are processed via a signal processing network running on a computer, and amplified (LP-2020A, Parts Express Inc.) after digital-to-analog conversion (Model 624, Mark of the Unicorn). The amplified signals drive the voice coil (Haptuator Mark II, Tactile Labs Inc.), returning the processed tactile signal to the finger with low latency (latency values are reported below). We use the same feedback signal in order to generate synchronous auditory feedback via a loudspeaker, headphone, or other device.

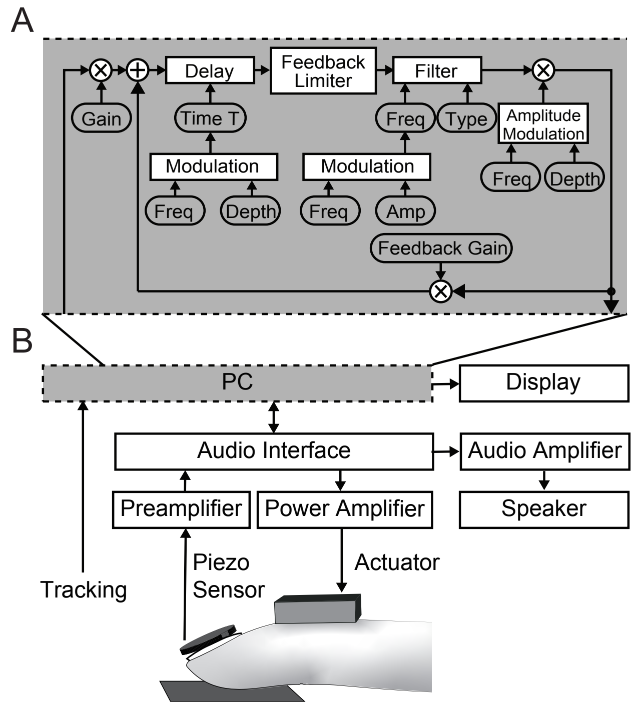

Figure 3.2: (A) The Tactile Echoes are generated from the input via a parametric signal processing network. It includes modulated delay, nonlinear feedback limiting, amplitude modulation (tremolo), and modulated filtering. This architecture is sufficient to produce a wide variety of parametrized audio effects. (B) System Diagram: A piezoelectric sensor worn on the finger captures vibrations in the fingertip. The vibrations are amplified and concurrently processed by a computer. A signal processing network parametrically modifies the signals, which are amplified and returned to the finger via an inertial voice-coil actuator, and to the ear via a loudspeaker or headphone.

Tactile Echoes effects are produced by a parametric signal processing network (described below). The processing to be applied may be modified based on the proximity of the finger to different objects in the surroundings using standard tracking methods. For example, in Section 7 below, we demonstrate how to apply this technique when tracking the spatial position of the finger using the integrated camera of a smart projector system (Touch Xperia, Sony Inc.) for augmenting touch feedback on a projected touch surface, or via an optical hand tracking device (Leap Motion, Ultraleap Inc.) for augmenting tactile feedback on passive proxy objects in virtual reality. In such applications, the position tracking does not need to be precise enough to capture the contact event with high temporal accuracy. Instead, our system identifies the nearest mapped surface and selects the appropriate Tactile Echo before the surface is touched. Thus, many different motion tracking technologies could be used (for a recent review, see [148]). Our use of proximity to select the mode of feedback (i.e., the Tactile Echo settings) allows the tactile feedback to be responsively and automatically generated, synchronous with the touch event, because the Tactile Echo itself is driven by vibrations in the skin that are generated through finger-object contact.

While there are inevitable delays between the capture of input vibrations and the first feedback returned to the finger, our design leverages even longer delays (from 10 to 30 ms) than are imposed by system requirements, in order to enhance the effects themselves. During the course of designing our system, we observed that providing the aforementioned minimum delays greatly enhanced the perceptual saliency of the feedback. We hypothesize that this enhancement is due to a reduction in tactile forward masking effects. Kaaresoja et al. found that delayed tactile feedback increased the perceived mass of an electronic button [91]. The feedback delays in our system also reduce sensor-actuator feedback instabilities by allowing within-skin vibrations additional time to decay. Prior findings from our lab show that contact-like vibrations applied to the skin decay within a few tens of milliseconds [101].

3.4.1 Tactile Echoes – Signal Processing

Touch elicited vibrations in the finger are processed in real-time via software to yield a variety of parametrically-controlled effects. In our initial prototypes of this system, we used a guitar multi-effects box to explore the tactile feedback generated by a set of 55 common audio effects during touch. These initial experiments revealed that some com-

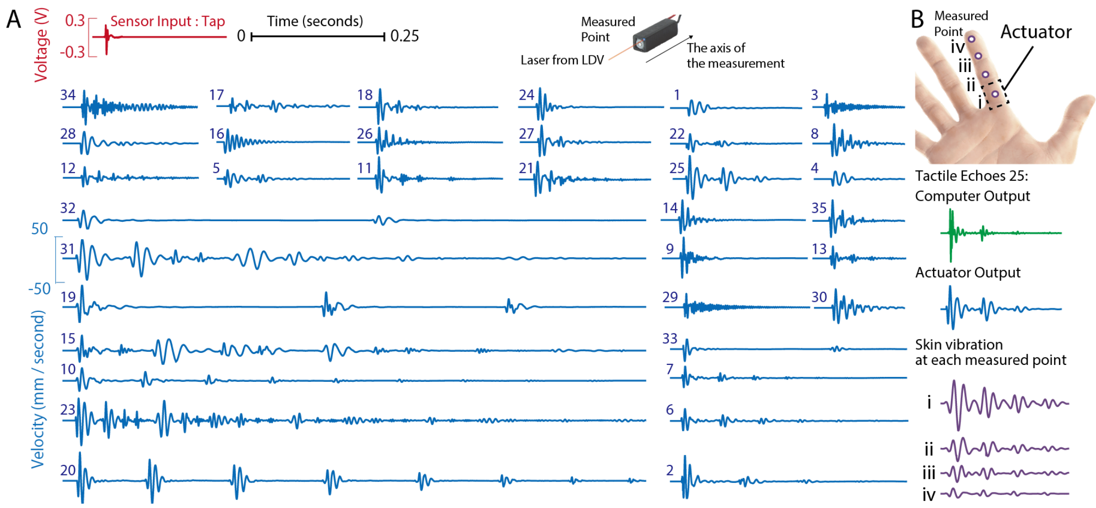

Figure 3.3: (A) Waveforms produced by 35 designed effects in response to a single, pre-recorded finger tap captured by the piezo sensor (shown in red). The generated waveforms (in blue) are the "echo" signals furnished to the skin by the actuator. They were measured via Laser Doppler Vibrometer (LDV) along the axis of actuator vibration (top center). Each Echo is specified via values of ten processing parameters. In applications, different output waveforms are produced by each Echo in response to different touch inputs, much like different natural tactile signals are felt when touching an object differently. These Echoes each comprise one stimulus used in the perception experiments (Sec. 3.5). (B) Computer voltage output (green trace) and actuator casing vibration (velocity, LDV measurements, blue trace) produced by a single echo, at four skin locations (i-iv, velocity, LDV measurements normal to skin surface, purple traces).

mon audio effects, such as too long reverberation and distortion, seemed uninteresting, while others were highly evocative. Informed by this experience, we designed our system software to comprise a flexible, digital signal processing network of selected audio effects, with parametric controls over different processing stages (Fig. 3.2A). We use this signal processing network to generate a variety of Tactile Echoes by manipulating the values of the parameters. The network comprises a feedback delay structure with a variable gain, a resonant multimode filter, and nonlinear limiting integrated in the forward path of the delay structure. The limiting stage suppresses feedback loop instabilities and provides adaptive gain functions. Low frequency sinusoidal oscillators can optionally modulate each of the processing stages. In total, there are ten parameters that may be selected to specify the processing: output gain, feedback gain, delay time, filter corner frequency, filter type (highpass, lowpass, bandpass), filter resonance (Q factor), delay time modulation frequency and depth, and amplitude modulation (tremolo) frequency and depth. In other embodiments, a variety of other processing stages could also be used.

The amplitude modulation stage mitigates feedback instabilities that can arise due to the physical proximity of the sensor and actuator. We selected this feedback suppression method based on prior research in our lab, which evaluated several alternatives [149]. Feedback suppression is also aided by the imposed delays, as noted in the preceding section. While we have observed that such instabilities can occur for select settings within the large parameter space of our system, this only very occasionally arose during spontaneous use by hundreds of visitors to demonstrations we have given. For our experiments (described below), we selected the parameter settings of the stimuli to avoid feedback instabilities (and confirmed their absence through signal observation during the experiments).

Depending on the selected parameter values, the signal processing network can produce a large variety of effects. Some of these can resemble audio effects that are used in music production and performance, such as echo, slap-back, reverb, filtering, tremolo, filter delays, flange, or chorus effects, among others. Such effects have less often been used for the design of haptic or multisensory feedback. Through informal experimentation, we found delay time to produce the most appreciable qualitative changes. Delay times between 30 and 500 ms yielded especially interesting effects. The delay time also included a fixed feed-forward delay, due to input-output buffering in the digital audio hardware mentioned above. For our system settings, we measured this delay to be 20 ms. This value could be reduced significantly through software optimization, and could be reduced to below 1 ms using off the shelf hardware and software methods. However, we found that much stronger perceptual effects were produced if we ensured that a delay time of at least 30 ms elapsed between the sensor input produced by a touch interaction. We conjecture that this perceptual effect is due to tactile forward masking. We intend to explore this phenomenon in future work.

3.4.2 Tactile Echoes – Design and Mechanical Characterization

The large size of the 10-dimensional parameter space of our signal processing network precluded systematic evaluation of all parameter combinations. However, through manual search we identified regions of the parameter space that yielded palpable feedback and others that did not. Guided by these observations, we performed a heuristic search based on which we identified parameter settings for 88 varied Tactile Echoes that we judged to be interesting. We then selected 35 Echoes which we felt approximated the expressive range of effects that could be produced using our system and with our parametric signal processing network. We observed the differences between these 35 Echoes by measuring the vibrations produced by the actuator when attached to a participant's finger (female, length of hand 16.5 cm, measured on right index finger). The hand from which measurements were captured arm was fixated to a vibration isolated table, with the measured finger left free. A non-contact Laser Doppler Vibrometer (Polytec PDV-100, Irvine, CA) measured the actuator velocity along the axis of vibration in response to the same, pre-recorded input from a discrete tap of the finger. The measured waveforms ranged in duration from 0.25 to 1 s, had varied densities of feedback, and different decay properties (Fig. 3.3A). While these sets of parameter values produced noticeably distinct waveforms, our heuristic selection process motivated the design of our experiments, which were based on user-supplied semantic labels and ratings, and an MDS analysis.

When reproduced via the wearable hardware, Tactile Echoes yield mechanical vibrations of the skin that propagate as viscoelastic waves [150, 101]. From physics, such vibrations are expected to attenuate with distance d in a manner that depends on their frequency content [104]. For a vibration component of frequency f, a decrease in amplitude A with distance d is expected, with an approximately exponential relationship,

$$A(d) \sim \exp(-\alpha d f), \tag{3.1}$$

where α is a damping coefficient. This damping contributes to the spatial localization of feedback in the finger, and reduces the influence of the actuator signal on the sensed signals. In our system, the combination of processing, feed-forward delay time, and damping in the skin reduce feedback instabilities, enabling larger gains to be used, and increasing dynamic range of the stimuli.

We empirically evaluated the vibrations imparted to the skin by the actuator when driven by Tactile Echoes waveforms using a non-contact scanning Laser Doppler Vibrometer (SLDV; Polytec PSV-500, Irvine, CA). The vibrometer measured the velocity of skin vibration in the direction normal to the volar skin surface at four locations (Fig. 3.3B). These measurements revealed that the Tactile Echoes system produced vibrations that were transmitted within the skin. The vibration waveforms at remote locations were similar to the those of the actuator signals. As expected from physics, the vibrations exhibit little change in signal phase with distance (Fig. 3B), due to the relatively large (> 2 cm) wavelengths that occur at tactile frequencies ($f < 1000$ Hz). The vibrations attenuated with distance as expected from wave mechanics [151, 104].

3.5 Perception Experiments

The goal of the experiments was to determine how touch interactions augmented by the Tactile Echoes were perceived and to identify a perceptual space that adequately described the perceptual similarity of different Tactile Echoes. The Tactile Echoes system can be applied to augment a wide variety of finger interactions such as sliding, grasping, tool-use, or scratching. We based our behavioral studies on a single gesture type, involving a discrete tap of the fingertip, which we judged to be an adequate proxy for transient contact events, such as initial skin-object contact, frequently occur during a large variety of manual interactions, such as pressing a switch, grasping an object, or touching a surface.

Our study design was informed by the fact that the Tactile Echoes stimuli are synthesized, and not intended to be realistic, and by our interest in avoiding biasing participant responses with our expectations about how the stimuli might be perceived. Our study is based on three perceptual experiments, a multidimensional scaling (MDS) procedure, and a regression analysis comparing the semantic ratings generated from the perceptual experiments with the MDS analysis. The three perceptual experiments consisted of a semantic labeling task, which employed a free verbalization method to elicit vocabulary which could be used to describe the sensations produced by the Tactile Echoes, a semantic sorting task, in which participants voted on the semantic labels to construct a unified set of 10 unipolar semantic labels to be used across participants, and a rating task, in which subjects rated the 35 Tactile Echoes based on semantic labels we determined via the preceding experiments. Our study was similar to those used in prior research [140, 141, 142]. This approach avoids difficulties that can arise if pre-determined adjective pairs are used [152]. Our system is also capable of producing multisensory feedback, by playing the Echoes as audio. To investigate the effect of this concurrent auditory feedback on how Tactile Echoes are perceived, we included both haptics-only and multisensory (audio-haptic) conditions.

3.5.1 Methods

Participants

In a first experiment, five native English speakers participated (ages 20 to 27, 3 male, 2 female). In a second experiment, a new set of seven native English speakers (ages 20 to 29, 4 male, 3 female) voted on the words that best described each stimulus. In a third experiment, fifteen new individuals (ages 20 to 50 years old, 10 male, 5 female) participated. All participants were right-hand dominant. Participants gave their written informed consent for the experiment, which was conducted according to the protocol approved by the UCSB institutional review board. Subjects were paid $10 per hour for participating.

Apparatus

All experiments used the Tactile Echoes system. Participants were seated in a well-illuminated quiet room in front of a computer. Participants' hands were cleaned and sanitized in advance. The device was worn on the participant's dominant hand (right hand in all cases). In two conditions, haptic or multisensory, participants felt the Tactile Echoes with or without sound. In the multisensory condition, tactile and auditory feedback were produced concurrently via the same waveform used to drive the actuator. All experiments incorporated both conditions, haptic and multisensory. Every participant completed both conditions, one after the other, in random order per participant. Participants wore noise-cancelling headphones to prevent auditory cues, outside of those being presented in the multisensory condition. A curtain obstructed the view of the hand. We used a plastic-coated plywood sheet as the touch surface for all perceptual experiments. The surface was flat and uniform.

Stimuli

We used the set of 35 designed stimuli in all experiments (Fig. 3.3A). Each stimulus setting was presented once, individually, one per trial, in random order. During each trial, participants repeatedly tapped the surface at a rate of 0.67 Hz (guided by a visual metronome) while maintaining a tapping force between 1 and 1.5 N. We provided this guidance to ensure that participants experienced the stimuli in similar conditions. Software estimated the tapping force from the piezoelectric sensor signal, calibrated based on measurements from a laboratory force sensor. A visual indicator showed when participants tapped with appropriate or inappropriate force. Before the experiment, participants briefly practiced the procedure and practiced tapping with the requisite force levels.

3.5.2 Experiment 1: Descriptive Word Harvesting

In a first experiment, participants provided descriptive labels for the stimuli in each of the haptic and multisensory conditions. On each of the 35 trials, participants provided as many verbs and adjectives as they could to describe how the stimuli felt to them. Participants could experience each stimulus for as many times as they preferred and could enter responses as they proceeded. The duration of the first experiment was about 40 minutes.

3.5.3 Experiments 2: Word Voting

In a second experiment, a new set of participants voted on the words that best described each stimulus. We aggregated all of the words from the first experiment, after merging similar words using dictionary definitions and thesaurus associations. During each trial, participants were presented with one stimulus and a master list, in randomized order, of all words that had been collected for any stimulus via the first experiment. For each stimulus, participants selected any and as many words from the entire list that described what they felt. For each stimulus, participants could tap for as long as they preferred while they responded. The second experiment lasted about 30 minutes in total.

3.5.4 Experiment 3: Semantic Scaling

In a third experiment, a new set of participants rated each of the stimuli on a set of twelve semantic differential scales derived from the semantic labeling experiments. During each trial, participants rated one of the stimuli on 12 semantic differential continua. Responses were entered via computer. We used continuum scales rather than Likert scales to avoid introducing quantization (rounding) errors that could lose information. The semantic differential labels were chosen as the eleven most voted labels in Experiment 2. One further label “Real” was added by the experimenters, but yielded ambiguous results. Each of the 12 scales consisted of the label at the left extreme of the visual analog scale, and a second “not” label, indicating the literal converse, at the opposite side. Participants could experience each stimulus for as long as they preferred while they responded. We collected informal written comments and verbal reports from participants about their experience after the experiment. The duration of the third experiment was 1 hour, including a ten minute break.

3.5.5 Data Analysis

Semantic Labeling

The data from experiment 1 consisted of word sets that were aggregated to form the word list for voting in experiment 2. The word lists and votes were not further analyzed. The data from experiment 3 consisted of semantic differential scale ratings of each of the 35 stimuli in each condition (haptic, multisensory) by each participant. We analyzed the haptic and multisensory stimuli separately.

MDS Analysis

To assess the number of independent perceptual dimensions needed to describe the responses, and to derive a space that parametrized how the Tactile Echoes are perceived, we used the Classical Multidimensional Scaling (MDS) algorithm. It minimizes the mean residual error, called the strain between Euclidean distances (dissimilarities) among the original response vectors for each of the 35 Tactile Echoes gathered from the scaling experiment and the distances between their projection in a lower-dimensional embedding space.

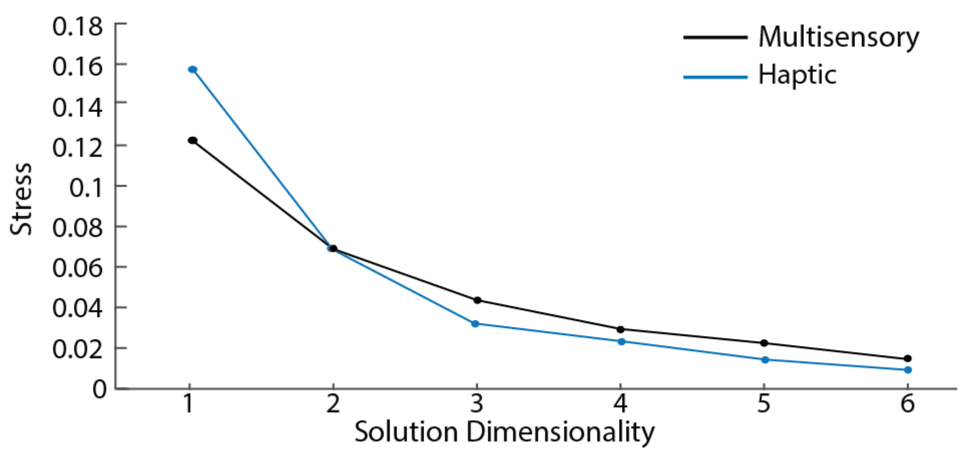

Figure 3.4: Scree plot showing the residual errors between the dissimilarity matrix and the MDS solutions as the number of dimensions increased.

We computed MDS embeddings of dimensions 1 to 6, and computed the strain residuals for each. We selected embedding dimensionalities ($M = 2, 3$) based on the knee in the plot of strain residual vs. dimension (scree plot, Fig. 3.4), see discussion below. We computed the corresponding MDS embeddings for each value of the dimension, yielding four spaces in total: two spaces for each condition and two spaces for each dimension. We computed mean response ratings for each stimulus and mapped each such value to one point in each MDS space.

Regression between Scales and MDS Spaces

We assessed the quality of the embeddings via Shephard diagrams – scatterplots of the dissimilarities vs. distances for each stimulus – and calculated R^2 values for each.

To further interpret the MDS mappings, and assess their quality, we used the entire dataset to fit the response data for each semantic differential scale as a function of the embedding coordinates. Regression of each scale yielded a line through the origin in each MDS space. We computed the R^2 values for each fit in order to assess the regression quality for each scale. This result allowed us to identify the semantic scales that were best predicted by the MDS coordinates, as those with the highest R^2 values. We identified orthogonal scales with high R^2 values (where $M = 2, 3$ is the embedding dimension) in order to interpret the MDS spaces in terms of participant-provided responses.

Similarity of the Semantic Labels

We used linear regression to map the perceptually-derived MDS spaces to each of the 12 semantic scales. Next, to investigate the perceptual dependence and independence of pairings of the response data for each semantic scale, we computed the relative angles between pairs of regression lines for each semantic scale in the MDS spaces (see Sec. 3.5.3) for both the haptic and multisensory conditions. For efficiency of presentation and to adhere to the length restrictions of this paper, we confined this further analysis to the 2D haptic and multisensory MDS spaces. We selected scales with $R^2 > 0.7$ for comparison. In brief, each regressed scale in each MDS space determined a vector with unit norm, $\mathbf{u}_i$, where $i = 1, 2, \ldots, 12$. The geometric angle θ_{ij} between each pair of scales in each MDS space was computed as $\theta_{ij} = \arccos(\mathbf{u}_i \cdot \mathbf{u}_j)$. Angles close to 0 degrees are interpreted as the semantic scales describing identical sensations, while angles of 90 degrees are interpreted as the semantic scales describing independent perceptual dimensions. Angles of 180 degrees are interpreted as the semantic scales describing bipolar sensations.

Comparison of Multisensory and Haptic Conditions

To compare the perception of Tactile Echoes in the multisensory and haptic conditions, we computed the distributions of pairwise distances of the mean stimulus response values in each MDS space. These distributions describe the perceptual similarity between the stimuli in each condition. We compared the multisensory and haptic distributions for both the 2D and 3D MDS embeddings and used a Wilcoxon signed-rank test to ascertain whether the median perceptual distance between stimuli was different between conditions.

Next, we investigated differences in descriptor ratings between the haptic and multisensory conditions. In order to conduct this comparison between the multisensory and haptic conditions for each stimulus type, condition, and each semantic differential label, we computed a three-way ANOVA (conditions and stimuli, and descriptors as within-participant factors) and applied a Bonferroni multiple comparisons test. Before computing the ANOVA, we checked for normality of residuals and homogeneity of variance. To check residual normality, the residuals from the model fit were analyzed graphically using Q-Q Plots; the residuals appeared normally distributed. Because there were 10,080 residuals, even small deviations from normality would be heavily penalized in conventional

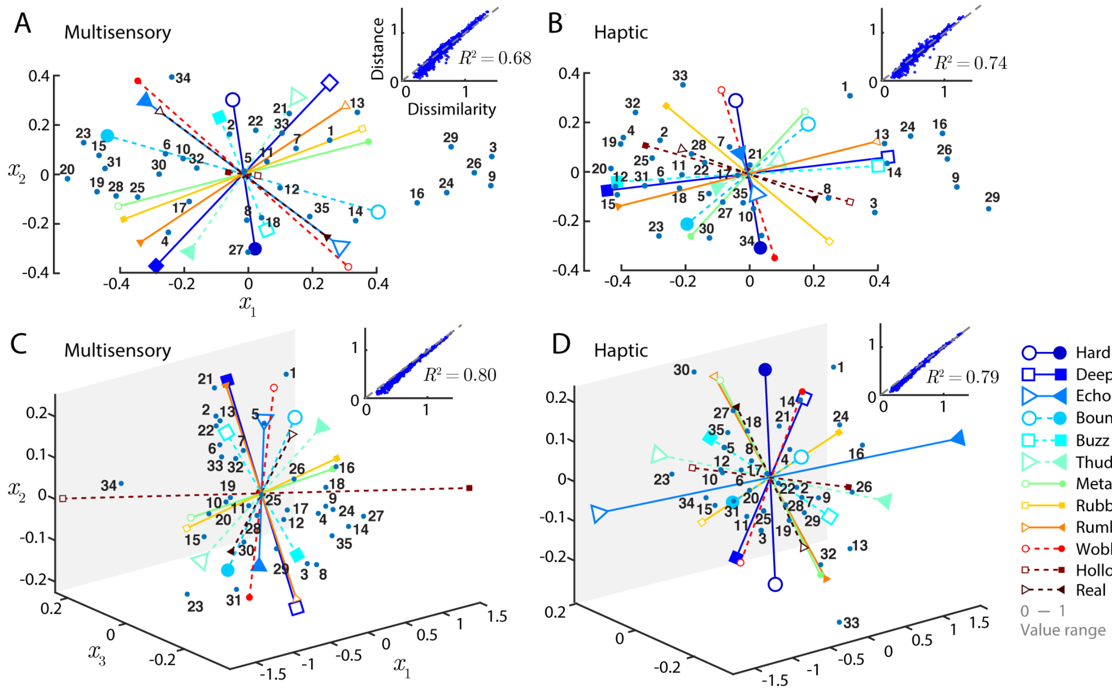

Figure 3.5: The MDS analysis yielded embeddings of the Tactile Echoes stimuli in low dimensional spaces. The MDS embeddings were computed so that stimuli that are embedded near to each other received similar ratings in the semantic differential scaling experiments. For each condition, we computed MDS spaces in two dimensions (A: Multisensory, B: Haptic) and three dimensions (C: Multisensory, D: Haptic). The lines represent regression axes from MDS spaces to the semantic differential scale values; they ranged from 0 (hollow symbol) to 1 (filled symbol). The line length for each axis is proportional to the R^2 value of the regression, with longest lines denoting highest R^2 values. The Shephard plots (inset figures) show that the embedding quality increased for 3 vs 2 dimensions. Figure adapted from the conference paper of which this article is a revised and extended version [125].

normality tests. To test for homogeneity of variance, we used multiple-sample tests for equal variances. After establishing significant main effects using an ANOVA, we used the Bonferroni multiple comparisons method to test for differences between the groupings of condition, descriptor and stimuli.

3.5.6 Results

Semantic Scaling

The results of Experiment 1 consisted of word sets that were aggregated to form a word list for voting in Experiment 2, which determined the semantic scales used in Experiment 3. We obtained 117 words in the haptic condition and 160 words in the multisensory condition. 46 words were common to both conditions.[1]

Perceptual Spaces

Each of the four MDS analyses yielded a monotonically decreasing stress residual as dimensionality increased (Fig. 3.4), as expected. In both the multisensory and haptic conditions, the stress declined most as the dimension increased from 1 to 2 and from 2 to 3. The stress began to plateau as we increased the MDS solution space dimensions from 3 to 4. Thus, we focused our analysis on MDS spaces of dimension 2 and 3. Retaining both values of M for analysis allowed us to better understand how the MDS solution quality varied with dimensionality.

For each stimulus, we computed the mean value of all ratings across all presentations and mapped the resulting vector to the corresponding MDS space (Fig 3.5). The set of stimuli were widely distributed in all four spaces. The MDS optimization is invariant to orthogonal transformations – rotations and reflections of the data – so the orientation within these spaces is not informative.

Comparing the mean stimulus positions in the haptic and multisensory conditions, some Tactile Echoes that were near to one another in the haptic condition remained so when audio was added (examples in the 2D plot include 19 vs. 20, 29 vs. 9, 2 vs. 22, 29

[1]The word lists are omitted for brevity. The lists, related results, and more details of the ten parameters in Tactile Echoes processing are summarized at this website: `http://spectrum2.mat.ucsb.edu/anzukawazoe/conf/TactileEchoes.html`.

vs. 9). Others that were near to one another in the haptic condition were farther apart in the multisensory condition (examples in the 2D plot include 10 vs. 34, 8 vs. 3, 2 vs. 25, 4 vs. 19). This is consistent with informal reports by participants that some Tactile Echoes features were perceived to be more prominent acoustically than haptically.

The linear regression analysis yielded a line representing each semantic scale in each MDS space (Fig 3.5). In the figure, line length is proportional to the R^2 value for the respective regression. The R^2 values ranged from 0.11 to 0.99. Several of the scales were nearly parallel, such as Wobbly and Echoing in the multisensory condition and Deep and Buzz in the haptic condition. These results suggest that these scales were interpreted redundantly by participants in each condition. Others, including Hollow, remained nearly orthogonal to the other scales in all MDS cases, suggesting these ratings captured complementary perceptual ratings to the others. While there is no objective threshold for what constitutes a meaningful relationship, other researchers have relied on the judgement that scales with R^2 values greater than about 0.7 reflect substantial relationships [143, 140, 141]. In all four analyses, Deep, Rubbery, Rumble, and Wobbly yielded R^2 values greater than 0.7. It is often desired in such analyses to identify subsets of the scales of the same dimension as the space itself with high R^2 values. Such subsets can be used to interpret the MDS embedding coordinates of different stimuli. Suitable pairs in the 2D analyses include Deep-Wobbly in both the haptic and multisensory conditions, and Wobbly-Rumble or Wobbly-Deep (among other possibilities) in the haptic condition. In the 3D MDS analysis, one can point to triplets such as Wobbly-Rumble-Buzz in the haptic condition, or to Rubbery-Buzz-Wobbly in the multisensory condition.

Perceptual Similarity Between Semantic Scales

The relative angles between pairs of semantic scale regression lines (with $R^2 > 0.7$) in the MDS spaces reflected the perceptual similarity between the scales. Several pairs of scales yielded small, nearly parallel angles (angle magnitude $<$15 degrees) reflecting high similarity, while several others were nearly orthogonal (90$\pm$10 degrees) indicating high perceptual independence (Table 3.1, shown in decreasing order of R^2 value).

Comparison of Multisensory and Haptic Conditions

The distribution of distances between mean stimuli ratings in the haptic and multisensory conditions was non-normal for both the 2D and 3D MDS embeddings. A Wilcoxon signed-rank test indicated a significant difference between the medians of the pairwise distances in the two conditions in 2D (median difference: 0.056, $Z = -3.7, p < 0.001$) and 3D (median difference: 0.057, $Z = -4.23, p < 0.0001$).

The three-way ANOVAs of the distributions of semantic ratings between conditions yielded residuals that were approximately normally distributed, with some light-tailed behavior, as determined graphically using Q-Q plots. Bartlett's multiple-sample tests showed that the variances in the semantic scale values across the stimuli, conditions, and descriptors were not significantly different ($p = 0.06$), supporting a constant variance analysis. The results of ANOVA test for all factors that were significant are shown in Table 3.2. The Bonferroni-corrected comparisons of semantic scale descriptors revealed that several descriptors were significantly different between the haptic and multisensory conditions (Table 3.3); ratings of Deep, Buzz, and Metallic were significantly higher, while ratings of Echoing, Bouncy, and Wobbly were significantly lower, in the haptic condition relative to the multisensory condition.

3.5.7 Perception Experiments: Discussion

Perceptual Spaces for Tactile Echoes

The descriptive word harvesting experiment revealed that participants employed a large variety of words to describe the effects. Examples included Wiggly, Thud, Twanging, Drop, Rattle, Thump, and Bouncy. In the haptic condition, words often evoked physical phenomena (Friction, Waves, Pulse, Thumping, Shock, and Reverberation). The multisensory experiment, which added auditory feedback, elicited a large number of descriptors that referred to material properties (Wood, Water, Marble, Glass, Liquid, Fluid, Woody, and Jelly) as well as words related to musical instruments (Drum, Banjo, and Guitar). The differences between the word lists in the haptic and multisensory conditions suggest that the presence of sound facilitated associations with material properties or objects, and that in the absence of sound, the effects evoked more abstract phenomena.

In prior studies, it has been observed the perception of Roughness, Softness, and Temperature are involved in material recognition [153] and, in texture perception, that Roughness, Softness, and Sticky or Slippery are important perceptual dimensions [141]. In our experiments, participants provided words that are associated with roughness and softness (Rough, Gritty, Hollow, Soft, and Hard), and words that were found in haptic texture studies (Sticky, Smooth, and Slippery). We did not obtain words related to other dimensions, like temperature, which are not frequently associated with vibration signals. Thus, although some of the Tactile Echoes stimuli appeared to evoke physical objects or processes, the association was limited in scope. In the voting experiment, the most commonly occurring word across both conditions was Bouncy. Others that were frequently selected included Echo, Short, Hard, Heavy, Rubbery, Rumble, and Light. Together, these comprised the most popular (top 15%) descriptors common to both conditions.

Table 3.1: Magnitudes of relative angles between semantic rating scale regression lines in the 2D MDS solution space (Left: Multisensory, Right: Haptic). Pairs with nearly orthogonal angles (90±15 degrees) bold, in red cells. Pairs with small angles (0±15 degrees) underlined in blue cells. Pairs with angles 180−15 degrees are green.

	Wobbly	Deep	Bouncy	Echoing	Rumble
Wobbly (0.944)	-				
Deep (0.8867)	**101.6**	-			
Bouncy (0.879)	28.6	73.0	-		
Echoing (0.8165)	<u>4.8</u>	**96.7**	23.8	-	
Rumble (0.7978)	**88.5**	<u>13.1</u>	59.8	**83.6**	-
Rubbery (0.7901)	74.1	27.5	45.5	69.3	<u>14.4</u>

	Deep	Buzz	Rumble	Rubbery	Wobbly
Deep (0.9568)	-				
Buzz (0.8851)	<u>4.1</u>	-			
Rumble (0.8926)	170.9	166.7	-		
Rubbery (0.7883)	55.1	51.0	115.7	-	
Wobbly (0.7367)	**84.2**	**80.1**	**93.4**	29.1	-
Hollow (0.72)	27.8	23.7	37.0	152.7	123.6

The MDS analysis revealed that despite the diversity of descriptors supplied by participants, and the ten different parameters used to design the stimuli, the perceptual similarity between the stimuli could be well-explained by just 2 or 3 dimensions. Several descriptors were highly correlated ($R^2 > 0.7$) with the MDS coordinates, including Deep, Buzz, Rumble, Rubbery, Wobbly, and Hollow in the haptic condition, and Wobbly, Deep, Bouncy, Echoing, Rumble, and Rubbery in the multisensory condition. In the further analysis of the 2D perceptual spaces, some pairs of the descriptors appeared to capture similar perceptual attributes, while others were complementary (Table 3.1). In the multisensory condition, Echoing and Wobbly captured very similar perceptual information, as did Rumble and Deep, and Rumble and Rubbery. Thus the 2D perceptual space in the multisensory condition could best be parameterized via Deep-Wobbly dimensions, while the 2D perceptual space in the haptic condition could best be parameterized by the Wobbly-Rumble dimensions.

These results reflect differences between the Tactile Echoes stimuli in the conditions of the experiments, which involved tapping at approximately constant rates and forces on a relatively stiff surface. Further research is needed in order to clarify how these results might change if the tactile interactions were different. We hypothesize that a greater diversity of interaction types (e.g., continuous sliding on smooth or textured surfaces, tapping on soft surfaces) would increase the range of perceptual responses.

Effects of the Sensory Conditions

As indicated by the ANOVA, we found a significant interaction between "stimuli" and "conditions" (Table 3.2). This significant interaction suggests that the presence of sound qualitatively altered how the stimuli were perceived. Further, the significant three-way interaction term between "conditions," "descriptors," and "stimuli" (Table 3.2) implies that the qualitative change in how the stimuli were perceived in the presence of sound was dependent on the specific descriptor being rated. In another line of analysis, we found that the variation in responses, considered as the median pairwise MDS distances for the stimuli, was significantly smaller in the haptic than in the multisensory condition, indicating that the presence of sound increased the variation in responses. This is consistent with previous findings on multisensory perception [154, 130, 155].

The post-hoc Bonferroni multiple comparisons test indicated that there were significant differences in 6 of 12 descriptors ratings between the multisensory and haptic condition (Table 3.3). Ratings of Deep, Buzz and Metallic were higher in the haptic condition, whereas ratings for Echoing, Bouncy, and Wobbly were higher in the multisensory condition. As for the reason for this difference in rating, it would appear that the auditory component made it possible to discriminate some stimuli that could not be dis-

Table 3.2: Three-way ANOVA result in which conditions, and stimuli, and descriptors are within-participant factors. This table shows degrees of freedom (df), F-value, Significance (Sig.). Asterisks (*), (**), (****) indicate statistical significance at levels 0.05, 0.01, or 0.001.

Source	df	F-Value	Sig.
Conditions	1	9.364	**
Descriptors	11	28.826	****
Stimuli	34	16.029	****
Conditions*Descriptors	11	35.998	****
Conditions*Stimuli	34	1.642	*
Descriptors*Stimuli	374	2.639	****
Conditions*Descriptors*Stimuli	374	1.933	****

tinguished from tactile information alone. Such difference could be due to the narrower tactile bandwidth limited below 100Hz by tactile actuator limitations above 700Hz by the rapidly decrease of tactile sensitivity. The results of the Bonferroni test, comparing the multisensory and haptic condition for each of the 35 stimuli, showed no significant difference between the mean semantic rating values for each stimulus. Thus, the presence of sound did not result in higher average ratings, although, as reported above, there was an effect when stimuli were grouped for each condition. The different results can be attributed to the conservative Bonferroni correction that is applied in the former case.

3.6 Demonstrating Applications

We explored demonstrations of our system, informed in part by approaches adopted in previous research projects that have used wearable systems to haptically supplement naturally-occurring sensations felt during touch contact with real, physical objects associated with digital objects in virtual or augmented reality environments [98, 156].

We implemented three demonstration applications to illustrate how Tactile Echoes can be applied in virtual and augmented reality, human-computer interaction, and gaming. Our applications highlight the practical ways in which Tactile Echoes can be used

Table 3.3: Multiple comparisons (Bonferroni's test) of descriptors differing between conditions. The asterisks (****) indicate statistical significance at the 0.001 level.

Descriptor	Mean Rating Difference (Multisensory - Haptic)	p-Value
Deep	-0.124	$p < 0.0001$****
Metallic	-0.120	$p < 0.0001$****
Buzzing	-0.100	$p < 0.0001$****
Thud	-0.068	$p = 0.068$
Rumble	-0.017	$p = 1$
Bouncy	0.221	$p < 0.0001$****
Echoing	0.152	$p < 0.0001$****
Wobbly	0.112	$p < 0.0001$****
Rubbery	0.061	$p = 0.245$
Hollow	0.055	$p = 0.754$
Real	0.016	$p = 1$
Hard	0.007	$p = 1$

to augment touch interactions with tactile feedback that is highly responsive, is parametrically and perceptually varied (as our experiments show), and can be assigned to different real or virtual objects, surfaces, or controls. The feedback is very responsive to the physics of the interaction because it is generated from vibrations in the skin that are produced when touching real objects. The applications also illustrate how different low-complexity tracking methods are sufficient for enabling distinct Tactile Echoes to be selectively assigned to different objects, surface regions, or actions.

3.6.1 Multisensory Memory Game in VR with Augmented Passive Tangible Proxy Objects

In one application, we created a Virtual Reality memory game, modeled after the classic electronic game "Simon" (Fig. 3.6A). In it, users wear a head-mounted virtual reality headset. In a virtual game environment, they experience four, three-dimensional colored blocks. The blocks must be tapped in a specified sequence, matching a pattern that is first shown by the computer. After a user successfully reproduces a given sequence, the computer demonstrates a longer sequence. This proceeds until the user makes an error. The goal is to reproduce the longest sequence, yielding a high score. In the demonstration, the virtual blocks are co-located with physical blocks, which serve as passive haptic proxy objects [147], at corresponding registered positions in the physical environment. Each block is assigned a different multisensory Tactile Echo which is felt and heard by the user when activating one of the blocks. When the computer demonstrates a sequence, a representative, pre-recorded signal is used to generate the Tactile Echo associated with each block, which is heard, but not felt, by the user. Thus, the challenge can be regarded as that of memorizing the sequence as determined by the color, position, and Tactile Echoes assigned to the block.

In the application, Tactile Echoes are elicited when users touch the objects with a finger wearing our device. A Leap Motion hand-tracking camera provides relatively coarse information about the position of the finger relative to the block. This information allows the system to pre-activate the Tactile Echo corresponding to a block well before it is touched. This process is transparent to the user, since the Tactile Echoes feedback is driven responsively by the real contact between the finger and the object. Thus, a user experiences a seamless association of each block with the corresponding Tactile Echoes.

3.6.2 Augmenting a 2D Tactile Drawing Application

In a second demonstration, we created a 2D finger drawing application in which drawing actions are interactively augmented with different Tactile Echoes (Fig. 3.6B). The application is presented via an augmented reality surface generated by a smart projector system (Touch Xperia, Sony Inc.) running the Android operating system. An integrated camera in the projector tracks the user's touch gestures. The user selects one of a large

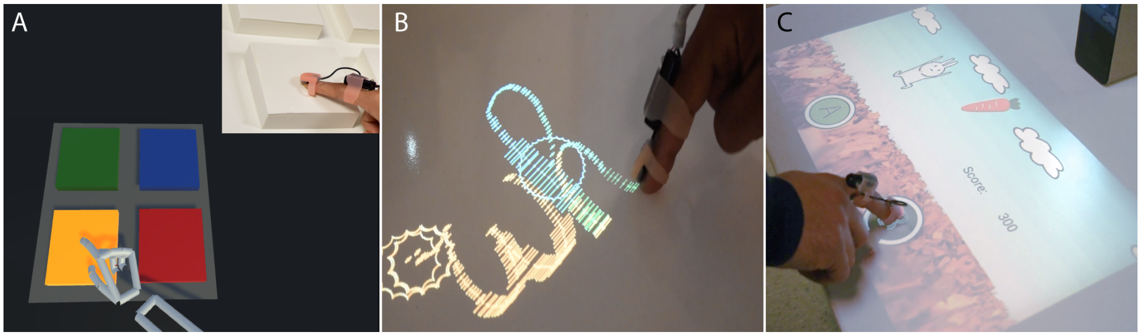

Figure 3.6: Applications of Tactile Echoes with audio in virtual and augmented reality and human-computer interaction. A) A memory game in virtual reality using four passive haptic proxy objects augmented with different Tactile Echoes. B) A drawing application augmenting planar stroking, tapping, or scratching interactions with Tactile Echoes that depend on the selected color. C) A side-scrolling game in which a user controls a hopping rabbit (capturing carrots) via tapping with haptic feedback.

variety of sprite shapes and colors from a palette for fingerpainting on the projected display. Each color and shape is associated with a different Tactile Echo, which, when interacting in the specified drawing region on the interface, evokes an artificial, texture-like effect. The interface allows for drawing with continuous strokes or discrete taps, yielding discrete or sustained Tactile Echoes feedback. When we demonstrated this application in an exhibition at our university, we observed a wide range of users, ranging from children to older adults, enjoy interacting with this multisensory creative experience. This application demonstrates how Tactile Echoes makes it possible to augment ordinary surfaces in the environment with continuously interactive projected interfaces that provide responsive tactile feedback.

3.6.3 Augmenting 2D Tactile Control Surfaces

In another demonstration, we used the same smart projector system to create a projected control surface. We mapped different tactile echoes to each of six colored regions (Fig. 3.1B). The dark areas of the interface, where no control button exists, are assigned to produce no Tactile Echoes feedback. In a separate application, we used the same approach and hardware to augment a projected touch screen based music controller (TouchOSC, Hexler, Ltd. [157]) with tactile feedback. The application provides a reconfigurable array of control surface elements, including sliders, dials, and buttons, for musical performance (see supplementary media and Fig. 3.1C). Tactile Echoes in this application are activated using control data transmitted via the Open Sound Control streaming network protocol [158]. Such augmented control surfaces can enable responsive, playful interfaces for creative applications. These applications demonstrate how it is possible to selectively assign tactile effects to different designer-specified control elements associated with a projected surface in a real environment.

3.6.4 Augmenting a 2D Video Game with Tactile Feedback

We created another simple demonstration in which we used Tactile Echoes to augment a controller for a side-scrolling video game based on a touch screen (Fig. 3.6C). The game runs on the smart projector system described above. In it, the player character, a rabbit, continuously travels to the right. The user is tasked with catching as many floating carrots as possible, which have been spawned at different heights, in the allotted time. In order to catch the carrots, the user taps on virtual buttons which make the rabbit jump. By tapping on the virtual buttons with more or less force, the user is able to control the height of the rabbit's jump; the harder the user taps, the higher the rabbit jumps. In order to estimate tapping force, we used the piezoelectric sensor in the Tactile Echoes wearable device (Figs. 3.1A, 3.2B) in the manner described in the perception experiment. The tapping force was also automatically reflected in the Tactile Echoes feedback. This demonstration shows how Tactile Echoes make it possible to augment playful touch screen interactions with tactile feedback.

3.6.5 User Study

In order to evaluate whether users found Tactile Echoes to provide a more engaging and immersive experience in an application setting when compared to that of traditional vibrotactile feedback, we performed a user study based on the rabbit game demonstration. In the experiment, two virtual buttons were placed in the lower third of the screen (Fig. 3.6C). Each button (which we denoted "A" and "B") was randomly assigned to provide either Tactile Echoes feedback or a simple vibrotactile notification, consisting of a 200 Hz vibration cue with fixed amplitude lasting 250 ms. 12 participants volunteered for the experiment (7 male, 5 female). All subjects gave their written informed consent. Before the experiment began, each subject underwent a short, three-minute training phase in which they were free to press both buttons (i.e., simple haptic feedback and Tactile Echoes feedback) and learn the mechanics of the game. After training, subjects played the game twice. In the first trial, the Tactile Echoes feedback and the simple notification feedback was randomly assigned to either button "A" or "B" (e.g. "A" provided Tactile Echoes feedback and "B" provided a simple notification). In the second trial, the feedback assigned to each button was swapped (e.g. "A" was assigned to provide a simple notification, while "B" provided Tactile Echoes feedback). Each trial lasted three minutes. Participants were naive with respect to the purpose of the experiment, and were not informed about the different feedback modes. After each trial, participants answered three questions for each of the two buttons that were based on standard presence questionnaires:

- How responsive was button A/B to motion?
- How engaging was button A/B?
- How much agency or control do you feel when using the A/B?

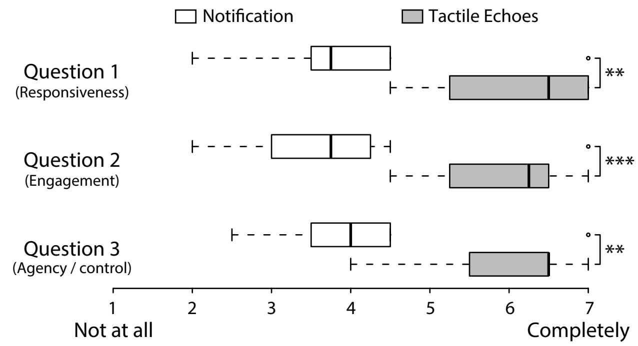

Figure 3.7: Results of the user study of Tactile Echoes in video gaming. Boxes, whiskers, and points present the medians and IQRs, the 1.5×IQR, and the outlier of evaluation value, respectively. The asterisks (**) and (***) indicate statistical significance at the 0.01 and 0.001 level, respectively.

Subjects answered using 7-point Likert scales (1 = Not at all; 4 = somewhat; 7 = completely). Subject responses were averaged across trials, resulting in 6 ratings per subject, 3 ratings describing how the Tactile Echoes feedback was perceived and 3 ratings describing how the simple notification feedback was perceived. We used a Wilcoxon signed-rank test to analyze the difference in median ratings between the two different types of feedback for question.

The median ratings for all questions were higher in the Tactile Echoes condition than in the control feedback condition. Participants judged the Tactile Echoes feedback to be more responsive to motion (median rating 6.5 vs. 4.0; W=65, Z=2.9, p=0.002, r=0.59), more engaging (6.25 vs. 3.75; W=66, Z=3.04, p=0.001, r=0.62), and more agency or control to facilitate (6.5 vs. 3.75; W=55, Z=3.0, p=0.002, r=0.605) [2]. This result suggests that Tactile Echoes could enhance user experiences in many applications that currently rely on simpler haptic notifications.

[2] W, Z, p, r are test statistics, critical z-value, p-value, and effect size, respectively.

3.7 Conclusion

This paper presents a wearable method and system for multisensory augmentation of manual touch interactions with objects and surfaces. This enables responsive haptic effects to be rendered during manual interactions involving direct contact with the skin. Our method allows tactile feedback to be introduced into naturally occurring interactions without requiring the touched object to be engineered and without imposing any device, such as a handheld controller or instrumented surface, between the skin and touched object. Thus, it can be used in a great variety of environments and interactions. This system represents a promising design approach for tactile augmented or mixed reality. It could be compared emerging visual augmented reality methods like those based on head mounted displays or projection systems. Our work also demonstrates how tactile feedback can be programmably assigned to objects or surface regions (Figure 3.6).

The Tactile Echoes system captures naturally occurring vibrations in the skin that are elicited via touch contact during manual interactions. It processes the vibrations and returns them to the hand as echoes of touch and to the ear as sound. The feedback automatically reflects the attributes of the contact event or touched object. Our system provides ten parameters to design these effects via a signal processing network. The same processing can be used to generate either only tactile feedback or concurrent tactile and auditory feedback, yielding multisensory experiences. Many other signal processing architectures and parameters can be used to realize such effects.

In perceptual experiments, we characterized how Tactile Echoes are perceived using semantic labels that were provided by participants. MDS analyses yielded low-dimensional, semantically grounded descriptions of the underlying perceptual spaces. While these results reflect design choices we adopted, and many other such choices are possible. The labels were often related to familiar physical processes or objects. We hypothesize that aspects of the perceptual mapping revealed here would be preserved in other embodiments of our approach, but further research is needed to clarify this hypothesis.

The promising nature of these results suggests several avenues for further investigation. First, the effects that we designed proved to be evocative and diverse, but not necessarily natural. Nonetheless, participants frequently described them using terms that referred to physical processes. Further research on how these effects might be designed to match natural touch sensations, or to modify the perceived properties of surfaces, is warranted. Second, individual differences in perception could arise from variations in the size, stiffness, and shape of the finger, as would be appropriate for further study. Third, as our applications demonstrate, this design can be used to generate responsive haptic effects in response to a variety of touch interactions, including tapping, textural sliding, and scratching, among others. Our perception experiments focused mainly on touch contact via tapping, while the applications also demonstrate sliding contact. Further research is warranted to investigate the perception of Tactile Echoes accompanying more general interactions. This research deduced perceptual spaces grounded in user-supplied semantic descriptors. It would be interesting to leverage these low-dimensional representations to simplify the design of Tactile Echoes effects. We plan to explore this design simplification in future work. Fourth, while we have presented several different demonstrations, the majority involve the haptic augmentation of nearly flat extended surfaces of objects. We have explored an array of potential interactive scenarios (including several not described here), and have informally found scenarios involving the augmentation of low-curvature surfaces to produce more interesting results than are typically obtained using three-dimensional objects. This could be due, in part, to the single-finger nature of the interactions involved, but other considerations may also be at play. We plan to investigate these issues further in future work.

We designed the physical implementations presented here based upon a piezoelectric vibration sensor, inertial voice coil actuator, motion sensing and display systems that were efficient to implement and appropriate for the experiments and demonstrations. However, many other variations on this system and these components are also possible. The implementations in our system are all tethered through physical wires, but this system can be made wireless and battery-powered, with wireless data transmission link to a remote desktop computer. We prototyped such a configuration in an earlier project in our lab [149]. The computing and motion sensing portions of the system could also be made wearable, leveraging contemporary head-mounted augmented reality glasses, goggles, and computer vision sensing, as we plan to explore in future work.

Chapter 4

Active Touch-Induced Forward Masking: Mechanisms and Effects on Tactile Perception

In the research of Chapter 3, we observed an unusual effect in which the intensity of tactile feedback provided in Tactile Echoes following touch contact increased as the latency with which the feedback was supplied increased. Similar perceptual phenomena, called tactile forward masking, have been previously studied in relation to passively applied haptic feedback, but such effects have not been previously identified in active touch. This motivated the study, presented in Chapter 4, of effects of time delay on the perception of haptic feedback in active touch.

At the time of writing, this chapter was being prepared for submission to the journal Scientific Reports under the title:

A. Kawazoe, G. Reardon, D. Goetz, M. D. Luca, Y. Visell,"Active Touch-Induced Forward Masking: Mechanisms and Effects on Tactile Perception," Scientific Reports.

4.1 Abstract

Tactile forward masking is a perceptual effect in which a first tactile stimulus inhibits the perception of a subsequent stimulus. While previous research has focused on passive touch, little is known about tactile forward masking in active touch. Here, we investigated masking effects that are driven by touch-elicited vibrations elicited by active touch contact of the finger with an object. Participants touched a surface with their index fingers and subsequently felt vibration feedback delivered via the surface. In several experiments, we characterized modulatory effects of the timing, vibration amplitude, and the perceptual similarity between the vibration feedback and the transient skin oscillations that were elicited via touch contact. We observed forward masking to attenuate the perceived intensity of the feedback that was delivered with no latency following touch contact by nearly 10 dB relative to feedback that was delivered after a delay of 100 ms, consistent with prior studies of masking in passive touch. Our findings reveal important modulatory effects of active touch on tactile processing, shed light on the interplay between perception and action in the somatosensory system, and have implications for the design of haptic interfaces.

4.2 Introduction

Touching an object produces transient skin oscillations that furnish a wealth of perceptual information about the touched object and contact event. Such stimuli can also alter the perception of subsequent tactile inputs, such as are felt during object exploration or, in haptic interfaces, when tactile feedback is supplied through the touched surface. Tactile forward masking is a manifestation of perceptual phenomena that occur when a first sensory stimulus, known as the masker, inhibits the perception of a subsequent stimulus, known as the target. Such masking effects have also been characterized in other sensory modalities, such as vision and audition. In the context of tactile perception, prior research has focused primarily on forward masking effects in passive touch, where the stimuli are presented to the skin without any active movement of the body. Several factors modulate forward masking effects, including the amplitude of the masker, the duration before the subsequent, target, stimulus is felt, and the perceptual similarity between the masker and target stimuli. Several studies have characterized the effects of active touch on the processing of tactile stimuli, highlighting the importance of considering the integration of sensory and motor processes in touch perception. However, there has been limited prior research on tactile forward masking effects produced by stimuli generated during active touch contact with objects. Thus, it is unclear to what extent such forward masking effects manifest in active touch, or how factors that modulate masking effects in passive touch may differ from those arising in active touch. Investigating the effects of contact-elicited stimuli generated during active touch on the perception of subsequent tactile stimuli, such as those felt during active object exploration, could provide insight into the complex interplay between perception and action in the somatosensory system, and neural mechanisms supporting active touch perception. Understanding these mechanisms also has implications for the usability and design of haptic interfaces and other technologies that furnish responsive tactile feedback.

Such masking effects have been proposed to be attributable to the persistence of the neural response to the masker stimulus, creating a refractory period during which subsequent stimuli are inhibited, or due to inhibitory neuronal effects that suppress activity that would otherwise be elicited by the target stimulus. Tactile forward masking can be explained not only by persistence but also by neural adaptation, similar to the mechanism of auditory forward masking [159]. Specifically, the neural response to a test stimulus changes due to a preceding masking stimulus. The work of Gescheidar and his colleagues supports these explanations [160, 161]. They investigated differences in the tactile forward masking effect between young and old individuals, taking advantage of the changes in neural persistence associated with aging. This assessment aimed to determine whether the tactile forward masking is due to sensory persistence and adaptation.

Forward masking effects, in which the first stimulus, known as the masking stimulus (masker) affects to diminish the perception of the second stimulus (test stimulus). Perceptual forward masking occurs when a brief sensory stimulus, known as the masker, inhibits the perception of a subsequent stimulus, known as the target. This effect has been observed and studied in vision, audition, and haptic perception. Prior haptics studies of tactile forward masking have involved passively presented stimuli presented in succession to the skin. Sherrick was the first to investigate tactile masking on the fingertip for tactile detection. The results showed that tactile masking shares similarities with auditory masking in several aspects. Firstly, tactile forward masking causes a greater elevation of thresholds than backward masking. Secondly, both forward and backward masking produce maximum effects when the interstimulus interval (ISI), the temporal interval between the offset of one stimulus and the onset of another, is zero. Finally, the time course over which maskers produce an elevation in threshold is longer for forward maskers than for backward maskers [162]. Subsequent research has revealed that several factors of the stimuli influence the amount of masking, including the amplitude, duration of the test and masking stimulus, and ISI. Makous et al. and Gescheider et al. characterized tactile forward masking in passive touch under conditions where the duration of the masking and test stimuli and the ISI varied with amplitude, and found that increasing the duration of the test stimulus and ISI decreased the amount of masking while increasing masking duration and magnitude had the opposite effect [163, 164, 165, 10]. These findings are consistent with other types of masking, such as backward and pedestal masking [166, 10]. Another important factor affecting the amount of tactile forward masking is the similarity between the masking and test stimuli. Tactile masking mostly occurs when both stimuli activate the same psychophysical channel. Some studies have investigated the effect of tactile masking over a wide range of frequencies (0.4 to 500 Hz) by applying conductors of varying sizes to different skin locations to understand the neural and psychophysical mechanisms underlying tactile masking [167, 168, 169, 170]. The result obviously presents more amount of tactile masking when the pair of the same frequency of masking and test stimuli are used rather than different pair of frequency. These findings indicate the independence of the psychophysical channel in tactile detection which enables the detection of tactile stimuli by one of four channels (P, NPI, NPII, NPIII) mediated by four mechanoreceptors (PC, RA, SA II, SA I). There are other researches that present the validation of neural independence in tactile masking under differences in ages, remote location, and other psychological methods [171, 172, 173, 174].

Less attention has been given to tactile masking effects in active touch, where sensory processing and motor control are tightly coupled. Here, in this study, we investigate the effect of tactile masking in active touch, in which we explore how the perceptual intensity of tactile feedback differs with delay time and the similarity between the masker (touch-elicited vibration) and test stimuli (tactile feedback). The goal of the study is to clarify how the perceptual intensity of tactile feedback differs with delay time after touch, and how the similarity of tactile masking affects the degree of tactile masking effect. The observed phenomena of the tactile forward masking effect occurring in active touch not only in passive touch or static touch conditions with vibration motivated us to investigate how tactile forward masking effect the perception of tactile feedback based on the delay time, physical intensity, and perceptual similarity. To achieve this goal, we conducted two experiments. In the first experiment, we will investigate the effect of delay time on the perceived intensity of tactile feedback. We will manipulate the delay time between touch contact and feedback, and assess how this affects the perceived strength of the

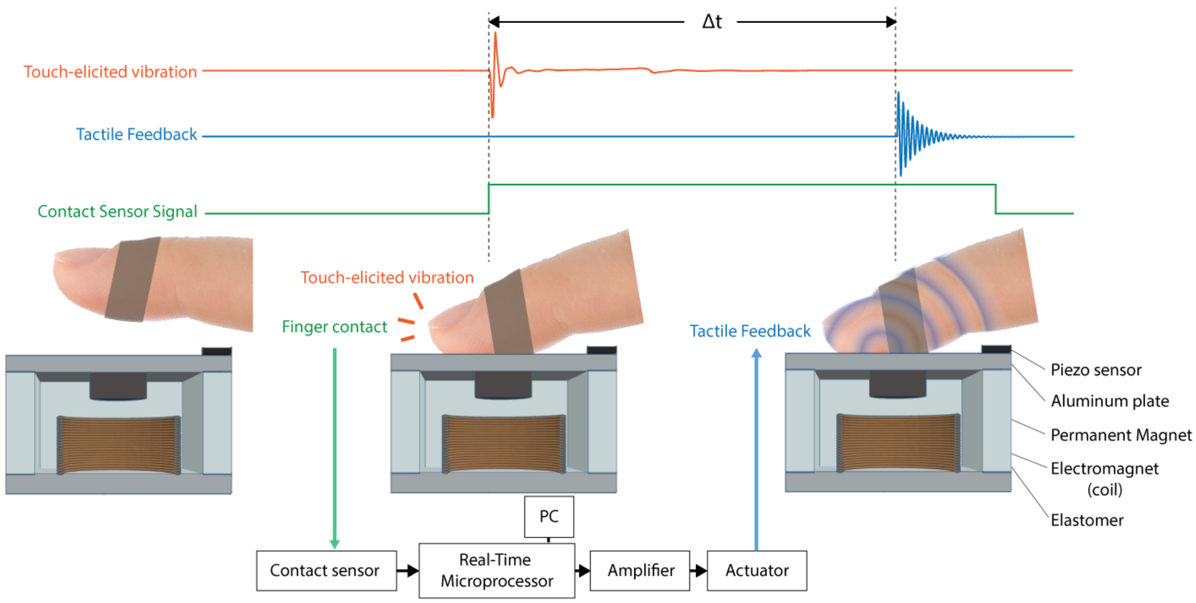

Figure 4.1: The concept and system of the effect of tactile masking in active touch. In the effect of tactile masking in active touch, touch-elicited vibration works as a masker for tactile feedback provided after touch. The duration of time delay (Δt) between the onset of touch-elicited vibration and the onset of tactile feedback is shorter the touch-elicited vibration works as a perceptual masker to decrease the perceptual intensity of tactile feedback. This experimental system consists of a contact sensor for touch detection, a real-time microprocessor to provide tactile feedback, an actuator, amplifier for the actuator. When the finger touched the surface of the actuator, the real-time microprocessor detects the electrical induce via conductive fabric from the electric-induced actuator surface.

feedback. In the second experiment, we will explore the relationship between perceptual similarity and the degree of tactile masking effect. We will manipulate the perceptual similarity between the masker and test stimuli, and assess how this affects the degree of masking. The contribution of this paper is the investigation of the tactile forward masking in active touch, presenting how much perceptual intensity of tactile feedback differs with delay time, and clarifying how the relationship between perceptual similarity and degree of tactile forward masking effect. The findings from this paper are practical for the design of the tactile device with touch interaction to adjust the intensity or delay of tactile feedback in order to obtain the desired intensity of tactile feedback.

In summary, this study aims to provide new insights into tactile forward masking in active touch and clarify how the delay time and perceptual similarity of tactile feedback affect its perceived intensity. Our findings will be of practical value to designers of haptic devices, as well as researchers interested in the perception of touch and haptic feedback.

4.3 Result

4.3.1 Experiments 1A and 1B - Tactile forward masking in active touch

If tactile feedback is provided with a short delay after touch, it should be perceived as less intense compared to tactile feedback with a longer delay. If this occurs, it confirms that tactile forward masking takes place in active touch, as the touch-elicited vibration serves as the masking stimulus, while the tactile feedback following touch acts as the test stimulus, similar to past investigations of tactile forward masking under passive conditions [163, 164, 165, 10]. One factor contributing to the magnitude of tactile forward masking is the interstimulus interval (ISI), the temporal interval between the offset of one stimulus and the onset of another. In this experiment, manipulating the time delay (indicated as Δt in Figure 4.1) of tactile feedback after touch also manipulates ISI, which affects the magnitude of tactile forward masking.

To investigate how the perceptual intensity of tactile feedback changes with the manipulation of time delay after touch, we conducted two experiments. In the first experiment (Experiment 1A), we employed a two-alternative forced-choice paradigm. Participants were asked to report which two stimuli felt stronger: the first stimulus was a recorded touch-elicited vibration from an actuator with a 30 ms delay time and 0 dB, and the second stimulus was a comparison stimulus that was the same recorded touch-elicited vibration but manipulated with 13 different amplitudes and 3 delay times. In the second experiment (Experiment 1B), participants rated the intensity of tactile feedback manipulated with 7 delay times and 3 amplitudes.

Experiment 1A aimed to determine how differences in delay time corresponded to changes in physical amplitude, while Experiment 1B, which manipulated more delay times than Experiment 1A, assessed how the magnitude of tactile forward masking changed over time. These experiments shed light on the interplay between perception and action in the somatosensory system during active touch.

Figure 4.2(a) presents the mean response proportions from Experiment 1A. Binary response data at each delay from each of the 13 participants were fitted to a cumulative normal distribution using a probit regression model, resulting in a total of 39 fits. The point of subjective equivalence (PSE) in the amplitude of tactile feedback was computed for each participant for each condition and subsequently averaged over the participants. Figure 4.2(b) displays the PSE values derived from the 50% point on the logistic function fitted to the psychometric function. Each plot illustrates the 50% proportion at which the comparison stimulus was judged for each delay time. Nonparametric repeated-measures tests contrasting all three delays revealed a significant effect of delay on PSE for all pairings ($p < 0.001$, Bonferroni corrected, BC). This result indicates that a 15 ms delay causes approximately a 2 dB difference in perceptual intensity. Furthermore, when comparing the proportion that the comparison stimulus was perceived as stronger at 0 dB of tactile feedback among the three delays, longer time-delayed tactile feedback was perceived as more intense due to the tactile forward masking effect, even when the physical intensity of tactile feedback remained the same.

In Experiment 1B, we investigated the effect of tactile masking in active touch across various time delays of tactile feedback by conducting a magnitude estimation experiment to measure the perceptual intensity at each delay for three amplitudes. We used tactile

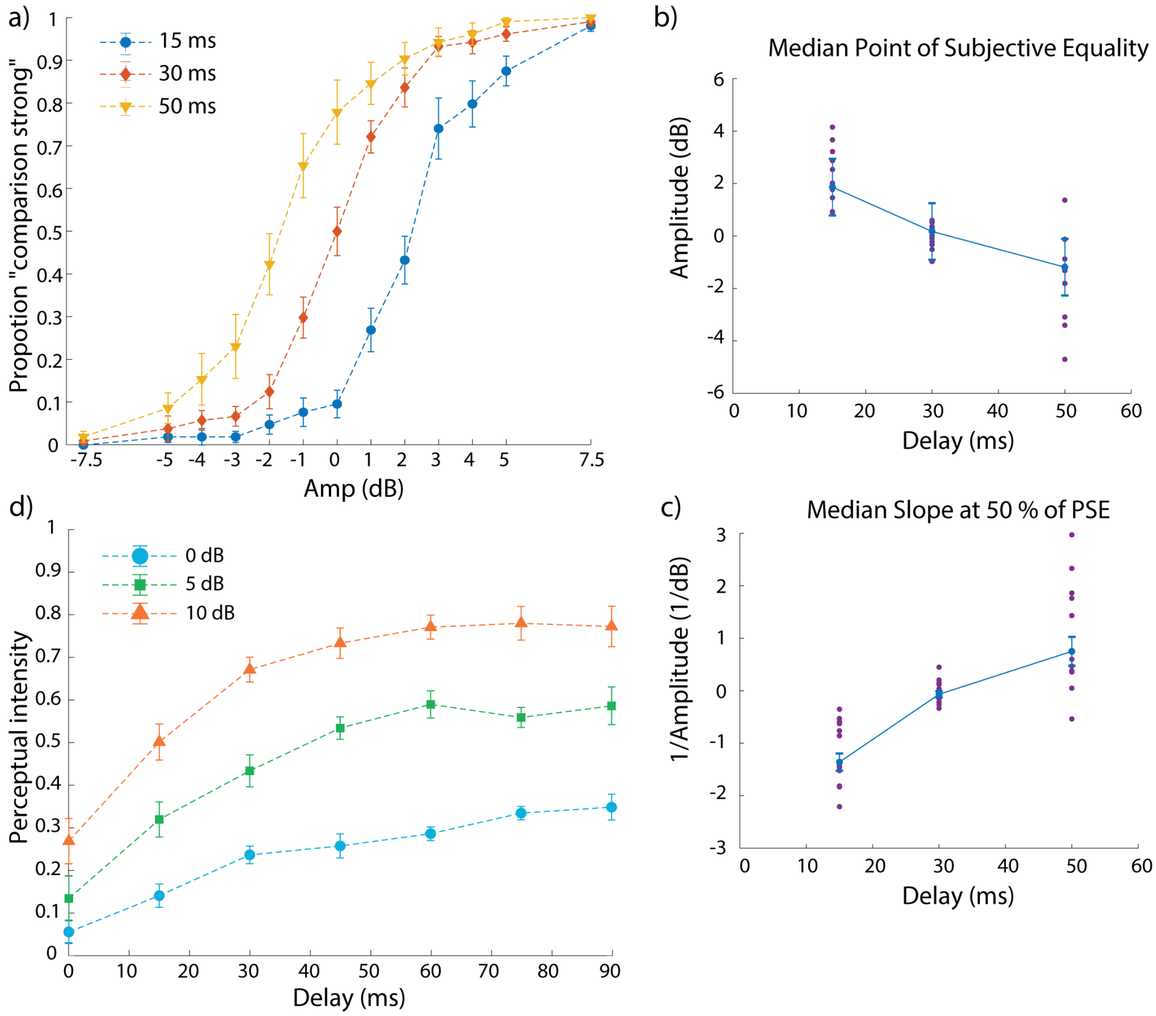

Figure 4.2: Results of Experiment 1. a) Mean proportion of comparison stimuli judged stronger than the standard in Experiment 1A. b) Median Point of Subjective Equality (PSE) in Experiment 1A. c) Median slope at the 50 % PSE level in Experiment 1A. d) Manipulation of perceptual intensity through varying delay times of tactile feedback in Experiment 1B.

feedback which has the same duration and similar properties to touch-elicited vibration. The results are shown in Figure 4.2(d). Tactile feedback with shorter delay times was perceived as less intense for each amplitude of tactile feedback. According to the pilot study conducted before the main experiment of Experiment 1B with 3 participants, we observed that the tactile masking effect persisted for approximately 90 ms when the touch-elicited vibration.

4.3.2 Experiments 2A and 2B - Effect of perceptual similarity on tactile forward masking in active touch

The results of Experiment 1 suggest that tactile forward masking occurs in active touch, whereby touch-elicited vibrations act as a masking stimulus to diminish the perceptual intensity of tactile feedback provided after touch contact. Previous studies of tactile forward masking in passive touch have shown that the amount of tactile forward masking is determined by whether the same psychophysical channel is evoked by the masking and test stimulus [167, 168, 169, 170]. However, it remains unclear how the amount of the tactile forward masking effect is influenced by the similarity between touch-elicited vibration and tactile feedback provided after touch in active touch.

To address this knowledge gap, Experiment 2 aimed to investigate the effect of varying vibration feedback properties on tactile forward masking in active touch. Experiment 2 consisted of two parts. In Experiment 2A, participants were asked to rate the similarity of each tactile feedback to a recorded touch-elicited vibration in the static hand condition, using a visual analog scale (VAS) based on the magnitude estimation method. In Experiment 2B, participants were asked to rate the intensity of tactile feedback after touch with 15 ms and 90 ms delays using a VAS, again based on the magnitude estimation method. The difference in perceptual intensity between the 90 ms and 15 ms delays was computed to determine the amount of tactile forward masking. A small difference in perceptual intensity between the 15 ms and 90 ms delays indicates weak tactile forward masking, while a large difference in intensity signifies a strong effect of tactile forward masking.

Touch-elicited vibrations were captured by the Laser Doppler Vibrometer (LDV) per participant, and in Experiment 2, this captured vibration (recorded tap) was used as a standard stimulus to compare the similarity with the comparison stimuli. In Figure

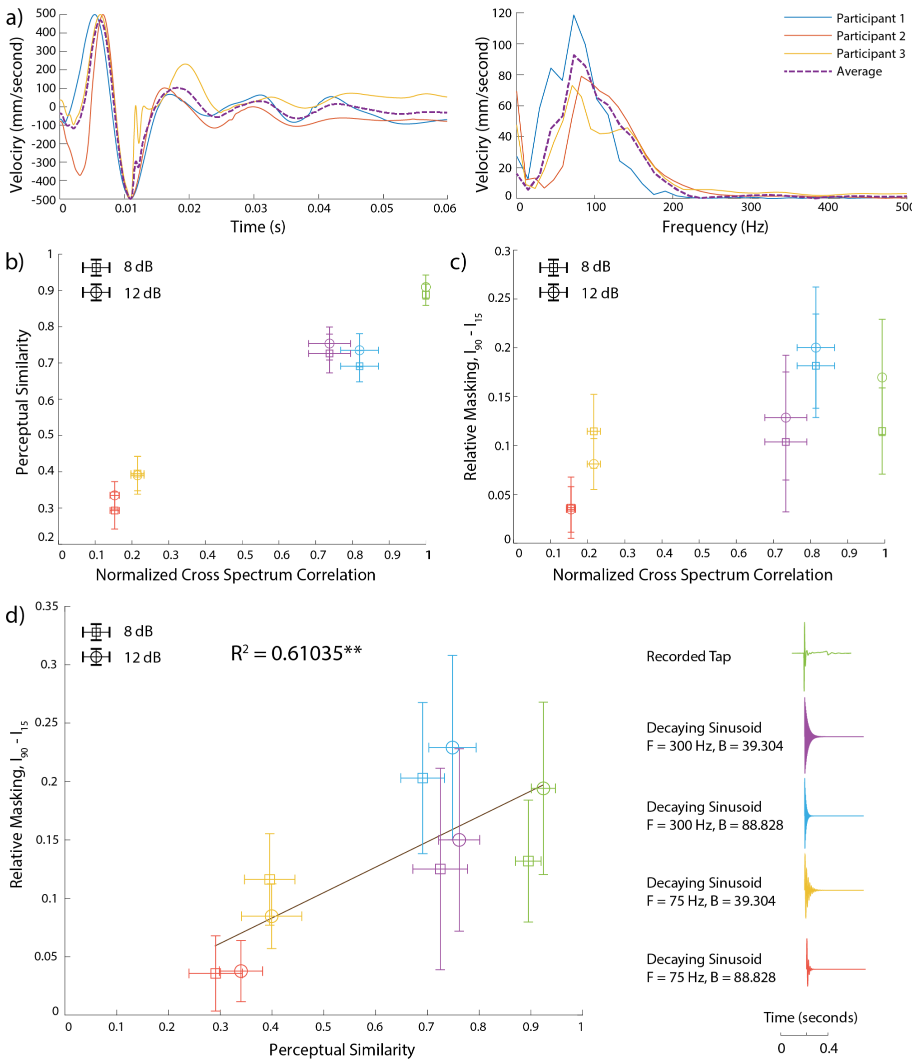

Figure 4.3: Figure depicting the outcomes of Experiment 2. a) The left side of the figure is time domain plots of touch-elicited vibration on the surface of the actuator captured by the Laser Doppler Vibrometer (LDV). The right side of the figure is the frequency domain plots of touch-elicited vibration on the surface of the actuator captured by LDV. In both plots, signal data of touch elicited vibration from 3 of 11 participants and the average of 11 participants is shown. b) This figure illustrates the normalized cross-spectrum correlation of each signal component and perceptual similarity measured in experiment 2A. c) This plot is a normalized cross-spectrum correlation of each signal and relative masking calculated by the difference between perceptual intensity in 90 ms and 15 ms. d) The plot presents the relationship between the perceptual similarity and difference of intensity which indicates how the similarity of tactile feedback and touch-elicited vibration decides the amount of tactile forward masking.

4.3(a), the whole averaged and 3 representative participant's time domain and frequency domain of LDV captured touch-elicited vibration is presented.

Figure 4.3(b) shows that as the normalized cross-spectrum correlation increased, the perceptual similarity increased. Normalized cross-spectrum correlation is the amount of similarity of frequency components in recorded tap signal and signal of comparison stimulus. Therefore, this Figure 4.3(b) shows the perceptual similarity increases when recorded tap and comparison stimuli are physically similar and have similar frequency components. Figure 4.3(d) presents the relationship between similarity and the difference in perceptual intensity between 15 ms and 90 ms delays for each tactile feedback. The plot of similarity and difference in intensity was calculated as the mean of all participants. Linear regression analysis was performed to predict the difference in perceptual intensity based on perceptual similarity. A significant regression equation was found ($F(1, 12) =$ 12.531, $p < 0.01$), with an R^2 of 0.61035. The results indicate that when the tactile feedback is perceived as more similar to the touch-elicited vibration, the amount of tactile forward masking effect increases, as evidenced by the larger difference in perceptual intensity between 15 ms and 90 ms delays. This finding highlights the influence of perceptual similarity on tactile forward masking.

Figure 4.3(c) presents how the relationship between the amount of tactile masking modified by the amount of similarity of frequency components in the recorded tap signal and signal of each comparison stimulus.

4.4 Discussion

Tactile forward masking occurs when the perception of vibration is impaired due to the presence of a preceding vibration. Past studies have demonstrated tactile forward masking in passive touch, where the finger remains static and vibrations are provided passively [162, 168, 10, 165, 164, 175, 176]. The amount of masking effect in tactile forward masking under passive conditions varies based on factors such as delay time, amplitude, masking duration, and tactile properties of masking and test stimuli [168, 164, 165, 10]. However, little is known about whether touch-elicited vibrations function as maskers and how they influence the perception of tactile feedback provided after touching in active touch.

In this study, we demonstrate that touch-elicited vibrations in active touch act as maskers, and the amount of masking effect is determined by factors such as delay time, amplitude, and tactile similarity between touch-elicited vibrations and tactile feedback. We found that participants judged longer-delayed tactile feedback as stronger, even when the intensity of tactile feedback was the same. Furthermore, the relationship between similarity and the difference in tactile intensity showed a positive correlation, indicating that the similarity between touch-elicited tactile feedback and tactile feedback determines the amount of tactile forward masking in active touch.

Our findings from Experiments 1A and 1B show how tactile forward masking manifests in active touch. In Experiment 1A, we measured the frequency with which comparison stimuli were judged to be stronger than the standard stimulus. The results suggested that longer-delayed tactile feedback was perceived as stronger compared to tactile feedback of the same amplitude. Moreover, 15 ms delayed tactile feedback corresponded to a 2 dB difference in perceived intensity. In Experiment 1B, we measured the perceptual intensity of tactile feedback manipulated by delay time and amplitude using the magnitude estimation method. The results revealed that tactile forward masking persisted for around 90 ms of delay time when using tactile feedback of the same duration and similar properties to touch-elicited vibrations. These findings reveal how tactile masking in active touch is intricately modulated by stimulus timing, amplitude, and perceptual similarity. These modulatory effects reflect the dynamical integration of temporally distinct stimuli by the somatosensory system during active touch.

The observed relationship between similarity and tactile intensity provides evidence that the perceptual system is sensitive to the properties of both masking and test stimuli in active touch. This sensitivity resonates with previous findings in passive touch, where the amount of masking was determined by whether the same psychophysical channel was evoked by the masking and test stimulus [167, 168, 169, 170]. The fact that tactile forward masking persists even in the presence of vanishingly short delay times emphasizes the efficiency of the perceptual system in integrating temporally separated stimuli. Moreover, the time delays over which tactile forward masking effects are largest are shorter than the temporal threshold for detecting tactile delays after hand movement (approximately 40 ms [177, 178]). In the visual-haptic, the threshold of detection exhibits significant variation, ranging from 20 to 200 ms. This discrepancy is influenced by the nature of the application and the specific form of haptic interaction involved. The latter can be subdivided into force feedback versus tactile feedback, discrete versus continuous force feedback, and active versus passive interaction [179]. In a collaborative virtual environment, where haptic information is reciprocally transmitted, the perception of haptic feedback delay could initiate from approximately 50 ms [180]. Furthermore, it has been observed that humans typically do not perceive delays less than 30 ms during continuous haptic interactions [181]. These observations suggest that tactile forward masking in active touch does not predominantly arise due to top-down effects.

The results from Experiments 2A and 2B demonstrate that the extent of the masking effect is influenced by the degree of tactile similarity between the masking and test stimuli. Interestingly, our findings reveal that tactile forward masking occurs even when the test stimulus is synthetic, such as a decaying sinusoid, and thus not identical to the touch-elicited vibration that serves as the masking stimulus. For all participants, the frequency content of the touch-elicited vibrations was predominantly concentrated below

75 Hz (Figure 4.3(a)). Higher-frequency synthesized vibrations, which are dissimilar to the masker, still exhibited masking effects. Nevertheless, our results underscore the importance of stimulus similarity, with stronger masking effects observed when the masking and test stimuli were more similar in their frequency content.

This observation aligns with previous studies reporting that tactile masking primarily occurs when masking and test stimuli activate the same psychophysical channel [168, 170, 174]. The modulation of masking effects based on the similarity of the stimuli contributes to a more nuanced understanding of the underlying mechanisms of tactile forward masking in active touch.

To contextualize our findings on tactile forward masking in active touch, it is valuable to compare them with previous studies on tactile forward masking in passive touch. The role of interstimulus interval (ISI) in determining the amount of tactile forward masking is consistent across studies, with shorter ISIs leading to stronger masking effects [165]. As previously noted, our findings are also consistent with prior characterizations of the effects of stimulus similarity on masking. These consistencies between the current study and prior work suggest that touch-elicited vibrations function similarly to passively supplied vibrotactile stimuli in the context of masking. This suggests that the impairment of tactile feedback perception in active touch can be explained by tactile forward masking, in contrast to other phenomena such as tactile suppression or tactile gating, in which motion influences detection.

4.5 Conclusion

In summary, our findings provide compelling evidence that the perception of tactile feedback in active touch is influenced by tactile forward masking. Two critical factors determine the strength of the masking effect: the onset timing of the feedback and the perceptual similarity between the touch-elicited vibration and the subsequent tactile feedback. Importantly, our findings are consistent with findings from prior investigations of forward masking in passive touch. These findings have significant implications for understanding the complex mechanisms of sensory perception and integration in active touch.

4.6 Methods

4.6.1 Participants

Experiment 1. In Experiment 1A, thirteen individuals (ages 23 to 35 years old, 7 male, 6 female) participated. In Experiment 1B, ten individuals (ages 23 to 35 years old, 5 male, 5 female) participated. All participants were right-hand dominant. Participants signed the informed consent for the experiment, which was conducted according to the protocol approved by the UCSB institutional review board. There was no compensation for their participation.

Experiment 2. In Experiment 2, ten individuals (ages 23 to 35 years old, 5 male, 5 female) participated. All participants were right-hand dominant. Participants signed the informed consent for the experiment, which was conducted according to the protocol approved by the UCSB institutional review board. There was no compensation for their participation.

4.6.2 Apparatus

Experiment 1. The experimental system consists of an actuator, a contact sensor, a real-time microprocessor, and an amplifier for the actuator (Figure 4.1). Participants wear the thin conductive tie near the tip of the finger and touch the surface of the actuator. On the surface of the actuator is induced 3V from the real-time microprocessor and contact on the actuator surface is detected by the electric flow from a thin conductive tie connecting to the analog read port to the real-time microprocessor. When finger contact is detected, the real-time microprocessor provides tactile feedback via the amplifier. The system delay from touch detection in the conductive sensor to tactile feedback from the actuator is 1 ms. The amplitude, delay time, and the kind of signal of tactile feedback are enabled to be switched from the computer with Open Sound Communication (OSC). The experimental software to present instructions and record participants' responses is on the computer. To avoid auditory bias, the participants put on earplugs and pink-noise-providing noise-canceling headphones to shut out environmental noises.

Experiment 2. In Experiment 2, the effect of tactile forward masking based on the similarity of tactile properties is investigated. To provide tactile feedback and detect a touch on the actuator surface, we used the same setup as Experiment 1. Regarding the stimuli, to have a variety of similarities, we prepared different similarity level tactile stimuli based on the pilot study in similarity measurement. There are 5 stimuli: recorded tap, 2 different curve parameters ($B = 88.828$ or 39.304) of sinusoidal decayed wave (300 and 75 Hz) as shown in the right part of Figure 4.3(d). The duration of the sinusoidal wave is the same as the duration of the recorded tap. A sinusoidal decayed wave was generated based on the past haptic study modeling touch vibration on the surface [182, 89, 183]. The equation is $Q(t) = A\exp(-Bt)\sin(2\pi ft)$ where the acceleration of vibration $Q[m/s^2]$ is determined by the amplitude coefficient $A[s^{-1}]$, decay rate $B[s^{-1}]$ of the sinusoid, and sinusoid frequency $f[Hz]$. According to the characteristics of touch perception, the perceptual intensity of stimuli is affected by the frequency components of tactile stimuli. To remove the bias of the perceptual intensity due to the frequency component, we equalized the perceptual intensity of all stimuli. To equal the perceptual intensity of all stimuli, in the pilot study, we adjusted all intensity to the same perceptual intensity as a recorded tap of 8 dB and 12 dB using the adjustment method with 5 repetitions.

4.6.3 Procedure

Experiment 1. At the beginning of Experiment 1, we collected recorded taps from each participant. Participants touch on the surface of the actuator in the same touch rhythm and similar force. A Piezo sensor on the surface sense force to maintain a touch force between 1 and 1.5 N. Green and red LEDs notify timing when participants can touch or keep their finger on the surface. We used each recorded tap for stimulus in Experiment 1 per each individual participant. Before this experiment, the Piezo sensor on the surface captured recorded tap. In Experiment 1A, the participants selected only one stimulus which they felt stronger comparing two stimuli derived from the 2IFC. In a trial, standard stimulus and comparison stimulus are provided. The standard stimulus is constant stimuli which are 0 dB and 30 ms delayed recorded tap. Comparison stimuli are recorded tap provided with 3 delay time values (15, 30, 50 ms) and 13 amplitude values (-7.5, -5, -4, -3, -2, -1, 0, 1, 2, 3, 4, 5, 7.5 dB). All comparison stimuli are repeated 8 times, and the total trial number is 312 trials. During each trial, participants compare the intensity of two tactile feedback provided aftertouch, and participants selected only one stimulus which they felt stronger. These responses were entered via computer. Until their response, the participants were allowed to experience each stimulus as long as they preferred. Experiment 1A lasted about an hour in total, including 10 minutes break.

In Experiment 1B, the participants rate the intensity of stimulus with a visual analog scale (VAS) derived from the method of magnitude estimation scale. First, participants experienced all stimuli in the practice trial and the main Experiment was conducted after. In each trial, participants rate the intensity of tactile feedback provided after the tap. In tactile feedback, the stimulus was randomly selected from 21 stimuli which is a combination of 3 amplitudes values (0, 5, 10 dB) and 7 delay time values (0, 15, 30, 45, 60, 75, 90 ms). VAS was labeled "No sensation" on the left side and "Most intense sensation" on the opposite side. Participants were able to experience each stimulus as long as they preferred while they responded. Each response of the magnitude estimation scale was entered into the computer. The total trials are 168 trials which are 7 repetitions of all stimuli. Experiment 1B lasted about 40 minutes including a practice trial, with 5 minute break time between the practice trial and the main Experiment.

Experiment 2. At the beginning of Experiment 2, we collected each participant's touch-elicited vibration on the surface of the actuator using Laser Doppler Vibrometer LDV (Polytec PDV 100, Irvine, CA). The recorded touch-elicited vibration is used as a standard stimulus in each participant's Experiment 2. In Experiment 2A, the participants rate the similarity of the standard stimulus (their recorded tap) and comparison stimulus which is one of the stimuli. In each trial, participants place their finger on the actuator, and when participants press right-click/left-click, a standard stimulus/comparison stimulus is provided from the surface of the actuator. Participants use a visual analog scale to rate the similarity of standard stimulus and comparison stimulus. Participants adjust the scale of the rate with the mouse wheel. The main Experiment is conducted after the practice trial to experience all stimuli and system manipulation for participants. The responses from participants are entered into the PC via Processing running experimental software.

In Experiment 2B, to measure the perceptual intensity, participants rated the intensity with VAS using the knob. In each trial, the participant touched the surface of the actuator, and a stimulus was provided from the surface of the actuator. Not to shorten the duration between each touch, we used LED (green and red lights) to tell them when the time participants allow touch, such as the red light was "stay finger on the place" and the green light was "can touch again". Participants touched the surface with similar force. The Piezo sensor estimates the touch force and white LED light flashes when they touch with proper force. Participants touched with a similar force of the touch with a separate duration between each touch. The response from participants was entered and saved to the PC via the experimental system. In the whole Experiment 2, participants wore noise-canceling headphone providing white noise and ear plug to prevent auditory bias that causes by the environmental sound. Experiment 2 lasted about an hour and 15 minutes in total including 10 minutes break.

4.6.4 Analysis

Experiment 1. In Experiment 1A, the proportion that comparison stimuli judged strong was calculated for each amplitude and delay time per participant, sum up all proportions of all participants, and compute the mean of the proportion that is judged comparison strong. The mean proportion for all participants was plotted. The median point of subjective Equality was calculated per participant, and we summed up and computed the median point of subjective equality of all participants. In Experiment 1B, the result from the magnitude estimation method is computed mean across participants.

Experiment 2. First, the 7 repetitions of similarity data of each tactile feedback from Experiment 2A were computed as the mean of similarity in each comparison stimulus per participant. Next, to obtain the difference in perceptual intensity between two delayed times per tactile feedback, we computed the mean of perceptual intensity by each participant. After that, the difference in perceptual intensity from 90 ms to 15 ms was computed. Finally, we plotted the relationship of similarity on the x-axis and the difference of perceptual intensity in two delayed times on the y-axis. The standard error in similarity and difference of perceptual intensity were attached as error bars on each plot of tactile feedback. To see the relationship, we compute linear regression to the plot. We computed ANOVA to check the significance of this regression model.

Chapter 5

BeaTactile: A Tactile Display for Low-Frequency Spatial Surfaces using Wave Interferences

Chapter 3 presents the wearable display with one actuator to interact surface and Chapter 4 demonstrates how tactile forward masking in active touch occurs and explores the possibility of delayed tactile feedback from one actuator. In a different approach from Chapters 3 and 4, using two actuators on the finger and surface rather than one actuator, Chapter 5 describes an exploration of a further method for augmenting touch interactions with surfaces, using feedback supplied not only to the finger but also via the touched surface. This system exploits vibrations supplied to a finger and a surface to augment surfaces with spatial vibration patterns formed in the finger by beat frequency interference.

5.1 Introduction

Tactile technologies are being adopted in many new devices and systems, including wearable devices, such as rings or wristwatches, and other devices, such as tablets or other touch screen displays. There are many new opportunities for integrating tactile input from wearable devices with feedback from location-based, tablet, or smart phone devices. Here, we propose methods for synergistically integrating vibrotactile feedback supplied via a wearable device on the finger with feedback from a touch screen device. We call this method BeaTactile. To illustrate the potential in this space, we show how simply supplying vibrotactile feedback at different single frequencies via a wearable device and touch screen device can elicit sensations of difference or beat frequencies. This can arise due to interference between vibration-elicited waves in the finger due to vibration sources in a wearable and touch-screen device. The frequencies of vibration-elicited waves reflect the difference in frequencies supplied by wearable and tablet devices. This effect can be reproduced with low-cost resonant vibration actuators, such as linear resonant actuators, that are integrated into many consumer devices.

Prior researchers have investigated how the interference of vibrations of different frequencies in the skin can give rise to vibrotactile difference frequencies that are perceived as low frequency modulation. In 1959, Békésy et al. described such interference effects in human skin. Many others, including Lim et al. [184], investigated the perception of vibrotactile difference ("beat") frequencies.

Here, we investigate how these phenomena can be exploited during the exploration of a touch surface via the hand when feedback is supplied by both a wearable and touch screen device. We refer to this method, described below, as BeaTactile. With it, interfering vibrations can be used in order to render textures, including low frequency textures, from a touch screen device. This interfering vibration is produced on the finger contact location and it enables to provides tactile sensation during direct finger interaction on the surface. Potential application areas include interactive interfaces that can be personalized or haptic touch screen gaming.

5.2 Background

The seminal study on interfering vibration elicited by two vibrations was conducted by von Békésy, who utilized a loudspeaker to create vibrations and observed the interfering vibration phenomena during the generation of two different frequencies within a broad bandwidth [185, 186]. In the wake of his research, multiple investigators have employed two vibrations to produce interfering vibration, thereby altering sensation.

Given the characteristics of the human hand, vibrations above 1 kHz are typically not perceptible. However, a study by Makino et al. contradicts this understanding, suggesting that such high-frequency vibrations become perceptible when a interfering vibration of 100 Hz is generated by the difference of high-frequency vibrations between two piezo vibrators [187].

Further advancing this research, Lim et al. developed a wearable display with two pins to probe the perception of interfering vibration [184]. Their findings demonstrated that participants could perceive beat frequencies with two vibrotactile stimuli, even when these stimuli were presented at distinct locations. Moreover, the detection of beat frequencies became easier to perceive as the carrier frequency of the beat vibration increased.

Notably, all these studies have been conducted under static or passive touch conditions, and the effects of attaching a vibrator to the interactive surface or finger have yet to be explored.

5.3 Methods

The BeaTactile display method involves simultaneous feedback from wearable vibration actuators and a touched display that provides concurrent tactile feedback at different frequencies (Fig. 5.1). Vibrations supplied by the wearable device and vibrating surface interfere in the finger due to the propagation of tactile waves in the skin [101]. When each single-frequency vibration source has a different frequency, the interference patterns that result are equivalent, at any point on the skin, to an amplitude modulated vibration source. In our demonstration, a 200 Hz sinusoidal vibration may be emitted from the finger-worn device and may combine in the skin with vibrations from a 210 Hz vibration supplied by the surface. The result is equivalent to the modulation of a 200 Hz vibration at the respective location by a 5 Hz modulation frequency. In our system, the interference of waves that produces the interfering vibration occurs in the skin. This is a different effect than can be produced using a single actuator with amplitude modulation. One salient difference is that the amplitude modulated signal is perceived as localized between the surface and the location of the actuator on the limb (for example, on a more proximal part of the finger). Our demonstration provides an exploration of the new possibilities created by the convergence of haptic feedback from wearable and surface-integrated haptic devices.

$$\sin 2\pi t f_A + \sin 2\pi t f_B = 2 \sin \tfrac{2\pi t(f_A + f_B)}{2} \cos \tfrac{2\pi t(f_A - f_B)}{2} \tag{5.1}$$

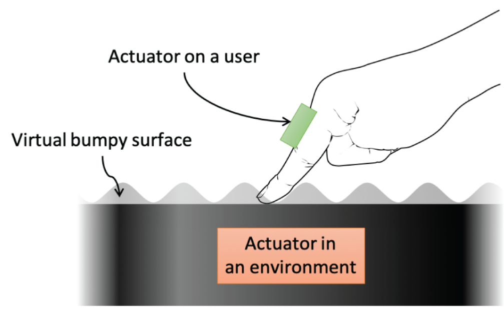

Figure 5.1: Overview of the BeaTactile display. Haptic feedback from a wearable and surface-integrated device produces an amplitude modulated feedback in the finger. When synchronized with scanning across the surface, this can yield the percept of a virtual bumpy surface.

5.4 Results

In order to ascertain whether the system elicits interfering vibrations onto the fingertip, a piezoelectric sensor mounted on the index fingertip records the signal produced there. Consequently, when Vibrator A (positioned on the index finger phalanx) and Vibrator B (located on the surface) introduce interfering vibrations, these vibrations are produced on the fingertip, as illustrated in Fig. 5.2. This phenomenon is observed not only when the finger is static upon the surface but also when it continuously moves across it.

These findings open up new possibilities for implementing interfering vibrations during interactions with surface devices. For instance, devices such as tablets, smartphones, and smartwatches, which have small actuators, combined with the introduction of an additional actuator worn on the finger, could enhance perceptual experiences due to the amplified intensity and diverse tactile sensations generated by the interfering vibrations. The potential applications of these vibrations span gaming as well as graphical user interfaces—including buttons, knobs, and sliders—to assist interaction by delivering tactile feedback and enriching the immersive experience.

With regard to the perceptual characteristics of interfering vibrations, several questions still warrant investigation. We have observed the elicited interfering vibrations at the site of finger contact during measurements. However, it is crucial to empirically determine the extent to which interfering vibrations are localized, and how perceptible they are on the finger when the frequency range of these vibrations is manipulated. Other pertinent inquiries involve determining the degree to which interfering vibrations enhance perceptual intensity compared to vibrations produced by a singular actuator, and the nature of the sensation that these interfering vibrations provide.

In conclusion, this chapter documents the development of the BeaTactile device, which generates interfering vibrations on the contacting finger using two actuators positioned on the surface and the finger. Measurements indicated that the piezoelectric sensor on the fingertip successfully captured these interfering vibrations. These interfering vibrations were captured under both static and moving conditions. As part of future work, I plan to conduct a perceptual study to further explore the characteristics of these interfering vibrations.

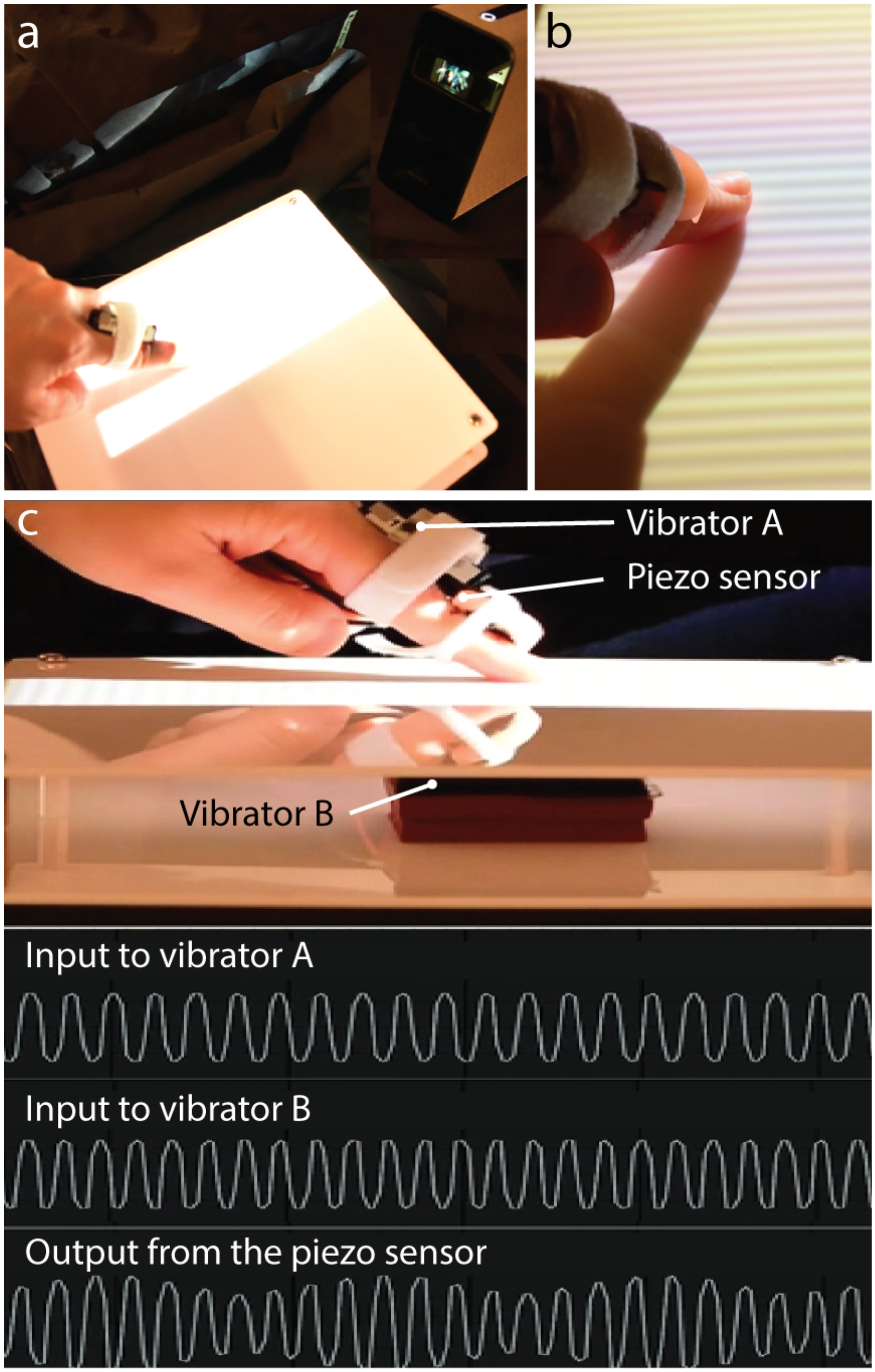

Figure 5.2: a) Top view of this BeaTactile system. b) On the touch surface, the visual texture is projected by the smart projector. c) A piezoelectric sensor captured the interfering vibration generated by vibrator A on the finger phalanx and vibrator B on the surface. The top of the figure shows the actual setup of the beatactile display. The bottom of the figure shows the signal of each vibrator input and the piezoelectric sensor captured interfering vibration.

Chapter 6

Time, Space, and Intensity in the Perception of Paradoxical Thermal Stimuli

The sensation of temperature is a crucial characteristic of surface touch perception. Using the cue of thermal sensation, we can recognize the materials we touch and determine the temperature of held objects, such as a cup of coffee. Rather than using the vibrotactile approach in Chapters 3, 4, and 5, Chapter 6 departs from the previous methods of tactile augmentation in investigating methods for augmenting surfaces with thermal sensations, using the thermal grill illusion.

The contents of Chapter 6 is adapted from the following reference [188]:

S. Patwardhan, A. Kawazoe, D. Kerr, M. Nakatani and Y. Visell, "Dynamics and Perception in the Thermal Grill Illusion," in IEEE Transactions on Haptics, vol. 12, no. 4, pp. 604-614, 1 Oct-Dec 2019, ©2019 IEEE. Reproduced here with permission from the IEEE, doi: 10.1109/TOH.2019.2904226.

Kawazoe's contributions to this study included the conception of the research, the design, fabrication, and iterative prototyping of the thermal grill device, the design and implementation of the electronic control system and control software for the device, the design and implementation of the psychophysical experiment, the piloting of the experiment, the analyses of the results of the psychophysical experiment, the preparation of the figures, and the preparation and editing of and manuscript.

6.1 Abstract

Thermal perception is important in the experience of touching objects, and thermal display devices are of growing interest for applications in virtual reality, medicine, and other areas. While most thermal percepts occur at relatively long timescales, measured in seconds, here we present an investigation of the thermal grill illusion, a perceptual effect in which burning sensations are rapidly elicited in response to stimulating the skin with juxtaposed warm and cool areas. We present experiments, using a new thermal display, in which we measured both response time and intensity in the thermal grill illusion. The experimental results revealed highly stereotyped responses. Perceived intensity increases, and response time decreases, monotonically with temperature differences. We developed a mathematical and numerical model of spatiotemporal heat exchange from a thermal grill display to the skin and used it to relate perception and tissue heating. Under accepted explanations, responses to thermal grill stimuli depend on temporal and spatial factors arising from tissue heating, neural transduction and integration, and the thermal properties and temperatures of stimuli applied to the skin. The results of this study could help to inform models accounting for these factors, enabling new uses of thermal feedback in computing interfaces, virtual reality, and medicine.

6.2 Introduction

Thermal cues play important roles in the haptic perception of objects [189], especially in material discrimination [190]. Thermal feedback is also of increasing interest in several application domains, including virtual reality, where thermal feedback is needed in order to enable realistic experiences of touch contact between the skin and simulated objects. Several applications of skin-interfaced thermal displays have also been proposed in medicine and wearable computing [191]. However, the systematic engineering and application of thermal displays is relatively recent, and both technologies [192] and knowledge of human factors [193] are improving.

Thermal touch involves the perception of the temperature or properties of objects through the exchange of heat that accompanies contact with the skin. This exchange is dynamic, because, in all cases of practical interest, thermal contacts and temperatures evolve through time. It is also spatially dependent, because contact differentially affects distinct skin areas, and because the temperature or properties of objects may vary across their surfaces. The normal temperature of human skin in homeostasis is between 31 and 35 °C. Temperatures are perceived as warm (31 to 35 °C), painfully hot (> 45 °C), cool (31 to 35 °C), or painfully cold (< 15 °C), based on interactions between distinct populations of thermoreceptive afferents innervating the skin [194], as well as nociceptive afferents associated with painful temperatures [195, 196]. As in other perceptual modalities, thermal perception involves the spatiotemporal integration of sensory signals, including input from both cold and warm thermoreceptors. Spatial summation is especially pronounced, and a larger area of stimulation leads to greater intensity of sensation. The time to respond to a thermal stimulus decreases with intensity, but for moderate temperatures response times are relatively slow, evidencing significant temporal integration. While not fully understood, the perceptual integration of thermal signals in space or time, and their interaction with other tactile modalities (such as nociception) has been found to give rise to several distinct perceptual effects.

The present work is an investigation of one such effect, the thermal grill illusion, and its ability to rapidly elicit intense sensations. The thermal grill illusion (TGI) was discovered by Torsten Thunberg (1896), who reported that innocuous warm and cool stimuli applied simultaneously to the skin by means of interlocking spiral tubes elicited burning sensations like those that accompany cold pain [197]. The illusion can be experienced by using shapes other than spiral tubes – alternating bars, checkerboard patterns, or grids. The thermal grill illusion does not change greatly with the number of stimuli or their spacing [198]. The thermal grill does not expose the skin to temperatures that are noxious or, in isolation, uncomfortable. Touching only the cold or hot bars individually thus elicits little discomfort, whereas an unambiguous and often rapid burning sensation is elicited when touching warm and cool bars with skin areas that are nearby, or that are represented proximally in the somatosensory system [199] [200].

Thermal perception involves heat exchange, which is a process of diffusion that evolves at a rate that depends on the temperature difference between the skin and the stimulus. Thermal transport in soft materials is limited by the dynamics of elastic vibrations, or phonon transport. From kinetic theory, thermal conductivity k is proportional to $\sqrt{E/\rho}$, where E is the elastic modulus and ρ the density [201]. Thus, soft materials are intrinsically insulating, and consequently non-noxious thermal interactions with the skin typically involve long timescales, measured in seconds. In contrast, the thermal grill illusion can evoke perceptual responses that are several times faster.

Current physiological explanations ascribe the thermal grill illusion to interactions between different thermally sensitive afferent pathways in early somatosensory processing. When touching the cold terminal of a thermal grill, normal discharge from coolness sensitive Aδ afferent fibers is suppressed due to the spatial summation of inputs that signal warmth in nearby skin regions [202]. In the absence of these nearby warm inputs, the Aδ inputs inhibit the activity of polymodal C-nociceptive afferent fibers, which otherwise cause burning sensations at only noxious cold temperatures ($< 15°$ C). When Aδ input is suppressed by input from nearby warm regions, a burning sensation occurs at merely cool ($< 24°$ C) temperatures. Brain imaging studies reveal that the thermal grill and the noxious hot and cold stimuli produce similar patterns of activation in the anterior cingulate cortex, whereas the warm and cool components of the thermal grill do not [203].

The intensity of the burning sensation evoked by the TGI increases with the magnitude of the temperature difference between warm and cool bars [204], indicating that it is not a digital phenomenon. TGI stimuli are felt by warm and cold thermoreceptive afferents within skin tissues, and the time course of response is determined by the dynamics of tissue heating and neural processing, including propagation times to the central nervous system. While response times for homogeneous thermal stimuli are relatively slow except at noxious temperatures [193], thermal grill stimuli elicit rapid and intense responses even at moderate (warm and cool) temperatures. The physics governing tissue heating due to uniform or spatially varying (thermal grill) stimuli is based on the time-dependent bioheat equation,

$$\rho c \frac{\partial T}{\partial t} = k \nabla^2 T + \omega \rho_b c_b (T_a - T) + q_{met} + q_{ext} \tag{6.1}$$

Here, $T = T(x, y, z, t)$ is the temperature of skin tissues at point (x, y, z) and time t, k is the effective thermal conductivity of skin, ρ and ρ_b are the density of skin tissue and blood, ω is the blood perfusion rate, T_a is the blood temperature, and q_{met} and q_{ext} capture tissue heating due to metabolic and external sources. Within this model, the tissue temperature in response to thermal touch is given by the solution with boundary condition $T(x, y_0, z, t)$ consisting of the temperature of the thermal grill at the skin surface y_0, in the case of thermal grill stimuli, or the constant temperature $T(x, y_0, z, t) = T_0$ of the touched surface, for homogeneous thermal stimuli [189].

As mentioned above, thermal grill stimuli are believed to engage thinly myelinated Aδ fibers, with conduction velocities of 2 to 30 m/s, and unmyelinated C fibers, whose conduction velocities are slower (2 m/s or less), and the engagement of each differs from those involved in purely hot or cold stimuli [205, 206]. This may partly explain why temporal properties of thermal grill induced percepts differ from those induced by either cool or warm stimuli in isolation [207]. Studies that have recorded participant responses during the course of application, through intensity ratings or temperature matching tasks, indicate that thermal grill percepts are time-dependent [208].

Further insight into temporal factors affecting TGI percepts could elucidate contributions of tissue heating and neural processing to thermal perception. This information would also be valuable for the design of devices that use the TGI alone or in combination with other modalities. However, there has been no prior quantitative assessment of response times to the onset of burning sensations in response to static thermal grill stimuli, as we provide here, or their relation to perceived intensity.

To investigate thermal display via the TGI, and time-dependent properties of the perception of the latter, we first investigated a mathematical model of tissue heating in response to the thermal grill. We then developed a new thermal grill display device capable of presenting a range of thermal grill temperatures under computer control. In a psychophysical experiment, we measured response time and perceived intensity as participants felt thermal grills, analyzed the results to quantify aspects of the perception of these stimuli, and compared the results with predictions of tissue heating from the model.

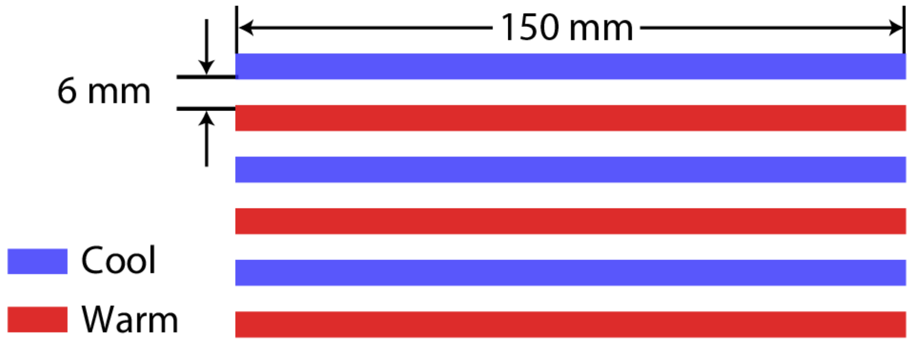

Figure 6.1: Thermal grill display concept. Dimensions correspond to those used in our device. The warm bars feel warm, the cool bars feel cool, but for a suitable difference in temperature between the two, the spatial pattern of alternating warm and cool bars (thermal grill) elicits a cold burning sensation.

6.3 Modeling tissue heating

When modeling the response of hand tissues to thermal stimuli, it is important to acknowledge the challenges associated with the fact that the human hand is a multi-layered complex system (Fig. 6.2) made up of multiple individual tissues and interacting solid and fluid components [209]. In addition, the extensive vascular network acts as a conduit for heat transfer between tissues and body areas. Thus, there is also the complexity of accounting for the heat transfer carried out by the skin blood perfusion, which is itself temperature-dependent [209]. At temperatures within physiological limits, effects of thermal damage and breakdown can be neglected. Nevertheless, heat exchange with the skin is generally far simpler than mechanical responses of skin, making it feasible and useful to pursue a mathematical description.

6.3.1 Mathematical modeling

A starting point for modeling tissue heating due to thermal contact with body tissues has typically been the time-dependent bioheat equation (6.1), as introduced by Pennes [211]. This was the first realistic model that quantified the heat transfer effect of blood

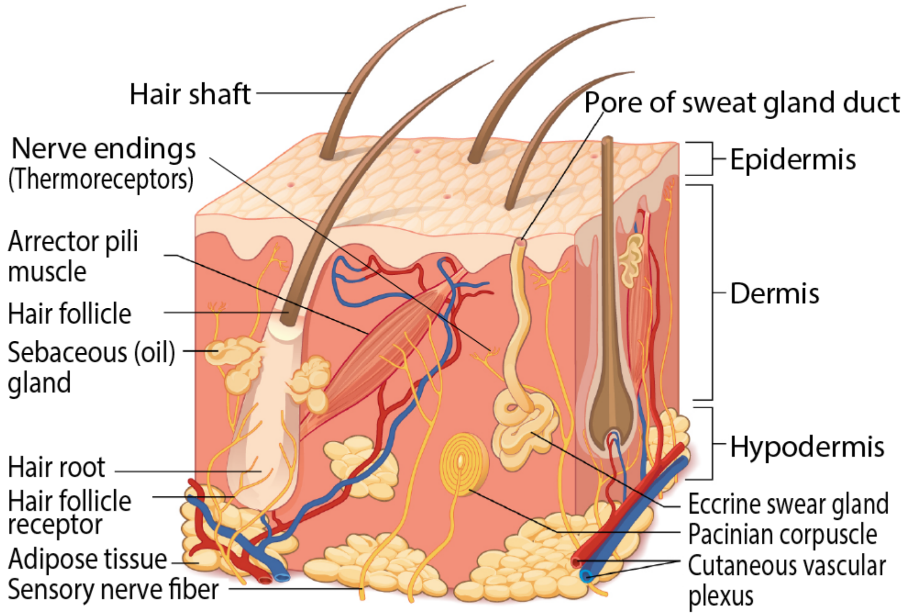

Figure 6.2: A diagram showing different layers of the skin such as epidermis, dermis and hypodermis. The thickness of these layers varies for different body parts. Figure reproduced under creative commons license from [210]

perfusion. Several authors have drawn on it in order to analyze thermal displays. Unusually, Benali-Khoudjal et al. [212] provided an explanation based on an electrical analogy. Jones and Ho [189] [213] proposed a thermal model that predicts the temporal response of the skin surface during contact with a surface at constant temperature. However, that model does not account for the change in temperature with depth, which is physiologically significant since thermoreceptive afferent nerves lie beneath the epidermis at depths that depend on body location [214]. The model also does not account for tissue heating due to contact with objects whose surface temperature varies with position, as in the case of the thermal grill.

The complex nature of the heat diffusion problem applied to the finger makes it difficult to account for all the heat sources and sinks adequately. Here, we adopt a model of heat exchange that assumes that the finger is composed of a homogeneous material, with thermal conductivity k. We ignore effects of perfusion and metabolic heating, or other factors, and model the stimulus at the skin surface as a temperature boundary condition. We further assume the thermal stimulus to vary along only one surface dimension x, corresponding to a boundary condition $T = T(x)$, and yielding a problem with two spatial dimensions plus time. The tissue temperature distribution is then given by $T = T(x, y, t)$, where x parametrizes distance along the skin surface, y is depth, and t is time. Under these assumptions, the time-dependent bioheat equation (6.1), describing thermal responses of skin tissues, becomes

$$\frac{\partial^2 T(x,y,t)}{\partial x^2} + \frac{\partial^2 T(x,y,t)}{\partial y^2} = \frac{1}{k}\frac{\mathrm{d}T(x,y,t)}{\mathrm{d}t} \tag{6.2}$$

To gain insight into tissue heating under these circumstances, we first consider a time-dependent analytical solution to (6.2) within a representative volume V of tissue of width a and depth b, then develop a numerical simulation. A boundary condition, $T(x, y_0, t) = T_{top}(x)\Omega(t)$, is imposed at the top y_0 of the skin, where $\Theta(t)$ is the heaviside step function, with $\Theta(t) = 1$ for $t > 0$ and $\Theta(t) = 0$ for $t < 0$. For the thermal grill stimuli, $T_{top}(x)$ will be a temperature profile corresponding to alternating hot and cold values. We assume that the other boundaries of the two-dimensional domain, which occur within the skin, are maintained at constant, ambient body temperature T_A, see Figure (6.3, top panel).

We use superposition to subtract the constant ambient body temperature T_A, and model the response through a tissue temperature variable $T(x, y, t) = \tilde{T}(x, y, t) - T_A$, where $\tilde{T}$ is the true tissue temperature. This yields boundary conditions $T(x, y, t) = 0$ for $x = 0, x = w$ and $y = d$, and $T_{top}(x) - T_A \equiv T_{TGI}(x)$, see Figure (6.3). Under thermal grill conditions, we assume the hot bars and cold bars to be respectively warmer and cooler than skin temperature T_A by the same amount, so that the boundary conditions are $T(x,0,t) = T_{TGI}(x) = \pm T_h$ within each surface domain of width a

$$\begin{aligned} T_{TGI}(x) &= \pm T_h \ \text{ if } \ x_n < x < x_{n+1}, \\ & x_n = na, \ n = 0,1,2,\ldots,N \end{aligned}$$

We fix the initial condition to be $T(x,y,0) = 0$, so that the initial tissue temperature is T_A. In this case, symmetry dictates that the temperature $T(x = x_n, y, t) = 0$ for positions x_n at the boundary between heating elements, for all y and all t. The solution to this problem is obtained by solving the heat equation within each each domain $x_n < x < x_{n+1}$ of width 10 mm (Fig. 6.4), with boundary conditions $T(0,y,t) = T(a,y,t) = 0$ and $T(x,0,t) = \pm T_h$. Since the heat equation is linear in T, the solutions $T(x,y,t)|_{\pm T_h}$ with boundary conditions T_h and $-T_h$ are related by $T(x,y,t)|_{T_h} = T(x,y,t)|_{-T_h}$

We divide the problem into its steady state and transient components and solve for each. The complete solution can be written $T(x,y,t) = T_{ss}(x,y) + T_t(x,y,t)$, where $T_{ss}(x,y) = \lim_{t\to\infty} T(x,y,t)$ is the steady state solution and $T_t(x,y,t)$ is the transient part. The steady state solution can be readily obtained when the temperature of the boundaries is held constant. It satisfies the time-independent heat equation

$$\frac{\partial^2 T}{\partial x^2} + \frac{\partial^2 T}{\partial y^2} = 0 \tag{6.3}$$

The solution with our boundary conditions is obtained using the method of separation of variables, and is given by [215]

$$T_{ss}(x,y) = T_s \sum_{n=1}^{\infty} \frac{2\left[1-(-1)^n\right]}{n\pi \sinh(n\pi b/a)} \sin\left(\frac{n\pi x}{a}\right) \sinh\left(\frac{n\pi y}{a}\right) \tag{6.4}$$

The steady-state solution over the entire domain is then obtained by concatenating the piecewise solutions for domains $ka < x < (k+1)a$ with alternating signs

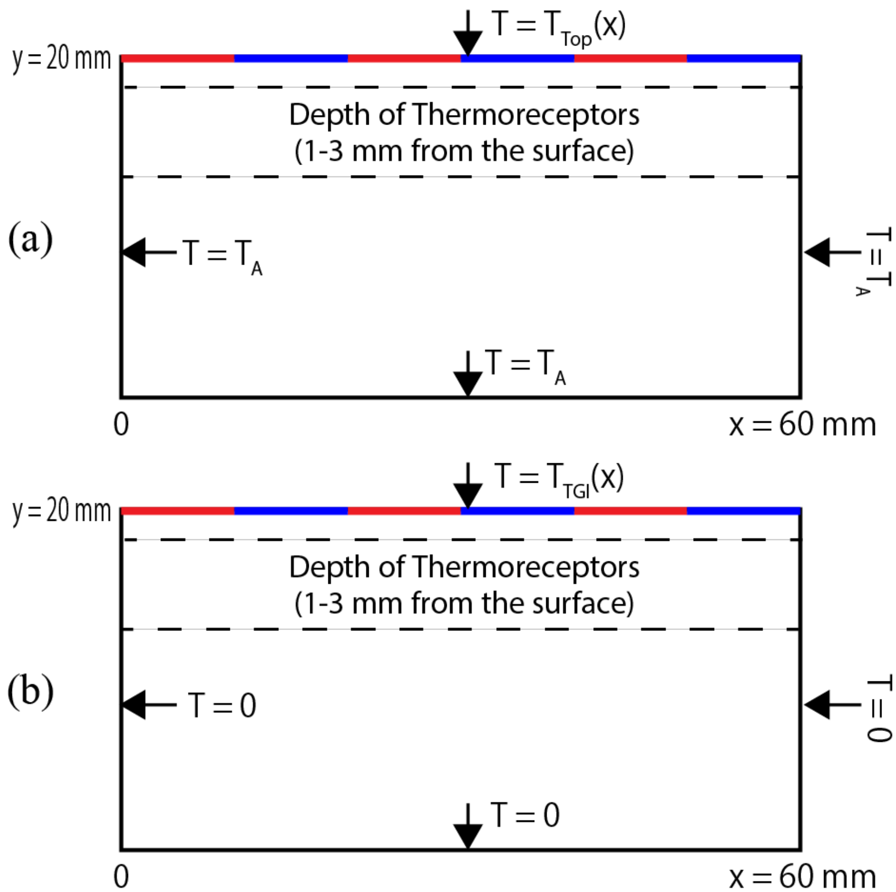

Figure 6.3: Boundary conditions for hand touching thermal grill. Top panel: The top boundary is held at the temperature of the thermal grill, while the other three are held at ambient body temperature. Bottom panel: The same boundary conditions after subtracting ambient body temperature T_A from all sides.

The transient part of the solution can likewise be obtained using the method of separation of variables, and can be written in the following form:

$$T_t(x, y, t) = \sum_{n=1}^{\infty} \sum_{m=1}^{\infty} C_{n,m} \sin\left(\frac{n\pi x}{a}\right) \sin\left(\frac{m\pi y}{b}\right) e^{\lambda t} \tag{6.5}$$

	x	y	Temperature $T(x,y,t)$
Left Boundary	$x=0$	$0 \leq y \leq b$	$T(0,y,0)=0$
Right Boundary	$x=a$	$0 \leq y \leq b$	$T(w,y,0)=0$
Bottom Boundary	$0 \leq x \leq a$	$y=0$	$T(x,0,0)=0$
Top Boundary	$0 \leq x \leq a$	$y=d$	$T(x,d,0)=T_{TGI}(x)$

Table 6.1: Boundary conditions for heat equation over the domain corresponding to the volume of body tissue near the surface of the skin after subtracting ambient body temperature T_A from all the sides

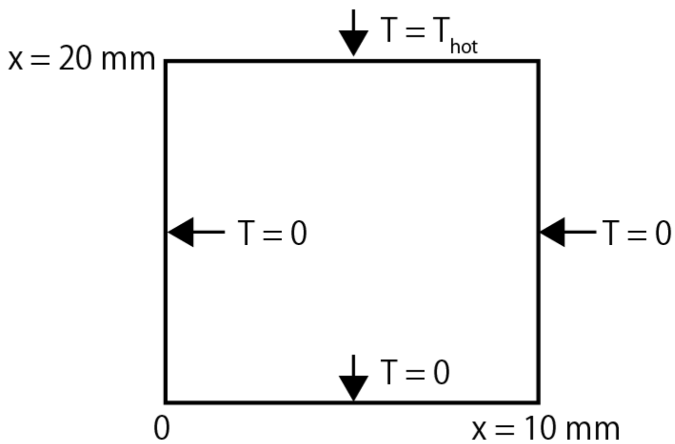

Figure 6.4: Using the method of superposition, the time-dependent solution to the heat equation can be reduced to that of a single unit cell corresponding to the volume of tissue beneath one element of the thermal grill, see text. The full solution is obtained by juxtaposition piecewise solutions with T_{hot} or $T_{cold} = -T_{hot}$

where

$$\lambda = -k\left(\left(\frac{n\pi}{a}\right)^2 + \left(\frac{m\pi}{b}\right)^2\right) \tag{6.6}$$

$$C_{n,m} = \frac{4}{ab}\int_0^b dy\, \sin\left(\frac{m\pi y}{b}\right)\left(T(x,y,0) - T_{ss}(x,y)\right) \times \int_0^a \mathrm{d}x\, \sin\left(\frac{n\pi x}{a}\right) \tag{6.7}$$

Parameter	Value
Simulation time	10 seconds
Frame rate	200 ms
Mesh size	3858×2060
Depth simulated	20 mm
Temperature at top boundary	$\pm T_{hot} = \pm 25°$C
Temperature at other boundaries	0° C
Thermal conductivity of tissue	$k = 0.3$ W m^{-1} k^{-1}

Table 6.2: Parameters used for the numerical simulation

6.3.2 Numerical Simulations

The analytical expressions for $T(x, y, t)$ illustrate the form of their dependence on time and space. However, for calculating tissue heating, these expressions are prove inconvenient, since numerical evaluation requires that the infinite sums and integrals be estimated. To avoid this, we numerically simulated the system using the finite element method. We modeled the problem domain using a rectangular mesh with dimensions 3858×2060. We used a value for the thermal conductivity of the skin of $k = 0.3$ W m^{-1} k^{-1}, which lies within the typical conductivity range of human dermis (0.293-0.322) and epidermis (0.209) [216].

The simulation spans ten seconds, and we captured the results at 50 instants with a spacing of by 200 ms. The initial conditions and boundary conditions matched those described above, and the time-dependent solution is shown for five instants in Figure 5. The dashed lines in the figures illustrate representative depths at which thermoreceptors in the hand can be located. Thermoreceptors lie at the regions of the dermis nearest to the epidermis, shown here as 1-3 mm, but depending in general on body location and other factors.

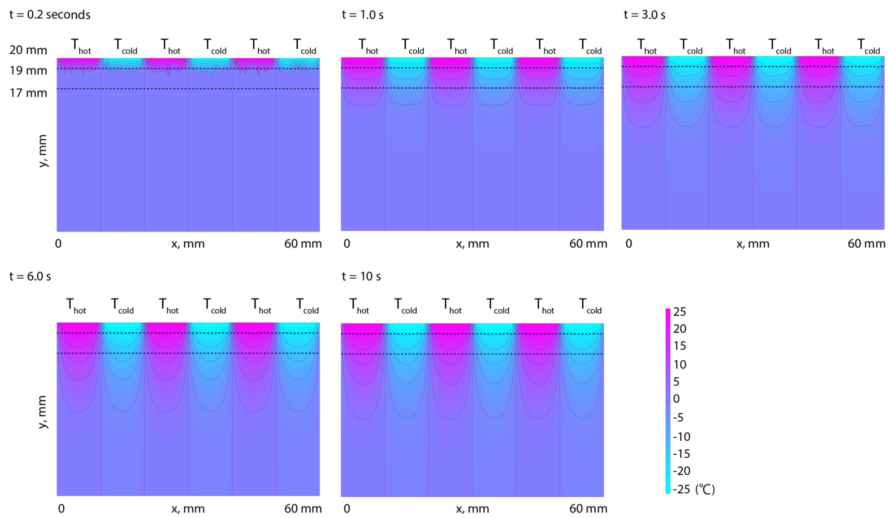

Figure 6.5: The time-dependent numerical solution for tissue heating at instants spanning ten seconds of the simulation, illustrating progressive heating of underlying tissues. The dashed black lines indicate the approximate range of depths of the epidermis-dermis interface, $1 - 3$ mm.

6.4 Thermal Grill Display Design

To empirically investigate factors reflecting how the thermal grill stimuli are perceived, and to explore the use of these stimuli in human-computer interfaces, we designed a new electro thermal display device. The device is comprised of a thermal grill surface, with heating apparatus, controller, sensors, and computer. The thermal grill surface is made of aluminum bars, each having dimensions $6 \times 6 \times 15$ mm. A total of 6 such bars are used. They are separated by 6 mm and arranged in an alternating pattern. In typical operation, half of the bars are heated (using the Peltier element on one side) and the remaining half are cooled (using that from the other side), but the bars may also be used to uniformly heat or cool.

The heating and cooling is done using Peltier devices (TEC1-12706 Thermoelectric Peltier Cooler 12 Volt, 92 Watt), semiconductor thermoelectric heat pumps that move heat heat from one side to another when an electric potential is applied across their

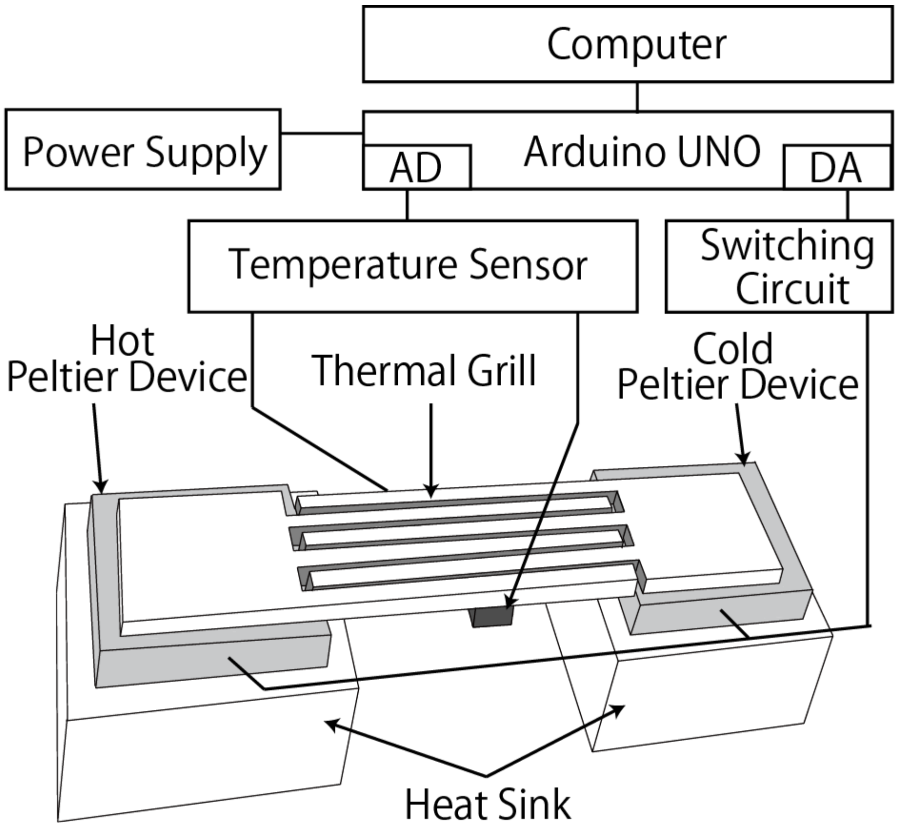

Figure 6.6: Thermal grill display device. Peltier thermoelectric pumps are electronically controlled independently for each of two sets of grill elements. A microcontroller sends control signals to the Peltier elements and reads signals from the temperature sensors. Heat sinks allow the thermoelectric device to operate relative to room temperature. Temperature sensors are affixed to the bottom of the touched portion of the grill. The temperature of the top surface of the device was calibrated in order to ensure that the specified temperature is felt by the skin on contact with the device.

terminals, causing one side to heat and the other to cool. An opposing side is maintained close to room temperature via a heat sink to ensure efficient operation. We employed two heat sinks to ensure that the Peltier elements could be positioned away from the touched grill area, which ensured that the warm and cool elements remained well decoupled. The temperature of the grill elements is monitored using surface temperature sensors that are attached to the bottom side of one hot and one cold element in the array, nearest to the touched interface, ensuring that the measured temperature reflects what is felt at the surface.

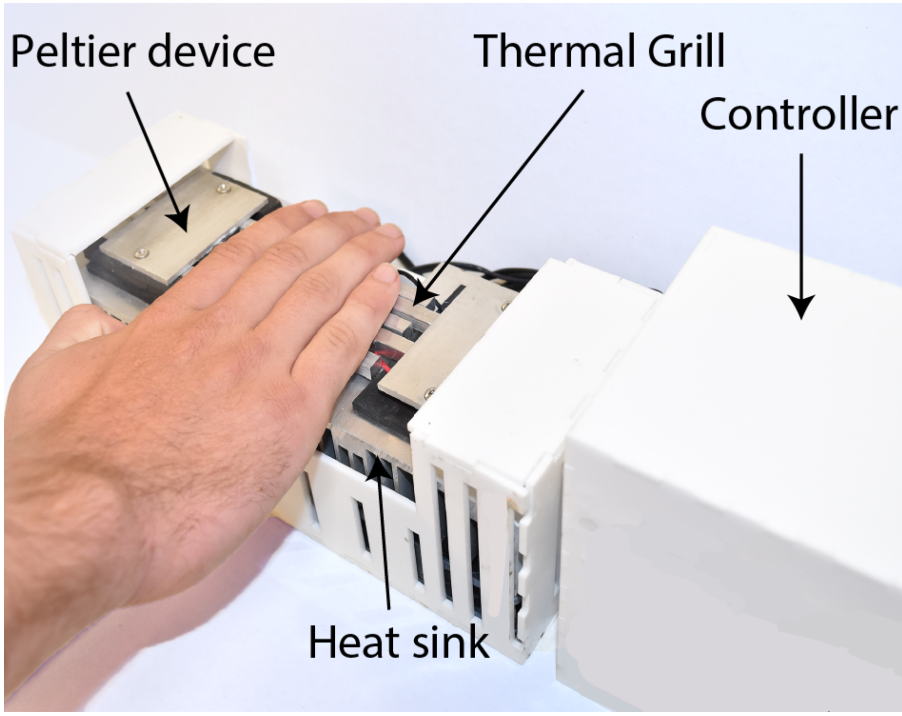

Figure 6.7: The thermoelectric haptic device used for the experiment. The participant kept their hand on the thermal grill and their responses were recorded.

In order to validate the performance of the device, we measured the temperature on the top surface using a contactless thermal probe and calibrated the temperature sensors to this value, ensuring that the specified temperature that is felt by the skin on contact with the device was within approximately $\pm 1°$ C of the specified temperature. The temperature control loop and sensor monitoring (sample frequency 100 Hz) is performed via a microcontroller (Arduino Uno, Arduino SRL, Italy), and commanded by desktop computer via serial communication. When a new temperature is commanded, it takes approximately one minute for a stable target temperature to be reached (we allowed for three minutes in the experiment below).

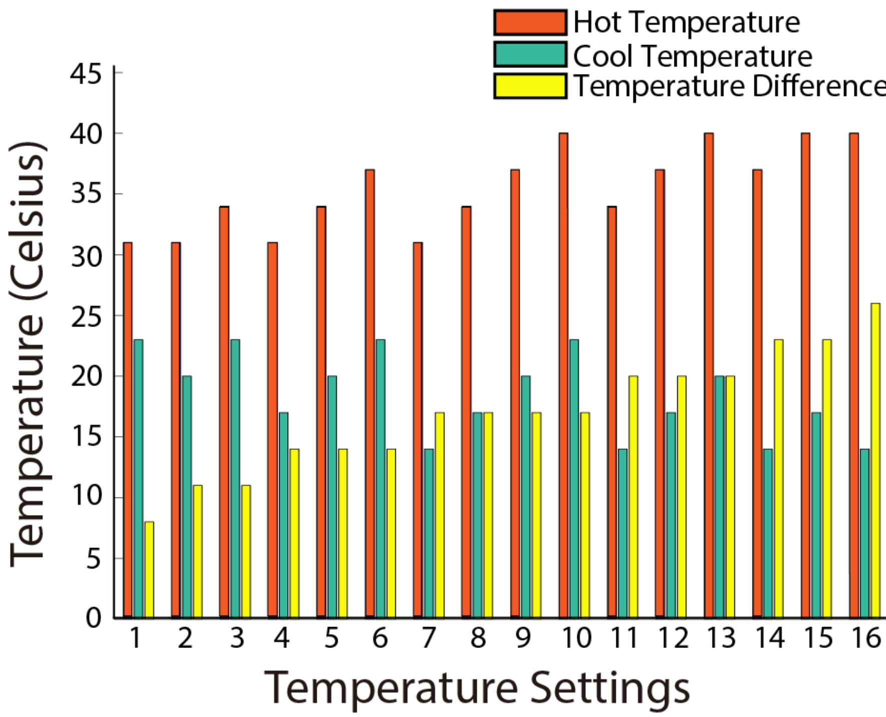

Figure 6.8: Temperature Settings for the thermal grill used in the study. Hot temperatures were varied between 31 to 40°C and cold temperatures were varied between 14 to 23°C. Four combinations each for hot and cold temperatures give 16 thermal grill settings.

6.5 Experiment: Time-dependent perception of the TGI

We designed a psychophysical experiment to apply this display, and to investigate the dynamics of thermal perception in the thermal grill illusion – and in particular the relation between the intensity of the sensations that it produced and the time that it took for these sensations to be elicited. In it, we assessed both intensity and reaction time, and analyzed the results to determine how they were related to the temperatures of the warm and cool bars.

6.5.1 Apparatus

The apparatus consisted of the thermal grill display device described in the previous section. We measured the response times during using an electronic sensor (switch), which recorded when the surface was touched and released by the hand of the participant. The ambient temperature during the experiment was climate controlled within a range from 20 and 22°C. The experiment was run under computer control using Python-based psychophysics software (Psychopy, University of Nottingham, UK), which selected the stimuli, commanded the thermal grill display, displayed the graphical user interface, and recorded participant responses.

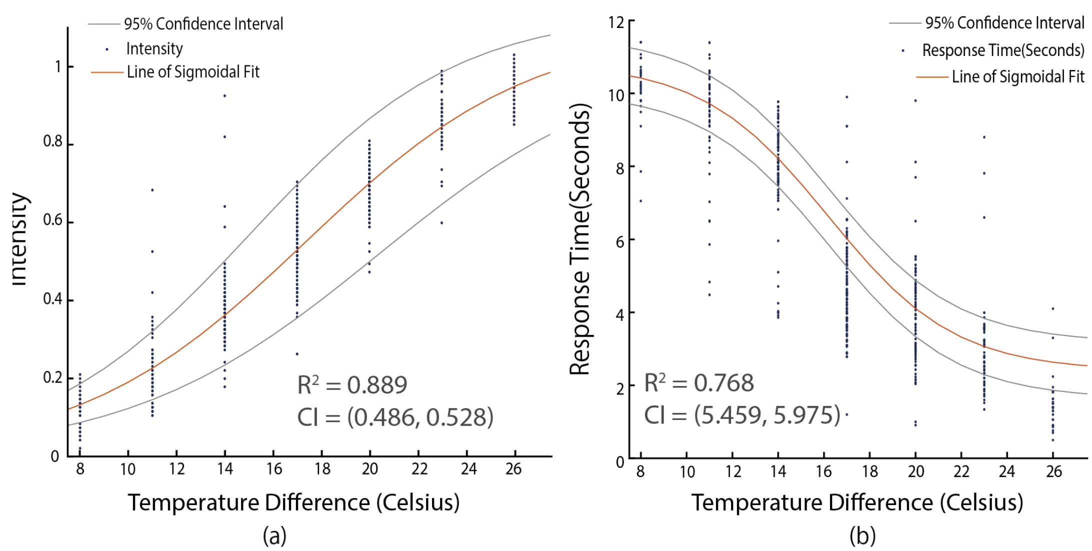

Figure 6.9: Perceived intensity and response time to thermal grill stimuli, data from all subjects and all trials in the experiment. The horizontal axis represents the temperature differential of the thermal grill. The vertical axis represents perceived intensity, from 0-1, on a scale rated according to extremal settings felt before the experiment. The perceived intensity shows a sigmoidal relationship with the temperature differential. (b) As in (a), except that the vertical axis represents the response time in seconds.

6.5.2 Methods and Stimuli

During the experiment, subjects felt the thermal grill at various temperature settings, consisting of the temperature of warm and cool elements, see Figure 6.8). Their response time and perceived intensity was recorded. The temperature settings of the thermal grill were changed between trials. There were a total of 16 temperature combinations (Figure 6.8). These temperature combinations were chosen to be well within the limits of thermal pain, so as that the individual elements were not perceived to be painful. The participants felt the thermal grill at the minimum and maximum settings prior to the experiment, in order to remove individual bias towards rating the perceived intensity.

6.5.3 Participants

A total of 10 participants volunteered for the experiment, five were female and five male, with ages ranging from 22 to 29 years old. Participants were compensated with $10 for their time. Participants reported no condition affecting normal use or sensation in the hands. All reported being right-hand dominant. All subjects gave informed consent. The experiments were approved and conducted according to the human subjects research policies of the University of California, Santa Barbara. Prior to the experiment, participants completed a short survey collecting anonymous demographic and screening information.

6.5.4 Procedure

Prior to the experiment, participants were asked to touch the thermal grill at the maximum and minimum temperature differential, and then rate the intensity of each trial accordingly. The total duration for each participant was 1 hour including a three minute break time between each temperature setting. This break time also enabled the thermal grill to reach a stable temperature.

The experiment was conducted in a quiet environment to limit distractions. Participants were seated at a desk equipped with a computer interface and the thermal grill. Participants completed a brief guided training phase before they proceeded to the main part of the experiment, during which they felt the thermal grill at the minimum (smallest temperature difference) and maximum (largest temperature difference) settings, and were informed that these corresponded to the least and most intense stimuli. During each trial, participants placed their palm flat on the grill. Participants were instructed to remove their hand from the display as soon as they felt a burning sensation similar to the one that they felt for the largest temperature difference stimulus, which they felt during the acclimation phase (see Methods and Stimuli). The response time was given by the time between initial contact and the removal of the hand, as recorded by the switch. If they did not respond within 10 seconds, participants were prompted to remove their hand from the display. Participants then rated the intensity using a continuous slider, ranging from 0 (least intense) to 1 (most intense). Subsequent trials proceeded similarly. We proceeded with three trials at each temperature setting, in succession, since no delay was required between them, and this permitted significantly more data to be collected, and averaged responses from the three. Different temperature settings were presented in random order. There were a total of 16 such settings in the experiment. The procedure was computer automated, and provided automated prompts as to when the thermal grill should be felt in each experimental condition.

6.5.5 Results

The rated intensity $I(\Delta T)$ increased, on average, monotonically with the temperature difference between warm and cool elements (Fig. 6.9a). The relationship between intensity and temperature difference was sigmoidal in shape. Fitting intensity I as a function of temperature difference ΔT with a sigmoidal function $I(\Delta T) = a(b + e^{-c\Delta T})^{-1} + d$ indicated a positive effect of temperature difference on intensity ($p < 0.01$). The R^2 value for the fit was 0.89. Differentiating this fitting function revealed that the maximum rate of increase in perceived intensity occurred at temperature difference ΔT =17° C.

On average, response time t_R decreased monotonically with temperature difference (Fig. 6.9b). We modeled the relationship via a sigmoidal function $t_R(\Delta T) = a(b + ce^{-d\Delta T})^{-1} + f$ and determined that the relationship was significant ($p < 0.01$) and that the R^2 value was 0.768. From the data, at the highest temperature difference, the response time was fastest. At the lowest temperature differences, the results reflect a mix of trials in which participants withdrew their hand based on what they felt and others in which they were prompted to do so after 10 seconds had elapsed. Nonetheless, a decrease in response time is seen with increasing temperature at these levels. Here too, the rate of decrease was fastest near 17° C. For each increase in ΔT by one degree, the response time decreased by 0.506 seconds, on average.

Across all temperature differences used in the experiment, there was, on average, a decrease in response time with intensity (Fig. 6). The relationship was approximately linear, and a linear fit yielded an R^2 value of 0.673. The lowest uncertainty was for the highest temperature differences ($\Delta T = 26°$ C), for which all data points clustered around a mean response time of approximately 1.5 seconds and an intensity of 0.9.

6.5.6 Discussion

The results (Figure 6.9a,b) indicate that as the temperature difference ΔT between the warm and cool bars increased, the perceived intensity increased, on average, while the response time t_R decreased. This suggests that the thermal grill illusion is not a

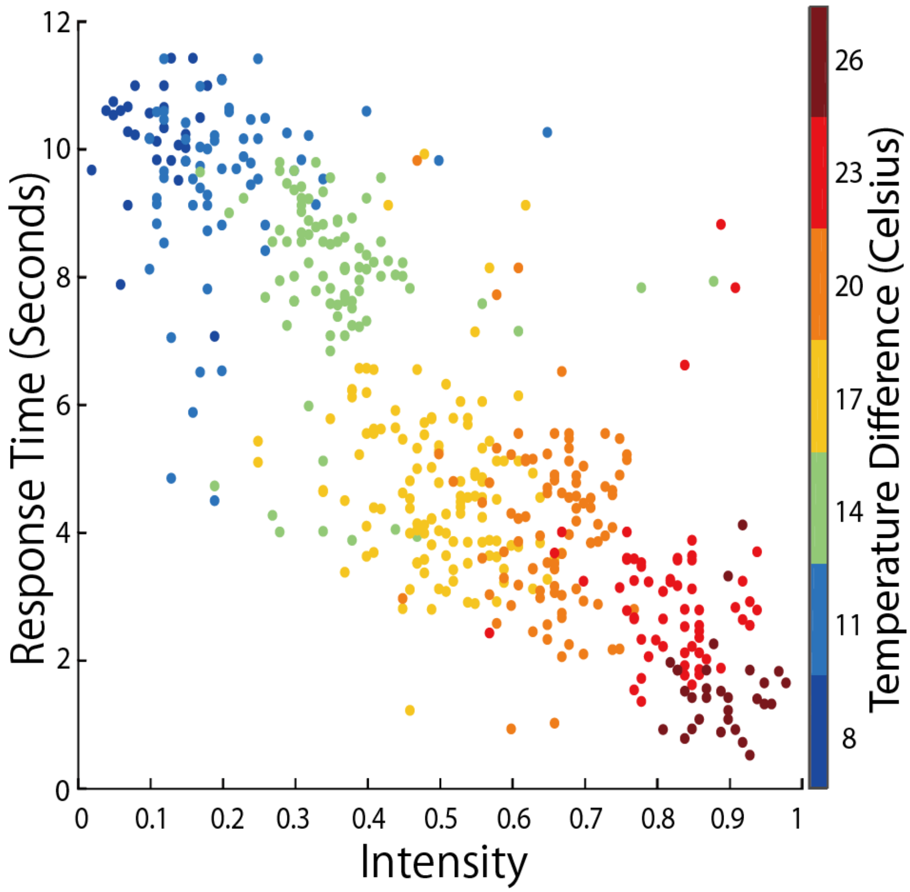

Figure 6.10: Response Time vs Perceived Intensity for the entire experimental data. Response time time varies inversely with the perceived intensity, with an approximately linear relationship. Positions along this relationship were approximately organized according to temperature differential.

digital phenomenon, and that there is a proportional effect of temperature difference on both intensity and response time, for temperatures in the range studied here. This is also consistent with prior observations [204], that the strength of the thermal grill illusion depends on the cold-warm differential rather than the individual cool and warm temperatures. The sigmoidal functions that we fit to the data may, in principle, be used in order to predict the intensity and response time to thermal grill stimuli as the temperature difference is varied, but the results likely also depend on factors including the surface area of contact [217]. Nonetheless, we expect qualitatively similar results to hold for thermal grill displays of different dimensions or configuration. The variability in intensity and response time were smallest (excluding limiting effects on response time measurements, see above) at the highest temperatures. The ratings and response times varied little among the entire participant population, underlining the robustness of this effect.

Possible relevance to neural mechanisms

There was no regime for which response times were (consistently) short for the lowest temperature differences studied; below about 20° C, the vast majority of responses took longer than three seconds. However, at the highest temperature differences (23 to 26° C), response times were almost always short, generally between 300 ms and 2.5 s. Participants feeling these stimuli responded very quickly after they placed their hand on the display. The values of the response times are remarkably short in comparison with the propagation time that would be suggested by the low neural conduction velocities of C fiber afferents. These velocities average less than about 2 m/s, which is too slow to account for the observed response times. Conduction speeds for Aδ afferents are faster, up to 30 m/s.

The difference in conduction speeds between these pathways may be relevant to understanding the dynamics of perception in the thermal grill illusion because, according to currently accepted explanations [202], the illusion arises due to a reduction of normal discharge in cold-sensitive Aδ afferents, which are suppressed due to spatial summation of inputs from adjacent warm regions. Normally, Aδ discharge has a disinhibiting effect on polymodal C-nociceptive fibers, preventing them from signaling pain in response to cool stimuli. Because the TGI elicits such rapid responses, it appears likely that the process involves activity of first order Aδ fibers that quickly reaches the central nervous system, where it disinhibits C fiber activity that is necessarily retrograde, associated with peripheral stimuli that must have occurred on the order of one second earlier. This picture is complicated by the dynamics governing tissue heating, which we discuss next, and further research is needed in order to clarify the mechanisms of dynamic perception in the thermal grill illusion.

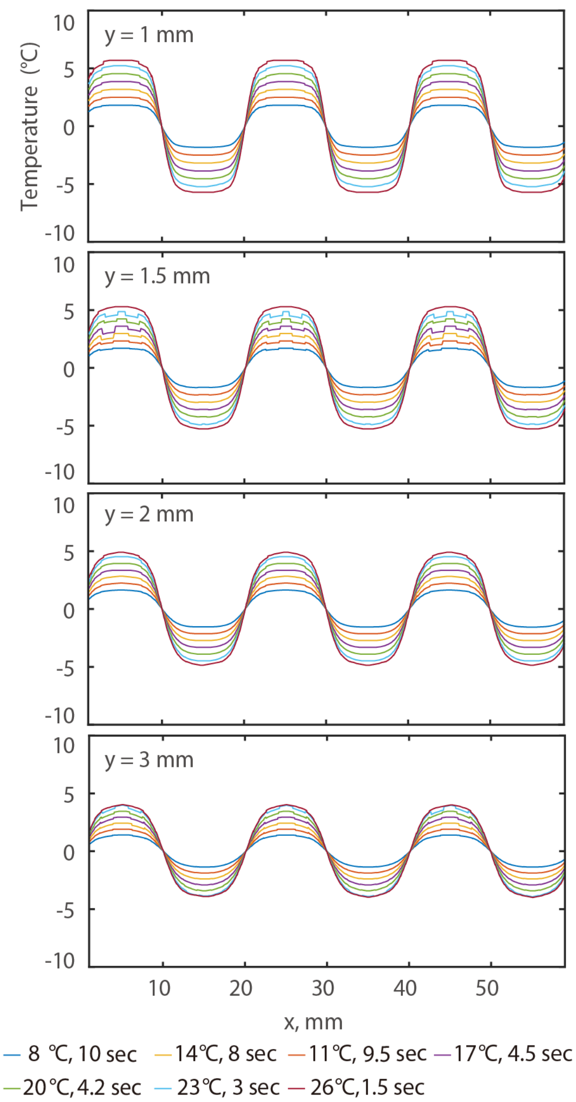

Figure 6.11: Simulated temperatures $T(x, y_T, t_R; \Delta T)$ as a function of displacement x along the direction of the thermal grill, at tissue depths d_T associated with thermoreceptive afferents. The mean tissue temperature was subtracted from the result, which is reported relative to 0 °C. Each curve represents a prediction of the simulation at a mean time t_R (range 1.5 to 10 seconds, as shown) that participants responded to stimuli with temperature difference ΔT (range 8 to 26 °C). See Table 3 for the associated mean response times and temperatures.

Temperature Difference ΔT (°C)	Response time t_R (s)
8	10
11	9.5
14	8
17	4.5
20	4.2
23	3
26	1.5

Table 6.3: Temperature differences and mean response times based on the experiment results, as used in the comparison with model predictions. The numerical solution for $T(x, y, t; \Delta T)$ was evaluated for each ΔT at the response time t_R listed in the table.

6.6 Integrating the thermal model and perception experiment

In order to obtain insight, however preliminary, into the role played by the dynamics of tissue heating in the perception of the thermal grill illusion, we combined the thermal model developed in Section 6.3.1 with the experimental results from Section 6.5. We first computed time-dependent numerical solutions $T(x, y, t; \Delta T)$ of the heat equation with thermal grill boundary conditions for each grill temperature difference, $\Delta T - T_{hot} - T_{cold}$, used in the experiment. Figure 6.5 shows an example of these results for a fixed value of the temperature difference. We then evaluated these solutions at depths d_T ranging from 1 to 3 mm (at positions $y{=}y_T{=}17$ to 20 mm with reference to the coordinate system of Section 3), corresponding to the presumptive range of depth of thermoreceptive afferents in glabrous skin, below the epidermal strata (corneum, lucidium, granulosum, spinosum, basale) [214, 218].

We then sought to estimate what was felt by participants when they responded to the thermal grill. We did this by determining the tissue temperature distribution at the nominal depths of the thermoreceptors that were predicted by the model at the response

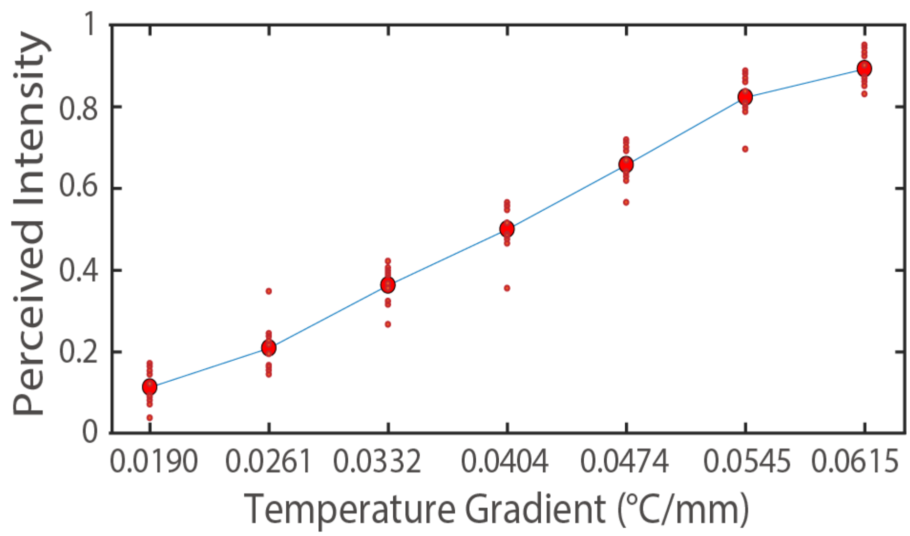

Figure 6.12: The average intensity reported by participants viewed as a function of the maximum value of the gradient of the simulated tissue temperature, $\max_x |\partial T(x, y, t; \Delta T)/\partial x|$, at the time t_R that participants responded. Results correspond to an assumed thermoreceptor depth of 1 mm (Fig. 11, top panel), and encompass all tested temperature differences from 8 to 26 °C. The proportional increase in subjective intensity with the gradient in tissue temperature provides a simplified explanation of the perceptual thermal grill illusion, although this explanation does not account for neural mechanisms or physiological factors affecting heat exchange.

time, which we obtained by selecting the mean response time $t_R(\Delta T)$ corresponding to temperature difference ΔT. These value pairs are reported in Table 6.3. For each temperature difference, the simulation was evaluated after an interval given by the corresponding time instant to respond. The spatial variation of tissue temperatures at the depth and time of interest was thus obtained from the numerical solutions, with $T(x, y_T, t_R; \Delta T)$. We subtracted the average tissue temperature (obtained from the equilibrium solution) in order to express temperatures relative to the ambient temperature in the tissue.

The resulting predictions for the tissue temperature at the response instant, for all seven values of ΔT, and four different tissue depths d_T (one per panel), are shown in Figure 6.11. Each plot represents the variation in temperature predicted by the model in a plane parallel to the skin surface, along the direction of change in the thermal grill. At each depth and temperature difference (and corresponding response time) the temperature pattern of the grill is reflected in the predicted temperature distribution in the tissue. At greater depths, the shape of the distribution becomes increasingly rounded, due to thermal diffusion. As position x varies, the temperatures at the hottest and coolest positions increases in proportion to the temperature difference of the grill. This proportional increase seemed to reflect the proportional increase in perceived intensity of the grill at the time participants reported it (which was the same time used to evaluate the simulation).

As a preliminary step toward understanding the relation between tissue heating and perceptual responses, we explored a simple hypothesis in which, as the temperature difference is varied, the perceived intensity $I(t_R)$ at the time of response t_R is proportional to the maximum value attained by the gradient of the temperature along the grill direction,

$$I(t_R) \approx \max_x \left| \frac{\partial T(x, y_T, t_R; \Delta T)}{\partial x} \right|, \tag{6.8}$$

at the assumed depth $y_T = y_0 - d_T$ of the thermoreceptors. The latter value was larger for higher temperature differences. We assessed this simple hypothesis using the thermal model predictions for tissue temperature at the time of response (Fig. 6.11) The results (Fig. 6.12) suggest a proportional, nearly linear, relationship between intensity ratings and temperature gradient, with relatively little variation. This suggests that internal tissue temperatures may be useful in understanding the time-dependent perception of the thermal grill illusion. However, because this explanation does not account for the accepted neural mechanisms of the illusion, which are required in order to explain the response times that are observed, and does not account for factors such as blood perfusion or internal heating, further research is merited.

6.7 Conclusions

Thermal perception is important in the experience of touching real objects, and thermal display devices are of growing interest for applications in virtual reality, medicine, and wearable technologies. In this study, we investigated the perception of the thermal grill illusion by developing a mathematical model of tissue heating, designing a new thermal display, and conducting a psychophysical experiment. We assessed the intensity of responses elicited by thermal grills with different temperature settings, and measured the response time until the onset of thermal grill sensations. We found that thermal grills elicited highly stereotyped responses. As the temperature difference increases, the intensity increases monotonically, while the response time decreases monotonically. Consequently, perceived intensity was inversely correlated with response time. A comparison of the psychophysical results with a model of tissue heating suggests that the responses may be predicted by accounting for the tissue temperature at the depth of the thermoreceptors, but more research is needed to clarify the relation between the tissue temperature and the time-dependent perception of the thermal grill illusion. Under current physiological explanations, responses to thermal stimuli depend on tissue heating, neural processing, and the spatial distribution of temperature, but do not account for internal temperatures of tissues. The results of this study could help to inform models accounting for these factors. Furthermore, this study has quantified the relation between display parameters and perceptual parameters. This could provided basic information needed to apply the thermal grill illusion in new application areas of human-computer interaction, VR, and medicine.

There are several areas of potential improvement of this study. In the perception experiment, the measurement method and analysis assumed that subjects would remove their hand due to discomfort at some finite time, whereas this was not necessarily true at the lowest temperatures. There may be some ordering bias, due to the repeated presentation of stimuli at the same temperature. While we attempted to control for this by introducing a delay between stimulus presentations, a fully randomized presentation order would be preferable. In practice, the slow heating time of the contact surface implies that this would require a relatively long experiment. A more detailed model of the TGI should account for the minimum temperature needed to elicit a TGI sensation at any temperature. More significantly, further research and theoretical analysis is needed about the relevance of different afferent pathways, and tissue heating, to the perception of the TGI. While we have presented a preliminary mathematical model for comparison with thermal grill responses, this model is simplified, and does not account for physiological factors affecting heat exchange, and does not quantitatively account for the accepted neural mechanisms of the thermal grill illusion, which are required in order to explain the response times that are observed. An improved computational model of thermal perception could, accounting for heat transfer and neural transduction and integration, could greatly inform our understanding of the thermal grill illusion, and of the perception of spatially and temporally varying thermal stimuli more generally, and is something that we hope to address in future work.

The thermal grill illusion is both an evocative example of sensory integration, and the relation between perception, physics, and physiology, and an intriguing example of very fast processing of thermal stimuli in the perceptual system. A better understanding of the mechanisms of fast perceptual processing of thermal stimuli could enable future thermal display methods that can evoke very fast perceptual responses. This could yield thermal displays with much wider applications than are currently envisaged.

Appendix

As the example of the use case in VR application with thermal grill illusion, "Impossible Touch" has developed (Fig. 6.13). Users have the ability to interact with potentially hazardous hot objects such as a heated pan on a lit stove, a steaming car body, and hot springs. This system holds practical implications for education and the creation of an authentic virtual environment imbued with a burning sensation. It would be intriguing to explore how this burning sensation enhances the immersive experience, the usability of the application, and the overall touch interaction.

Figure 6.13: Impossible Touch represents a compelling use case of the Thermal Grill illusion within the realm of virtual reality, specifically in augmented haptic reality. By thermal feedback to create a sensation of fake burning heat, users are able to interact with objects that would typically be too hot to physically touch with their hands in Virtual Reality and experience fake burning heat.

Chapter 7

Conclusion

This PhD research was motivated by the engineering challenges of developing a haptic device that allows us free-hand interaction to augmentation haptically these touch interactions in VR and AR. This goal is still far from realization regardless of over decades. The reason for this challenge is touch sensation is sub modality that includes vibration, pressure, temperature, and pain, and touch sensation is easily affected by the property of stimuli and condition, touch interaction, of body movement because touch sensation is temporally and spatially integrated and process in the brain.

This PhD dissertation contributes to the knowledge of several different approaches in attempts to serve longstanding goals by presenting the tactile augmentation reality to augment haptically in free-hand touch interaction. Chapters 3, 4, 5 presented the new design and perceptual research for tactile augmented reality with vibrotactile feedback in free-hand touch interaction, and how usability is improved by the free-hand interaction. Chapter 6 showed the augmented surface haptically with thermal feedback.

The field of haptics is highly interdisciplinary, encompassing multiple disciplines such as engineering, psychophysics, biomechanics, anatomy, and physics. The present PhD research was motivated by the need to understand touch perception in active touch interaction. While the field of haptic research has made significant progress in recent years, there is still room for research on the method, perception, and usability of tactile augmentation.

Chapter 3 of this dissertation introduces a novel wearable method and system for multisensory augmentation of manual touch interactions with objects and surfaces, with the goal of enhancing haptic touch interaction in virtual and augmented reality. The system, called Tactile echoes, is a wearable tactile device that enables responsive haptic effects to be rendered during manual interactions involving direct contact with the skin. The perceptual study of the new wearable display showed that it provided various sensations of tactile feedback to modify the surface, which was explained by the MDS perceptual space labeled by hard, deep, echoing, bouncy, buzz, thud, metallic, rubbery, rumble, wobbly, hollow, and real. Moreover, in a user study with Tactile echoes in an AR game, it was found that responsiveness, engagement, and agency were significantly enhanced in playing the AR game. This method allows tactile feedback to be introduced into naturally occurring interactions without requiring the touched object to be engineered or imposing any device between the skin and the touched object, such as a handheld controller or instrumented surface. Therefore, this system represents a promising design approach for tactile augmented or mixed reality. The findings of this research also demonstrate how tactile feedback can be programmable and assigned to objects or surface regions.

Chapter 4 investigates the tactile forward masking effect in active touch. This research is motivated by observations of diminished perception of tactile feedback with a short delay after touch, compared to a longer delay in the wearable tactile device demonstrated in Chapter 3. We conducted two parts of perceptual experiments to reveal how the perceptual intensity of tactile feedback is affected by the masking of touch-elicited vibration in active touch, manipulating delay time, amplitude, and property of tactile feedback. The results of the experiment show modulatory effects of timing, vibration amplitude, and the perceptual similarity of the vibration feedback with the transient skin oscillations elicited through touch contact. Our findings are consistent with previous investigations of passive touch and demonstrate the important modulatory effects of active touch behavior and events on tactile processing. They shed light on the interplay between perception and action in the somatosensory system and have implications for the design of haptic interfaces.

Chapter 5 introduces a novel method for synergistically integrating vibrotactile feedback provided via a wearable device on the finger with feedback from a touch screen device. The method involves supplying vibrotactile feedback at different single frequencies via the wearable and touch screen devices, which can elicit sensations of difference, or beat frequencies, due to interference between vibration-elicited waves in the finger resulting from the vibration sources in the wearable and touch screen devices. The low frequencies reflect the difference in frequencies supplied by wearable and tablet devices. This effect can be reproduced with low-cost resonant vibration actuators, such as linear resonant actuators, which are integrated into many consumer devices. These interfering vibrations can be used to render textures, including low-frequency textures, from a touchscreen device. Potential application areas for this technology include interactive interfaces that can be personalized or haptic touchscreen gaming.

Finally, Chapter 6 of this PhD dissertation investigates perception of the thermal grill illusion. Thermal grill illusion is a perceptual effect in which burning sensations are rapidly elicited in response to stimulating the skin with juxtaposed warm and cool areas, despite most thermal percepts occurring at relatively long timescales, measured in seconds. We conducted experiments using a new thermal display to measure both response time and intensity in the thermal grill illusion. The results revealed highly stereotyped responses, with perceived intensity increasing and response time decreasing monotonically with temperature differences. We developed a mathematical and numerical model of spatiotemporal heat exchange from a thermal grill display to the skin and used it to relate perception and tissue heating. The responses to thermal grill stimuli depend on temporal and spatial factors arising from tissue heating, neural transduction and integration, and the thermal properties and temperatures of stimuli applied to the skin, as explained in accepted explanations. The results of this study could inform models accounting for these factors, enabling new uses of thermal feedback in computing interfaces, virtual reality, and medicine. Indeed, this study was conducted in collaboration with David Kerr, Director of Diabetes Research and Innovation at the Sansum Diabetes Research Institute, to explore new methods of diagnosing neuropathy in diabetes patients.

In summary, these chapters appear to build on each other by first introducing a new wearable haptic device allowing free-hand interaction (Chapter 3), understanding how tactile masking, a perceptual phenomenon found in Chapter 3, affects the perception of tactile feedback in active touch (Chapter 4), integrating interfered vibrotactile feedback generated by two vibrations from the actuator on touchscreens and a finger to explore the approach to provide feedback on the finger contact location (Chapter 5), and then adding knowledge of perceptual characteristics of a thermal sensation for establish future tactile immersion experience (Chapter 6). These represent a systematic exploration of various methods and factors that can enhance haptic free-hand interaction in AR and VR.

7.1 Future Research direction

This dissertation contributes to the knowledge of human perception in haptic interaction and the design of the tactile display to haptically augment an immersive world and presents effective approaches to augment surface with free-hand interaction. These methods have a great possibility to integrate haptic technology in virtual, augmented, and mixed reality. However, there are still remaining questions and room for consideration for further research.

Although the result of Chapter 3 provides that the developed wearable tactile display allows tactile feedback to be introduced into naturally occurring interactions without requiring the touched object to be engineered and without imposing any device, such as a handheld controller or instrumented surface, between the skin and touched object, there is still room for improving the design of the wearable device to minimize and design wireless to expand the degree of freedom in haptic interaction. The computing and motion sensing portions of the wearable device system could also be made wearable, leveraging contemporary head-mounted augmented reality glasses, goggles, and computer vision sensing.

Chapter 4 presents a perceptual investigation on tactile forward masking in active touch. Further investigation is necessary to determine the masking effect with varying duration of tactile feedback, and remote tactile forward masking for designing a wearable tactile display attached separately from the fingertip.

In Chapter 6, the perceptual intensity and response speed of thermal sensation evoked by the thermal grill illusion were addressed. Further research is needed to minimize the thermal grill device or design a wearable thermal grill display to pursue more practical use cases in virtual and augmented reality for free-hand interaction.

The research also proposed several avenues for future investigation that may contribute to the overarching challenge of wearable tactile display in free-hand interaction, some of which are being pursued by me and my colleagues.

- Chapter 3 presents the findings of a new wearable tactile device that allows for free-hand interaction in augmented and virtual reality. The advantage of this wearable display is to provide responsive feedback accompanying active touch during object interaction. As a further development beyond what is described in Chapter 3, there is a possibility to develop a multi-finger wearable tactile device. The multi-finger wearable tactile device will allow the user to grasp, pinch, explore haptically, and perform multi-finger manipulations. To develop a multi-finger wearable tactile display, an investigation into the effects of stimulation in multi-finger interactions is essential.

- The results from Chapter 4 overturns the brief of design haptic technology which eliminates delay in the system as the best tactile device. The reason is that touch-elicited vibration eliminates the sensation of tactile feedback provided in a short delay in active touch, and even in the perceptual delay time, this tactile forward masking effect lasts. As a further investigation, it is interesting to develop a tactile feedback system that manipulates only the latency of tactile feedback rather than its physical intensity to explore how tactile sensation can be varied and how tactile feedback with varied latency contributes to helping the control of the graphic application with its tactile cue.

- Chapter 5 introduces a novel method for rendering coarsely textured, bumpy surfaces by utilizing beat frequencies generated within the finger. It is essential to carry out perceptual experiments to empirically ascertain the extent of localization of interfering vibrations and their perception on the finger when the frequency range of these vibrations is manipulated. Further important investigations include evaluating to what degree interfering vibrations augment perceptual intensity compared to vibrations produced by a singular actuator, and identifying the specific nature of the sensation these interfering vibrations evoke.

- The perceptual investigation of thermal grill display in Chapter 6 is a great guideline for designing a fast and intense burning sensation. This knowledge of providing the fastest and strongest burning sensation can be used in virtual and augmented reality applications. As a further development beyond what is described, I developed the virtual reality system named “Impossible Touch.” In this system, the user can touch dangerously hot objects such as a hot pan on the firing stove, the hot steamed car body, and hot springs (Fig. 6.13). This system is practical for education and building a real virtual environment with a burning sensation. It is interesting to investigate how the burning sensation improves the immersive experience, usability of the application, and touch interaction.

The scope of the phenomena examined in this PhD, coupled with the relative newness of this field to the haptics research community, implies that the outcomes of this dissertation could have implications that extend beyond the current research focus, thereby informing various future advancements that are yet to be conceived.

Appendix A

Supplemental materials

A.1 Tactile Echoes

The supplemental media of applications and experiments can be retrieved here: https://youtu.be/HrR5WuPiMmU

All supplemental materials are archived here: http://doi.org/10.25349/D9BS5G

A.2 BeaTactile

The supplemental media of applications and experiments can be retrieved here: https://youtu.be/-E11GiZSUzA

A.3 Impossible Touch

The supplemental media of applications and experiments can be retrieved here: https://youtu.be/6wIGpiepTos

Bibliography

[1] L. Jones, *Haptics.* The MIT Press, 2018.

[2] A. Kawazoe, G. Reardon, E. Woo, M. D. Luca, and Y. Visell, *Tactile echoes: Multisensory augmented reality for the hand*, *IEEE Transactions on Haptics* **14** (2021), no. 4 835–848.

[3] P. Cipresso, I. A. C. Giglioli, M. A. Raya, and G. Riva, *The past, present, and future of virtual and augmented reality research: A network and cluster analysis of the literature*, *Frontiers in Psychology* **9** (2018).

[4] S. J. Lederman and R. L. Klatzky, *Haptic perception: A tutorial*, *Attention, Perception, & Psychophysics* **71** (2009) 1439–1459.

[5] F. P. McGlone, A. B. Vallbo, H. Olausson, L. S. Loken, and J. Wessberg, *Discriminative touch and emotional touch.*, *Canadian journal of experimental psychology = Revue canadienne de psychologie experimentale* **61 3** (2007) 173–83.

[6] E. Kandel, J. Koester, S. Mack, and S. Siegelbaum, *Principles of Neural Science, Sixth Edition.* McGraw-Hill Education, 2021.

[7] E. R. Kandel, J. H. Schwartz, T. M. Jessell, S. A. Siegelbaum, and A. J. Hudspeth, *Principles of neural science*, vol. 4. McGraw-hill New York, 2000.

[8] A. Gescheider, S. J. Bolanowski, and K. Hardick, *The frequency selectivity of information-processing channels in the tactile sensory system*, *Somatosensory & Motor Research* **18** (2001) 191 – 201.

[9] R. T. Verrillo, *Effect of contactor area on the vibrotactile threshold*, *Journal of the Acoustical Society of America* **35** (1963) 1962–1966.

[10] G. A. Gescheider, S. J. Bolanowski, and R. T. Verrillo, *Vibrotactile masking: effects of stimulus onset asynchrony and stimulus frequency.*, *The Journal of the Acoustical Society of America* **85 5** (1989) 2059–64.

[11] Y. Vardar, B. Güçlü, and C. Basdogan, *Tactile masking by electrovibration*, *IEEE Transactions on Haptics* **11** (2018), no. 4 623–635.

[12] I. Darian-Smith and K. O. Johnson, *Thermal sensibility and thermoreceptors.*, *The Journal of investigative dermatology* **69 1** (1977) 146–53.

[13] A. Brown, *Somatic sensation: Peripheral aspects. textbook of physiology*, 1989.

[14] A. Patapoutian, A. Peier, G. M. Story, and V. Viswanath, *Thermotrp channels and beyond: mechanisms of temperature sensation*, *Nature Reviews Neuroscience* **4** (2003) 529–539.

[15] D. C. Spray, *Cutaneous temperature receptors.*, *Annual review of physiology* **48** (1986) 625–38.

[16] J. C. Stevens and K. K. Choo, *Temperature sensitivity of the body surface over the life span.*, *Somatosensory & motor research* **15 1** (1998) 13–28.

[17] L. E. Williams and J. A. Bargh, *Experiencing physical warmth promotes interpersonal warmth*, *Science* **322** (2008) 606 – 607.

[18] H. Ijzerman and G. R. Semin, *The thermometer of social relations*, *Psychological Science* **20** (2009) 1214 – 1220.

[19] G. Lakoff and M. Johnson, *Philosophy In The Flesh: The Embodied Mind And Its Challenge To Western Thought*. Collection of Jamie and Michael Kassler. Basic Books, 1999.

[20] A. Adilkhanov, M. Rubagotti, and Z. Kappassov, *Haptic devices: Wearability-based taxonomy and literature review*, *IEEE Access* **10** (2022) 91923–91947.

[21] A. J. Silva, O. A. D. Ramírez, V. P. Vega, and J. P. O. Oliver, *Phantom omni haptic device: Kinematic and manipulability*, *2009 Electronics, Robotics and Automotive Mechanics Conference (CERMA)* (2009) 193–198.

[22] H. I. Son, A. Franchi, L. Chuang, J. Kim, H. H. Bülthoff, and P. R. Giordano, *Human-centered design and evaluation of haptic cueing for teleoperation of multiple mobile robots*, *IEEE Transactions on Cybernetics* **43** (2013) 597–609.

[23] A. F. Siu, E. J. Gonzalez, S. Yuan, J. B. Ginsberg, and S. Follmer, *Shapeshift: 2d spatial manipulation and self-actuation of tabletop shape displays for tangible and haptic interaction*, in *Proceedings of the 2018 CHI Conference on Human Factors in Computing Systems*, CHI '18, (New York, NY, USA), p. 1–13, Association for Computing Machinery, 2018. https://doi.org/10.1145/3173574.3173865.

[24] B. Long, S. A. Seah, T. Carter, and S. Subramanian, *Rendering volumetric haptic shapes in mid-air using ultrasound*, *ACM Trans. Graph.* **33** (nov, 2014) [https://doi.org/10.1145/2661229.2661257].

[25] A. Adel, M. M. Micheal, M. A. Seif, S. Abdennadher, and I. S. M. Khalil, *Rendering of virtual volumetric shapes using an electromagnetic-based haptic interface*, *2018 IEEE/RSJ International Conference on Intelligent Robots and Systems (IROS)* (2018) 1–9.

[26] E. Whitmire, H. Benko, C. Holz, E. Ofek, and M. Sinclair, *Haptic revolver: Touch, shear, texture, and shape rendering on a reconfigurable virtual reality controller*, in *CHI '18*, 2018.

[27] E. J. Gonzalez, E. Ofek, M. Gonzalez-Franco, and M. Sinclair, *X-rings: A hand-mounted 360° shape display for grasping in virtual reality*, in *The 34th Annual ACM Symposium on User Interface Software and Technology*, UIST '21, (New York, NY, USA), p. 732–742, Association for Computing Machinery, 2021. https://doi.org/10.1145/3472749.3474782.

[28] A. Zenner, D. Degraen, F. Daiber, and A. Krüger, *Demonstration of drag:on - a vr controller providing haptic feedback based on drag and weight shift*, *Extended Abstracts of the 2020 CHI Conference on Human Factors in Computing Systems* (2020).

[29] G. Nikolakis, D. Tzovaras, S. Moustakidis, and M. G. Strintzis, *Cybergrasp and phantom integration : Enhanced haptic access for visually impaired users*, 2004.

[30] S. B. Schorr and A. M. Okamura, *Fingertip tactile devices for virtual object manipulation and exploration*, *Proceedings of the 2017 CHI Conference on Human Factors in Computing Systems* (2017).

[31] M. Zhu, A. H. Memar, A. Gupta, M. Samad, P. Agarwal, Y. Visell, S. Keller, and N. Colonnese, *Pneusleeve: In-fabric multimodal actuation and sensing in a soft, compact, and expressive haptic sleeve*, *Proceedings of the 2020 CHI Conference on Human Factors in Computing Systems* (2020) [https://doi.org/10.1145/3313831.3376333].

[32] D. Prattichizzo, F. Chinello, C. Pacchierotti, and M. Malvezzi, *Towards wearability in fingertip haptics: A 3-dof wearable device for cutaneous force feedback*, *IEEE Transactions on Haptics* **6** (2013) 506–516.

[33] M. Wiertlewski, D. D. Leonardis, D. J. Meyer, M. A. Peshkin, and J. E. Colgate, *A high-fidelity surface-haptic device for texture rendering on bare finger*, in *EuroHaptics*, 2014.

[34] S. Asano, S. Okamoto, and Y. Yamada, *Vibrotactile stimulation to increase and decrease texture roughness*, *IEEE Transactions on Human-Machine Systems* **45** (2015) 393–398.

[35] H. Culbertson, J. Unwin, and K. J. Kuchenbecker, *Modeling and rendering realistic textures from unconstrained tool-surface interactions*, *IEEE Transactions on Haptics* **7** (2014) 381–393.

[36] V. Yem and H. Kajimoto, *Wearable tactile device using mechanical and electrical stimulation for fingertip interaction with virtual world*, in *2017 IEEE Virtual Reality (VR)*, pp. 99–104, 2017.

[37] I. Choi, Y. Zhao, E. J. Gonzalez, and S. Follmer, *Augmenting perceived softness of haptic proxy objects through transient vibration and visuo-haptic illusion in virtual reality*, *IEEE Transactions on Visualization and Computer Graphics* **27** (2020) 4387–4400.

[38] G. Reardon, N. Kastor, Y. Shao, and Y. Visell, *Elastowave: Localized tactile feedback in a soft haptic interface via focused elastic waves*, *2020 IEEE Haptics Symposium (HAPTICS)* (2020) 7–14.

[39] U. Gollner, T. Bieling, and G. Joost, *Mobile lorm glove: introducing a communication device for deaf-blind people*, *Proceedings of the Sixth International Conference on Tangible, Embedded and Embodied Interaction* (2012) [https://doi.org/10.1145/2148131.2148159].

[40] H. Uchiyama, M. A. Covington, and W. D. Potter, *Vibrotactile glove guidance for semi-autonomous wheelchair operations*, in *ACM-SE 46*, 2008. https://doi.org/10.1145/1593105.1593195.

[41] A. Karime, H. A. Osman, W. Gueaieb, and A. E. Saddik, *E-glove: An electronic glove with vibro-tactile feedback for wrist rehabilitation of post-stroke patients*, *2011 IEEE International Conference on Multimedia and Expo* (2011) 1–6.

[42] A. Israr, S. Zhao, K. McIntosh, J. Kang, Z. Schwemler, E. Brockmeyer, M. Baskinger, and M. Mahler, *Po2: Augmented haptics for interactive gameplay*, in *ACM SIGGRAPH 2015 Emerging Technologies*, SIGGRAPH '15, (New York, NY, USA), Association for Computing Machinery, 2015. https://doi.org/10.1145/2782782.2792489.

[43] T. Hachisu, B. Bourreau, and K. Suzuki, *Enhancedtouchx: Smart bracelets for augmenting interpersonal touch interactions*, in *Proceedings of the 2019 CHI Conference on Human Factors in Computing Systems*, CHI '19, (New York, NY, USA), p. 1–12, Association for Computing Machinery, 2019. https://doi.org/10.1145/3290605.3300551.

[44] G. Sziebig, B. Solvang, C. Kiss, and P. Z. Korondi, *Vibro-tactile feedback for vr systems*, *2009 2nd Conference on Human System Interactions* (2009) 406–410.

[45] C. Gaudeni, L. Meli, L. A. Jones, and D. Prattichizzo, *Presenting surface features using a haptic ring: A psychophysical study on relocating vibrotactile feedback*, *IEEE Transactions on Haptics* **12** (2019) 428–437.

[46] A. T. Maereg, A. K. Nagar, D. Reid, and E. L. Secco, *Wearable vibrotactile haptic device for stiffness discrimination during virtual interactions*, *Frontiers Robotics AI* **4** (2017) 42.

[47] A. Girard, M. Marchal, F. Gosselin, A. Chabrier, F. Louveau, and A. Lécuyer, *Haptip: Displaying haptic shear forces at the fingertips for multi-finger interaction in virtual environments*, *Frontiers ICT* **3** (2016) 6.

[48] S.-W. Kim, S. H. Kim, C. S. Kim, K. Yi, J.-S. Kim, B. J. Cho, and Y. Cha, *Thermal display glove for interacting with virtual reality*, *Scientific Reports* **10** (2020).

[49] M. Gabardi, D. D. Leonardis, M. Solazzi, and A. Frisoli, *Development of a miniaturized thermal module designed for integration in a wearable haptic device*, *2018 IEEE Haptics Symposium (HAPTICS)* (2018) 100–105.

[50] G. Chernyshov, K. Ragozin, C. Caremel, and K. Kunze, *Hand motion prediction for just-in-time thermo-haptic feedback*, *Proceedings of the 24th ACM Symposium on Virtual Reality Software and Technology* (2018) [https://doi.org/10.1145/3281505.3281573].

[51] S. Gallo, G. Rognini, L. Santos-Carreras, T. Vouga, O. Blanke, and H. Bleuler, *Encoded and crossmodal thermal stimulation through a fingertip-sized haptic display*, *Frontiers Robotics AI* **2** (2015) 25.

[52] N. Ranasinghe, P. Jain, S. Karwita, D. Tolley, and E. Y.-L. Do, *Ambiotherm: Enhancing sense of presence in virtual reality by simulating real-world environmental conditions*, *Proceedings of the 2017 CHI Conference on Human Factors in Computing Systems* (2017) [https://doi.org/10.1145/3025453.3025723].

[53] R. L. Peiris, W. Peng, Z. Chen, and K. Minamizawa, *Exploration of cuing methods for localization of spatial cues using thermal haptic feedback on the forehead*, *2017 IEEE World Haptics Conference (WHC)* (2017) 400–405.

[54] Y. Ishikawa, A. Kawazoe, G. Chernyshov, S. Fujii, and M. Nakatani, *The thermal feedback influencer: Wearable thermal display for enhancing the experience of music listening*, in *International Conference on Haptic Interaction - Science, Engineering and Design*, 2018.

[55] S. Akiyama, K. Sato, Y. Makino, and T. Maeno, *Thermon: thermo-musical interface for an enhanced emotional experience*, in *International Semantic Web Conference*, 2013. https://doi.org/10.1145/2493988.2494326.

[56] T. Narumi, T. Akagawa, Y. ah Seong, and M. Hirose, *Characterizing the space by thermal feedback through a wearable device*, in *HCI*, 2009.

[57] K. Parida, H. Bark, and P. S. Lee, *Emerging thermal technology enabled augmented reality*, *Advanced Functional Materials* **31** (2021).

[58] J. Lee, H. Sul, W. Lee, K. R. Pyun, I. Ha, D. Kim, H. Park, H. Eom, Y. Yoon, J. Jung, D. Lee, and S. H. Ko, *Stretchable skin-like cooling/heating device for reconstruction of artificial thermal sensation in virtual reality*, *Advanced Functional Materials* **30** (2020).

[59] J. Patten, H. Ishii, J. Hines, and G. Pangaro, *Sensetable: A wireless object tracking platform for tangible user interfaces*, in *Proceedings of the SIGCHI Conference on Human Factors in Computing Systems*, CHI '01, (New York, NY, USA), p. 253–260, Association for Computing Machinery, 2001. https://doi.org/10.1145/365024.365112.

[60] S. Jordà, G. Geiger, M. Alonso, and M. Kaltenbrunner, *The reactable: Exploring the synergy between live music performance and tabletop tangible interfaces*, in *Proceedings of the 1st International Conference on Tangible and Embedded Interaction*, TEI '07, (New York, NY, USA), p. 139–146, Association for Computing Machinery, 2007. https://doi.org/10.1145/1226969.1226998.

[61] H. ISHII, *Bottles : A transparent interface as a tribute to mark weiser*, *IEICE Transactions on Information and Systems, D* **87** (jun, 2004) 1299–1311.

[62] J. Underkoffler and H. Ishii, *Urp: A luminous-tangible workbench for urban planning and design*, in *Proceedings of the SIGCHI Conference on Human Factors in Computing Systems*, CHI '99, (New York, NY, USA), p. 386–393, Association for Computing Machinery, 1999. https://doi.org/10.1145/302979.303114.

[63] K. Ryokai, S. Marti, and H. Ishii, *I/o brush: Drawing with everyday objects as ink*, in *Proceedings of the SIGCHI Conference on Human Factors in Computing Systems*, CHI '04, (New York, NY, USA), p. 303–310, Association for Computing Machinery, 2004. https://doi.org/10.1145/985692.985731.

[64] D. A. Chacon, E. Velloso, T. Hoang, and K. Wolf, *Spinallog: Visuo-haptic feedback in musculoskeletal manipulation training*, in *Proceedings of the Thirteenth International Conference on Tangible, Embedded, and Embodied Interaction*, TEI '19, (New York, NY, USA), p. 5–14, Association for Computing Machinery, 2019.

[65] B. Ullmer and H. Ishii, *The metadesk: Models and prototypes for tangible user interfaces*, in *Proceedings of the 10th Annual ACM Symposium on User Interface Software and Technology*, UIST '97, (New York, NY, USA), p. 223–232, Association for Computing Machinery, 1997. https://doi.org/10.1145/263407.263551.

[66] H. Ishii, C. Ratti, B. Piper, Y. Wang, A. Biderman, and E. Ben-Joseph, *Bringing clay and sand into digital design — continuous tangible user interfaces*, *BT Technology Journal* **22** (Oct., 2004) 287–299.

[67] B. Piper, C. Ratti, and H. Ishii, *Illuminating clay: A 3-d tangible interface for landscape analysis*, in *Proceedings of the SIGCHI Conference on Human Factors in Computing Systems*, CHI '02, (New York, NY, USA), p. 355–362, Association for Computing Machinery, 2002. https://doi.org/10.1145/503376.503439.

[68] B. Piper, C. Ratti, and H. Ishii, *Illuminating clay: A tangible interface with potential grass applications*, 2002.

[69] K. Kobayashi, M. Hirano, A. Narita, and H. Ishii, *A tangible interface for ip network simulation*, in *CHI '03 Extended Abstracts on Human Factors in Computing Systems*, CHI EA '03, (New York, NY, USA), p. 800–801, Association for Computing Machinery, 2003. https://doi.org/10.1145/765891.766000.

[70] K. Kobayashi, A. Narita, M. Hirano, I. Kase, S. Tsuchida, T. Omi, T. Kakizaki, and T. Hosokawa, *Collaborative simulation interface for planning disaster measures*, in *CHI EA '06*, 2006. https://doi.org/10.1145/1125451.1125639.

[71] H. Zhang and X. Gong, *Tmusic: A music player based on tangible user interface*, in *2015 International Conference on Electromechanical Control Technology and Transportation*, pp. 216–219, Atlantis Press, 2015/11.

[72] J. Patten, B. Recht, and H. Ishii, *Interaction techniques for musical performance with tabletop tangible interfaces*, in *Proceedings of the 2006 ACM SIGCHI International Conference on Advances in Computer Entertainment Technology*, ACE '06, (New York, NY, USA), p. 27–es, Association for Computing Machinery, 2006. https://doi.org/10.1145/1178823.1178856.

[73] M. Spindler, V. Cheung, and R. Dachselt, *Dynamic tangible user interface palettes*, in *Human-Computer Interaction – INTERACT 2013* (P. Kotzé, G. Marsden, G. Lindgaard, J. Wesson, and M. Winckler, eds.), (Berlin, Heidelberg), pp. 159–176, Springer Berlin Heidelberg, 2013.

[74] S. Okamoto, H. Nagano, and Y. Yamada, *Psychophysical dimensions of tactile perception of textures*, *IEEE Transactions on Haptics* **6** (2013) 81–93.

[75] O. Shogo, *Tactile transmission system and perceptual effects of delayed tactile feedback.* PhD thesis, Tohoku University, 2010.

[76] T. Yamauchi, S. Okamoto, M. Konyo, Y. Hidaka, T. Maeno, and S. Tadokoro, *Real-time remote transmission of multiple tactile properties through master-slave robot system*, in *2010 IEEE International Conference on Robotics and Automation*, pp. 1753–1760, 2010.

[77] A. M. Okamura, M. R. Cutkosky, and J. T. Dennerlein, *Reality-based models for vibration feedback in virtual environments*, *IEEE/ASME Transactions on Mechatronics* **6** (2001), no. 3 245–252.

[78] K. J. Kuchenbecker, J. Fiene, and G. Niemeyer, *Improving contact realism through event-based haptic feedback*, *IEEE Transactions on Visualization and Computer Graphics* **12** (2006) 219–230.

[79] Y. Ikeda and S. Hasegawa, *Characteristics of Perception of Stiffness by Varied Tapping Velocity and Penetration in Using Event-Based Haptic*, in *Joint Virtual Reality Conference of EGVE - ICAT - EuroVR* (M. Hirose, D. Schmalstieg, C. A. Wingrave, and K. Nishimura, eds.), The Eurographics Association, 2009.

[80] S. Asano, S. Okamoto, Y. Matsuura, and Y. Yamada, *Toward quality texture display: vibrotactile stimuli to modify material roughness sensations*, *Advanced Robotics* **28** (2014), no. 16 1079–1089, [https://doi.org/10.1080/01691864.2014.913502].

[81] Y. Ochiai, T. Hoshi, J. Rekimoto, and M. Takasaki, *Diminished haptics: Towards digital transformation of real world textures*, in *EuroHaptics*, 2014.

[82] L. B. Porquis, M. Konyo, and S. Tadokoro, *Representation of softness sensation using vibrotactile stimuli under amplitude control*, *2011 IEEE International Conference on Robotics and Automation* (2011) 1380–1385.

[83] A. Ikeda, T. Suzuki, J. Takamatsu, and T. Ogasawara, *Producing method of softness sensation by device vibration*, *2013 IEEE International Conference on Systems, Man, and Cybernetics* (2013) 3384–3389.

[84] Y. Visell and S. Okamoto, *Vibrotactile sensation and softness perception*, in *Multisensory Softness*, 2014.

[85] J. Kildal, *3d-press: Haptic illusion of compliance when pressing on a rigid surface*, in *International Conference on Multimodal Interfaces and the Workshop on Machine Learning for Multimodal Interaction*, ICMI-MLMI '10, (New York, NY, USA), Association for Computing Machinery, 2010.

[86] J. Kildal, *Kooboh: Variable tangible properties in a handheld haptic-illusion box*, in *Haptics: Perception, Devices, Mobility, and Communication* (P. Isokoski and J. Springare, eds.), (Berlin, Heidelberg), pp. 191–194, Springer Berlin Heidelberg, 2012.

[87] K. Higashi, S. Okamoto, and Y. Yamada, *What is the hardness perceived by tapping?*, in *EuroHaptics*, 2016.

[88] K. Higashi, S. Okamoto, Y. Yamada, H. Nagano, and M. Konyo, *Hardness perception based on dynamic stiffness in tapping*, *Frontiers in Psychology* **9** (2019).

[89] T. Hachisu and H. Kajimoto, *Vibration feedback latency affects material perception during rod tapping interactions*, *IEEE Transactions on Haptics* **10** (2017) 288–295.

[90] H. Ohnishi and K. Mochizuki, *Effect of delay of feedback force on perception of elastic force: A psychophysical approach*, *IEICE Trans. Commun.* **90-B** (2007) 12–20.

[91] T. Kaaresoja, E. E. Hoggan, and E. Anttila, *Playing with tactile feedback latency in touchscreen interaction: Two approaches*, in *INTERACT*, 2011.

[92] M. Hollins and S. R. Risner, *Evidence for the duplex theory of tactile texture perception*, *Perception Psychophysics* **62** (2000) 695–705.

[93] T. Yamauchi, S. Okamoto, M. Konyo, Y. Hidaka, T. Maeno, and S. Tadokoro, *Real-time remote transmission of multiple tactile properties through master-slave robot system*, *2010 IEEE International Conference on Robotics and Automation* (2010) 1753–1760.

[94] M. Konyo, S. Tadokoro, A. Yoshida, and N. Saiwaki, *A tactile synthesis method using multiple frequency vibrations for representing virtual touch*, *2005 IEEE/RSJ International Conference on Intelligent Robots and Systems* (2005) 3965–3971.

[95] A. M. Okamura, M. R. Cutkosky, and J. T. Dennerlein, *Reality-based models for vibration feedback in virtual environments*, 2001.

[96] R. Lundström, *Local vibrations–mechanical impedance of the human hand's glabrous skin.*, *Journal of biomechanics* **17 2** (1984) 137–44.

[97] T. Maeda, R. L. Peiris, M. Nakatani, Y. Tanaka, and K. Minamizawa, *Wearable haptic augmentation system using skin vibration sensor*, in *VRIC '16*, 2016.

[98] O. Bau, I. Poupyrev, M. L. Goc, L. Galliot, and M. Glisson, *Revel: tactile feedback technology for augmented reality*, in *SIGGRAPH Emerging Technologies*, 2012.

[99] C. Bermejo and P. Hui, *A survey on haptic technologies for mobile augmented reality*, *CoRR* **abs/1709.00698** (2017) [arXiv:1709.0069].

[100] A. Matsubayashi, Y. Makino, and H. Shinoda, *Direct finger manipulation of 3d object image with ultrasound haptic feedback*, in *Proceedings of the 2019 CHI Conference on Human Factors in Computing Systems*, CHI '19, (New York, NY, USA), pp. 87:1–87:11, ACM, 2019.

[101] Y. Shao, V. Hayward, and Y. Visell, *Spatial patterns of cutaneous vibration during whole-hand haptic interactions*, *Proceedings of the National Academy of Sciences* (2016).

[102] Y. Shao, V. Hayward, and Y. Visell, *Compression of dynamic tactile information in the human hand*, *Science Advances* ((In Press), 2020).

[103] H. Shaefer, Z. Wells, Y. Shao, and Y. Visell, *Transfer properties of touch elicited waves vary with hand posture and contact conditions*, in *Proc. IEEE World Haptics Conference*, 2017.

[104] B. Dandu, Y. Shao, A. Stanley, and Y. Visell, *Spatiotemporal haptic effects from a single actuator via spectral control of cutaneous wave propagation*, in *Proc. IEEE World Haptics Conference*, 2019.

[105] K. J. Kuchenbecker, J. Fiene, and G. Niemeyer, *Improving contact realism through event-based haptic feedback*, *IEEE Transactions on Visualization and Computer Graphics* **12** (March, 2006) 219–230.

[106] A. M. Okamura, M. R. Cutkosky, and J. T. Dennerlein, *Reality-based models for vibration feedback in virtual environments*, *IEEE/ASME Transactions on Mechatronics* **6** (Sep, 2001) 245–252.

[107] T. Hachisu and H. Kajimoto, *Vibration feedback latency affects material perception during rod tapping interactions*, *IEEE Transactions on Haptics* **10** (April-June, 2017) 288–295.

[108] T. Hachisu and H. Kajimoto, *Hachistack: dual-layer photo touch sensing for haptic and auditory tapping interaction*, in *2013 ACM SIGCHI Conference on Human Factors in Computing Systems, CHI '13, Paris, France, April 27 - May 2, 2013*, pp. 1411–1420, 2013.

[109] H.-Y. Yao, V. Hayward, and R. E. Ellis, *A tactile magnification instrument for minimally invasive surgery*, in *Medical Image Computing and Computer-Assisted Intervention – MICCAI 2004* (C. Barillot, D. R. Haynor, and P. Hellier, eds.), (Berlin, Heidelberg), pp. 89–96, Springer Berlin Heidelberg, 2004.

[110] M. Bouzit, G. Burdea, G. Popescu, and R. Boian, *The rutgers master ii-new design force-feedback glove*, *IEEE/ASME Transactions on Mechatronics* **7** (Jun, 2002) 256–263.

[111] "CyberGrasp force feedback system and CyberTouch tactile feedback system. Online , Last accessed on July, 2018.."

[112] J. Hummel, J. Dodiya, G. A. Center, L. Eckardt, R. Wolff, A. Gerndt, and T. W. Kuhlen, *A lightweight electrotactile feedback device for grasp improvement in immersive virtual environments*, in *2016 IEEE Virtual Reality (VR)*, pp. 39–48, March, 2016.

[113] F. Chinello, M. Malvezzi, C. Pacchierotti, and D. Prattichizzo, *Design and development of a 3rrs wearable fingertip cutaneous device*, in *2015 IEEE International Conference on Advanced Intelligent Mechatronics (AIM)*, pp. 293–298, July, 2015.

[114] M. Solazzi, A. Frisoli, and M. Bergamasco, *Design of a novel finger haptic interface for contact and orientation display*, in *2010 IEEE Haptics Symposium*, pp. 129–132, March, 2010.

[115] D. Prattichizzo, F. Chinello, C. Pacchierotti, and M. Malvezzi, *Towards wearability in fingertip haptics: A 3-dof wearable device for cutaneous force feedback*, *IEEE Trans. Haptics* **6** (oct, 2013) 506–516.

[116] C. Pacchierotti, G. Salvietti, I. Hussain, L. Meli, and D. Prattichizzo, *The hring: A wearable haptic device to avoid occlusions in hand tracking*, in *2016 IEEE Haptics Symposium (HAPTICS)*, pp. 134–139, April, 2016.

[117] S. B. Schorr and A. M. Okamura, *Fingertip tactile devices for virtual object manipulation and exploration*, in *Proceedings of the 2017 CHI Conference on Human Factors in Computing Systems*, pp. 3115–3119, May, 2018. https://doi.org/10.1145/3025453.3025744.

[118] E. Whitmire, H. Benko, C. Holz, E. Ofek, and M. Sinclair, *Haptic revolver: Touch, shear, texture, and shape rendering on a reconfigurable virtual reality controller*, in *CHI 2018*, ACM, April, 2018.

[119] J. Fleureau, Y. Lefevre, F. Danieau, P. Guillotel, and A. Costes, *Texture rendering on a tactile surface using extended elastic images and example-based audio cues*, vol. 9774, pp. 350–359, 07, 2016.

[120] M. Wiertlewski, D. Leonardis, D. J. Meyer, M. A. Peshkin, and J. E. Colgate, *A high-fidelity surface-haptic device for texture rendering on bare finger*, in *Haptics: Neuroscience, Devices, Modeling, and Applications* (M. Auvray and C. Duriez, eds.), (Berlin, Heidelberg), pp. 241–248, Springer Berlin Heidelberg, 2014.

[121] M. Niwa, T. Nozaki, T. Maeda, and H. Ando, *Fingernail-mounted display of attraction force and texture*, in *Haptics: Generating and Perceiving Tangible Sensations*, (Berlin, Heidelberg), pp. 3–8, Springer Berlin Heidelberg, 2010.

[122] K. Sakai, T. Hachisu, and Y. Hashimoto, *Characteristics of illusory vibration in the toe pad induced by vibration applied to toenail and toe force to surface*, pp. 281–286, 06, 2017.

[123] S. Asano, S. Okamoto, and Y. Yamada, *Toward augmented reality of textures: Vibrotactile high-frequency stimuli mask texture perception to be rougher or smoother?*, *2013 IEEE International Conference on Systems, Man, and Cybernetics* (2013) 510–515.

[124] M. Chartier, N. Thomas, Y. Shao, and Y. Visell, *Toward a wearable tactile sensory amplification device: Transfer characteristics and optimization*, in *Work in Progress of the 2016 Haptic Symposium Conference.*, pp. 546–551, IEEE., 2016.

[125] A. Kawazoe, M. Di Luca, and Y. Visell, *Tactile echoes: A wearable system for tactile augmentation of objects*, in *Proceedings of the 2019 IEEE World Haptics Conference*.

[126] Y. Makino, M. Murao, and T. Maeno, *Life log system based on tactile sound*, in *Haptics: Generating and Perceiving Tangible Sensations* (A. M. L. Kappers, J. B. F. van Erp, W. M. Bergmann Tiest, and F. C. T. van der Helm, eds.), (Berlin, Heidelberg), pp. 292–297, Springer Berlin Heidelberg, 2010.

[127] K. Minamizawa, Y. Kakehi, M. Nakatani, S. Mihara, and S. Tachi, *Techtile toolkit: a prototyping tool for design and education of haptic media*, in *Proceedings of the 2012 Virtual Reality International Conference*, p. 26, ACM, 2012.

[128] T. Maeda, R. Peiris, M. Nakatani, Y. Tanaka, and K. Minamizawa, *Wearable haptic augmentation system using skin vibration sensor*, in *Proceedings of the 2016 Virtual Reality International Conference*, pp. 25:1–25:4, ACM, 2016. https://doi.org/10.1145/2927929.2927946.

[129] T. Maeda, K. Tsuchiya, R. Peiris, Y. Tanaka, and K. Minamizawa, *Hapticaid: Haptic experiences system using mobile platform*, in *Proceedings of the Eleventh International Conference on Tangible, Embedded, and Embodied Interaction*, pp. 397–402, ACM, 2017.

[130] V. Jousmäki and R. Hari, *Parchment-skin illusion: sound-biased touch*, *Current Biology* **8** (1998), no. 6 R190 – R191.

[131] M. Zampini and C. Spence, *The role of auditory cues in modulating the perceived crispness and staleness of potato chips*, *Journal of Sensory Studies* **19** (2004), no. 5 347–363.

[132] P. von Schiller, *Die rauhigkeit als intermodale erscheinung (roughness as an intermodal phenomenon)*, *Zeitschrift für Psychologie Bildung* **127** (1932) 265–289.

[133] J. K. Koehn and K. J. Kuchenbecker, *Surgeons and non-surgeons prefer haptic feedback of instrument vibrations during robotic surgery*, *Surgical Endoscopy* **29** (2014) 2970–2983.

[134] S. Jeon and S. Choi, *Haptic augmented reality: Taxonomy and an example of stiffness modulation*, *PRESENCE: Teleoperators and Virtual Environments* **18** (2009) 387–408.

[135] H. Culbertson and K. J. Kuchenbecker, *Ungrounded haptic augmented reality system for displaying roughness and friction*, *IEEE/ASME Transactions on Mechatronics* **22** (2017) 1839–1849.

[136] B. T. Gleeson and D. E. Johnson, *Expressive haptic rendering with cartoon-inspired effects*, *2010 IEEE Haptics Symposium* (2010) 191–194.

[137] S. Okamoto, M. Konyo, and S. Tadokoro, *Vibrotactile stimuli applied to finger pads as biases for perceived inertial and viscous loads*, *IEEE Transactions on Haptics* **4** (October, 2011) 307–315.

[138] S. Yoshimoto, Y. Kuroda, M. Imura, and O. Oshiro, *Material roughness modulation via electrotactile augmentation*, *IEEE Transactions on Haptics* **8** (April, 2015) 199–208.

[139] S. Jeon and S. Choi, *Haptic augmented reality: Taxonomy and an example of stiffness modulation*, *Presence* **18** (Oct, 2009) 387–408.

[140] M. Holliins, R. Faldowski, S. Rao, and F. Young, *Perceptual dimensions of tactile surface texture: A multidimensional scaling analysis*, *Perception & Psychophysics* **54** (Nov, 1993) 697–705.

[141] M. Hollins, S. Bensmaïa, K. Karlof, and F. Young, *Individual differences in perceptual space for tactile textures: Evidence from multidimensional scaling*, *Perception & Psychophysics* **62** (Dec, 2000) 1534–1544.

[142] W. M. B. Tiest and A. M. Kappers, *Analysis of haptic perception of materials by multidimensional scaling and physical measurements of roughness and compressibility*, *Acta Psychologica* **121** (2006), no. 1 1 – 20.

[143] Q. Liu, H. Z. Tan, L. Jiang, and Y. Zhang, *Perceptual dimensionality of manual key clicks*, in *2018 IEEE Haptics Symposium (HAPTICS)*, pp. 112–118, March, 2018.

[144] D. Ternes and K. E. Maclean, *Designing large sets of haptic icons with rhythm*, in *International Conference on Human Haptic Sensing and Touch Enabled Computer Applications*, pp. 199–208, Springer, 2008.

[145] J. Luk, J. Pasquero, S. Little, K. MacLean, V. Levesque, and V. Hayward, *A role for haptics in mobile interaction: initial design using a handheld tactile display prototype*, in *Proceedings of the SIGCHI conference on Human Factors in computing systems*, pp. 171–180, ACM, 2006.

[146] K. Hinckley, R. Pausch, J. C. Goble, and N. F. Kassell, *Passive real-world interface props for neurosurgical visualization*, in *Proceedings of the SIGCHI Conference on Human Factors in Computing Systems*, CHI '94, (New York, NY, USA), pp. 452–458, ACM, 1994.

[147] L.-P. Cheng, E. Ofek, C. Holz, H. Benko, and A. D. Wilson, *Sparse haptic proxy: Touch feedback in virtual environments using a general passive prop*, in *Proceedings of the 2017 CHI Conference on Human Factors in Computing Systems*, CHI '17, (New York, NY, USA), p. 3718?3728, Association for Computing Machinery, 2017.

[148] M. Yahya, J. A. Shah, K. Kadir, Z. M. Yusof, S. Khan, and A. Warsi, *Motion capture sensing techniques used in human upper limb motion: a review*, *Sensor Review* **39** (2019) 504–511.

[149] H. Schafer, *Touch amplification for human computer interaction*, Master's thesis, UC Santa Barbara, 2017.

[150] R. R. Z. H. Chunhui Li, Guangying Guan and R. K. Wang, *Determining elastic properties of skin by measuring surface waves from an impulse mechanical stimulus using phase-sensitive optical coherence tomography*, *J R Soc Interface* **9** (2011), no. 70 831–41.

[151] L. R. Manfredi, A. T. Baker, D. O. Elias, J. F. Dammann III, M. C. Zielinski, V. S. Polashock, and S. J. Bensmaia, *The effect of surface wave propagation on neural responses to vibration in primate glabrous skin*, *PloS one* **7** (2012), no. 2.

[152] S. Okamoto, H. Nagano, and Y. Yamada, *Psychophysical dimensions of tactile perception of textures*, *IEEE Transactions on Haptics* **6** (First, 2013) 81–93.

[153] L. Jones and S. Lederman, *Human Hand Function*. Oxford University Press, 2006.

[154] S. Guest, C. Catmur, D. Lloyd, and C. Spence, *Audiotactile interactions in roughness perception*, *Experimental Brain Research* **146** (Sep, 2002) 161–171.

[155] M. Zampini and C. Spence, *The role of auditory cues in modulating the perceived crispness and staleness of potato chips*, *Journal of Sensory Studies* **19** (2004), no. 5 347–363, [https://onlinelibrary.wiley.com/doi/pdf/10.1111/j.1745-459x.2004.080403.x].

[156] S. V. Salazar, C. Pacchierotti, X. de Tinguy, A. Maciel, and M. Marchal, *Altering the stiffness, friction, and shape perception of tangible objects in virtual reality using wearable haptics*, *IEEE Transactions on Haptics* **13** (2020) 167–174.

[157] A. Gräf, *A touchosc midi bridge for linux*, 2014.

[158] A. Freed and A. Schmeder, *Features and future of open sound control version 1.1 for nime*, in *In Proceedings of the 9th Conference on New Interfaces for Musical Expression*, pp. 116–120, 2009.

[159] J. J. DiGiovanni, E. E. Lynch, N. K. Nagaraj, and D. T. Ries, *Dominance of persistence over adaptation in forward masking*, *Attention, Perception, & Psychophysics* **80** (2018) 1863–1869.

[160] G. A. Gescheider, A. A. Valetutti, M. C. Padula, and R. T. Verrillo, *Vibrotactile forward masking as a function of age.*, *The Journal of the Acoustical Society of America* **91 3** (1992) 1690–6.

[161] R. T. Verrillo, *Effects of aging on the suprathreshold responses to vibration*, *Perception & Psychophysics* **32** (1982) 61–68.

[162] C. E. Sherrick, *Effects of double simultaneous stimulation of the skin.*, *The American journal of psychology* **77** (1964) 42–53.

[163] J. Makous, G. A. Gescheider, and S. J. Bolanowski, *Decay in the effect of vibrotactile masking.*, *The Journal of the Acoustical Society of America* **99 2** (1996) 1124–9.

[164] G. A. Gescheider, K. E. Santoro, J. Makous, and S. J. Bolanowski, *Vibrotactile forward masking: effects of the amplitude and duration of the masking stimulus.*, *The Journal of the Acoustical Society of America* **98 6** (1995) 3188–94.

[165] G. A. Gescheider and N. Migel, *Some temporal parameters in vibrotactile forward masking.*, *The Journal of the Acoustical Society of America* **98 6** (1995) 3195–9.

[166] G. A. Gescheider, K. Hoffman, M. A. F. Harrison, M. Travis, and S. J. Bolanowski, *The effects of masking on vibrotactile temporal summation in the detection of sinusoidal and noise signals.*, *The Journal of the Acoustical Society of America* **95 2** (1994) 1006–16.

[167] G. A. Gescheider, R. T. Verrillo, and C. V. Doren, *Prediction of vibrotactile masking functions.*, *The Journal of the Acoustical Society of America* **72 5** (1982) 1421–6.

[168] G. A. Gescheider, M. J. O'Malley, and R. T. Verrillo, *Vibrotactile forward masking: evidence for channel independence.*, *The Journal of the Acoustical Society of America* **74 2** (1983) 474–85.

[169] G. A. Gescheider, S. J. Bolanowski, J. V. Pope, and R. T. Verrillo, *A four-channel analysis of the tactile sensitivity of the fingertip: frequency selectivity, spatial summation, and temporal summation*, *Somatosensory & Motor Research* **19** (2002) 114 – 124.

[170] R. D. Hamer, R. T. Verrillo, and J. J. Zwislocki, *Vibrotacile masking of pacinian and non-pacinian channels.*, *The Journal of the Acoustical Society of America* **73 4** (1983) 1293–303.

[171] B. Güçlü and C. Oztek, *Tactile sensitivity of children: effects of frequency, masking, and the non-pacinian i psychophysical channel.*, *Journal of experimental child psychology* **98 2** (2007) 113–30.

[172] J. Makous, R. F. Friedman, and C. Vierck, *A critical band filter in touch*, in *Journal of Neuroscience*, 1995.

[173] B. Güçlü and S. J. Bolanowski, *Vibrotactile thresholds of the non-pacinian i channel: I. methodological issues*, *Somatosensory & Motor Research* **22** (2005) 49 – 56.

[174] Y. Tanaka, S. Matsuoka, W. M. B. Tiest, A. M. L. Kappers, K. Minamizawa, and A. Sano, *Frequency-specific masking effect by vibrotactile stimulation to the forearm*, in *EuroHaptics*, 2016.

[175] R. D. Gilson, *Vibrotactile masking: Some spatial and temporal aspects*, *Perception & Psychophysics* **5** (1969) 176–180.

[176] R. T. Verrillo, G. A. Gescheider, B. G. Calman, and C. L. V. Doren, *Vibrotactile masking: Effects of oneand two-site stimulation*, *Perception & Psychophysics* **33** (1983) 379–387.

[177] S. Okamoto, M. Konyo, S. Saga, and S. Tadokoro, *Identification of cutaneous detection thresholds against time-delay stimuli for tactile displays*, in *2008 IEEE International Conference on Robotics and Automation*, pp. 220–225, 2008.

[178] S. Okamoto, M. Konyo, S. Saga, and S. Tadokoro, *Detectability and perceptual consequences of delayed feedback in a vibrotactile texture display*, *IEEE Transactions on Haptics* **2** (2009) 73–84.

[179] I. M. L. C. Vogels, *Detection of temporal delays in visual-haptic interfaces*, *Human Factors: The Journal of Human Factors and Ergonomics Society* **46** (2004) 118 – 134.

[180] C. Jay, M. Glencross, and R. J. Hubbold, *Modeling the effects of delayed haptic and visual feedback in a collaborative virtual environment*, *ACM Trans. Comput. Hum. Interact.* **14** (2007) 8.

[181] N. Colonnese, A. F. Siu, C. M. Abbott, and A. M. Okamura, *Rendered and characterized closed-loop accuracy of impedance-type haptic displays*, *IEEE Transactions on Haptics* **8** (2015) 434–446.

[182] A. Okamura, M. Cutkosky, and J. Dennerlein, *Reality-based models for vibration feedback in virtual environments*, *IEEE/ASME Transactions on Mechatronics* **6** (2001), no. 3 245–252.

[183] T. Kaaresoja, S. Brewster, and V. Lantz, *Towards the temporally perfect virtual button: Touch-feedback simultaneity and perceived quality in mobile touchscreen press interactions*, *ACM Trans. Appl. Percept.* **11** (2014) 9:1–9:25.

[184] S.-C. Lim, K.-U. Kyung, and D.-S. Kwon, *Effect of frequency difference on sensitivity of beats perception*, *Experimental Brain Research* **216** (Jan, 2012) 11–19.

[185] G. von Békésy, *Sensations on the skin similar to directional hearing, beats, and harmonics of the ear*, *Journal of the Acoustical Society of America* **29** (1957) 489–501.

[186] G. von Békésy, *Synchronism of neural discharges and their demultiplication in pitch perception on the skin and in hearing*, *Journal of the Acoustical Society of America* **31** (1959) 338–349.

[187] Y. Makino, T. Maeno, and H. Shinoda, *Perceptual characteristic of multi-spectral vibrations beyond the human perceivable frequency range*, *2011 IEEE World Haptics Conference* (2011) 439–443.

[188] S. Patwardhan, A. Kawazoe, D. Kerr, M. Nakatani, and Y. Visell, *Dynamics and perception in the thermal grill illusion*, *IEEE Transactions on Haptics* **12** (2019) 604–614.

[189] H.-N. Ho and L. A. Jones, *Thermal model for hand-object interactions*, in *Haptic Interfaces for Virtual Environment and Teleoperator Systems, 2006 14th Symposium on*, pp. 461–467, IEEE, 2006.

[190] L. A. Jones and M. Berris, *Material discrimination and thermal perception*, in *Haptic Interfaces for Virtual Environment and Teleoperator Systems, 2003. HAPTICS 2003. Proceedings. 11th Symposium on*, pp. 171–178, IEEE, 2003.

[191] H.-N. Ho and L. A. Jones, *Contribution of thermal cues to material discrimination and localization*, *Perception & Psychophysics* **68** (2006), no. 1 118–128.

[192] R. Ma, Z. Zhang, K. Tong, D. Huber, R. Kornbluh, Y. S. Ju, and Q. Pei, *Highly efficient electrocaloric cooling with electrostatic actuation*, *Science* **357** (2017), no. 6356 1130–1134.

[193] H.-N. Ho, K. Sato, S. Kuroki, J. Watanabe, T. Maeno, and S. Nishida, *Physical-perceptual correspondence for dynamic thermal stimulation*, *IEEE transactions on haptics* **10** (2017), no. 1 84–93.

[194] A. Craig, *Temperature sensation*, in *Encyclopedia of Neuroscience* (L. R. Squire, ed.), pp. 903 – 907. Academic Press, Oxford, 2009.

[195] D. C. Spray, *Cutaneous temperature receptors*, *Annual Review of Physiology* **48** (1986), no. 1 625–638.

[196] I. Darian-Smith and K. O. Johnson, *Thermal sensibility and thermoreceptors*, *Journal of Investigative Dermatology* **69** (1977), no. 1 146–153.

[197] T. Thunberg, *Förnimmelserna vid till samma ställe lokaliserad, samtidigt pågående köld-och värmeretning*, *Uppsala Läkfören Förh* **2** (1896), no. 1 489–495.

[198] X. Li, L. Petrini, L. Wang, R. Defrin, and L. Arendt-Nielsen, *The importance of stimulus parameters for the experience of the thermal grill illusion*, *Neurophysiologie Clinique/Clinical Neurophysiology* **39** (2009), no. 6 275–282.

[199] P. Bach, S. Becker, D. Kleinböhl, and R. Hölzl, *The thermal grill illusion and what is painful about it*, *Neuroscience letters* **505** (2011), no. 1 31–35.

[200] F. Lindstedt, B. Johansson, S. Martinsen, E. Kosek, P. Fransson, and M. Ingvar, *Evidence for thalamic involvement in the thermal grill illusion: an fmri study*, *PLoS one* **6** (2011), no. 11 e27075.

[201] D. W. Hahn and M. N. Azisik, *Heat conduction.* John Wiley & Sons, 2012.

[202] A. Craig and M. Bushnell, *The thermal grill illusion: unmasking the burn of cold pain*, *Science* **265** (1994), no. 5169 252–256.

[203] A. D. Craig, E. M. Reiman, A. Evans, and M. C. Bushnell, *Functional imaging of an illusion of pain*, *Nature* **384** (Nov 21, 1996) 258–60.

[204] D. Bouhassira, D. Kern, J. Rouaud, E. Pelle-Lancien, and F. Morain, *Investigation of the paradoxical painful sensation (âillusion of painâ) produced by a thermal grill*, *Pain* **114** (2005), no. 1 160–167.

[205] A. I. Basbaum, D. M. Bautista, G. Scherrer, and D. Julius, *Cellular and molecular mechanisms of pain*, *Cell* **139** (2009), no. 2 267–284.

[206] R. H. LaMotte and J. N. Campbell, *Comparison of responses of warm and nociceptive c-fiber afferents in monkey with human judgments of thermal pain*, *Journal of neurophysiology* **41** (1978), no. 2 509–528.

[207] J. Hunter, R. Dranga, M. Wyk, and J. Dostrovsky, *Unique influence of stimulus duration and stimulation site (glabrous vs. hairy skin) on the thermal grill-induced percept*, *European journal of pain* **19** (2015), no. 2 202–215.

[208] A. Y. Leung, M. S. Wallace, G. Schulteis, and T. L. Yaksh, *Qualitative and quantitative characterization of the thermal grill*, *Pain* **116** (2005), no. 1 26–32.

[209] F. Xu and T. Lu, *Introduction to Skin Biothermomechanics and Thermal Pain*, vol. 7. Springer, 2011.

[210] O. College, *Anatomy and Physiology*, OpenStax CNX. http://cnx.org/contents/14fb4ad7-39a1-4eee-ab6e-3ef2482e3e22@8.81.

[211] H. H. Pennes, *Analysis of tissue and arterial blood temperatures in the resting human forearm*, *Journal of applied physiology* **1** (1948), no. 2 93–122.

[212] M. Benali-Khoudjal, M. Hafez, J.-M. Alexandre, J. Benachour, and A. Kheddar, *Thermal feedback model for virtual reality*, in *Micromechatronics and Human Science, 2003. MHS 2003. Proceedings of 2003 International Symposium on*, pp. 153–158, IEEE, 2003.

[213] H.-N. Ho and L. A. Jones, *Modeling the thermal responses of the skin surface during hand-object interactions*, *Journal of Biomechanical Engineering* **130** (2008), no. 2 021005.

[214] L. A. Jones and S. J. Lederman, *Human hand function*. Oxford University Press, 2006.

[215] V. Ganesan and A. Mills, *Heat Transfer 2/E*. Pearson Education, 2009.

[216] M. L. Cohen, *Measurement of the thermal properties of human skin. a review*, *Journal of investigative dermatology* **69** (1977), no. 3 333–338.

[217] L. A. Jones and M. Berris, *The psychophysics of temperature perception and thermal-interface design*, in *Haptic Interfaces for Virtual Environment and Teleoperator Systems, 2002. HAPTICS 2002. Proceedings. 10th Symposium on*, pp. 137–142, IEEE, 2002.

[218] H. Hensel, *Die intracutane temperaturbewegung bei einwirkung aèusserer temperaturreize*, *Pflügers Archiv European Journal of Physiology* **252** (1950), no. 2 146–164.